Addendum

(p. 35, following line 13):

In addition to SP, the perivascular endings of trigeminovascular fibers contain another neuropeptide that has been implicated in inflammation: calcitonin gene-related peptide (CGRP) (Uddman *et al.* 1988, McCulloch *et al.* 1986). This section reviews the biology of CGRP and then compares between the roles of CGRP and SP in neurogenic inflammation.

(p. 60, following line 2):

Routine histological staining does not allow the characterization of microglia (Berry *et al.* 2002). Specific immunohistochemical staining for these cells was nor performed in this study as there is no indication in the literature that these cells have any role in the alteration of BBB permeability and cerebral edema. Furthermore, although the study of Lai *et al.* (2000) described the presence of SP-IR in human microglia, this study was conducted in vitro on isolated microglia cultured from human fetal brains. It is well documented that microglia are greatly dependent on the CNS microenvironment for expression of their phenotypic structure and function (Schmidtmayer *et al.* 1994, Sievers *et al.* 1994). This has been shown to involve direct contact with surrounding astrocytes and interaction with neurons (Neumann *et al.* 1998). In the study by Lai *et al.*, however, microglia were isolated for several weeks in an artificial medium in which they represented 99% of the cellular constituents. Thus, it is not clear whether or not these results are applicable to microglia in situ.

(p. 115, following line 10):

As explained in the methodology section, no attempt was made to characterize SP-IR in microglia. However, irrespective of the expression of SP-IR in microglia, the results of this study suggest that astrocytes are the most important cells in any effect that SP may have on the BBB in the settings of infarction and contusion.

(Cont'd on inside of back cover)

THE ROLE OF SUBSTANCE P IN CEREBRAL EDEMA ASSOCIATED WITH RAT AND HUMAN INFARCTION AND CONTUSION

Islam Khamis Hassan
MBBCh, MAIMS

Department of Pathology
University of Adelaide
Adelaide, South Australia

and

Hanson Institute Centre for Neurological Diseases
Institute of Medical and Veterinary Science
Adelaide, South Australia

A Thesis Submitted to the University of Adelaide in Fulfillment of the Requirements for the Degree of Master of Medical Science

August 2006

Table of Contents

Abstract

Cerebrovascular stroke is the third commonest cause of death in industrialized countries while traumatic brain injury (TBI) is the leading cause of mortality and disability in individuals below 40 years of age. An important influence on the severity of both TBI and stroke is cerebral edema. The mechanism of cerebral edema in both is poorly understood.

Recent evidence suggests that substance P (SP) plays a role in this edema and, specifically, that injured SP-containing perivascular nerve fibers are involved.

The present study examined tissue obtained from rat models of infarction and contusion as well as human post mortem infarct and contusion tissue at several timepoints. Immunohistochemistry was used to characterize and correlate, in the cores of the lesions and their margins, the presence and distribution of SP and extravascular albumin, an indicator of vasogenic edema. In addition, the tissues were examined to identify injured perivascular SP-containing nerve fibers using amyloid precursor protein (APP) as an indicator of axonal injury.

Our results demonstrated, in all examined rat and human tissue, that perivascular SP-IR was present in astrocytic processes rather than in nerve fibers. Furthermore, no APP-immunoreactive perivascular nerve fibers were observed. This implies that perivascular astrocytic processes might be more

important than perivascular nerve fibers in any effect that SP may have on the blood-brain barrier (BBB) in the settings of infarction and contusion. In addition, the results generally showed, in rat infarcts and contusions, an increase in SP-immunoreactivity (SP-IR) and albumin-immunoreactivity (albumin-IR). This suggests that, in the rat, increased SP in the setting of infarction and contusion might contribute to vasogenic edema. Human tissue, however, showed no increase in SP-IR following infarction or contusion in spite of the presence of albumin-IR. These observations in human tissue might be related to the unavailability of tissue for examination at earlier timepoints post-insult and further investigation is warranted to provide greater detail on any possible involvement of SP with edema in these settings.

Declaration

I certify that this thesis contains no material which has been accepted for the award of any other degree or diploma in any university or other tertiary institute and, to the best of my knowledge and belief, contains no material previously published or written by any other person, except where due reference is made in the text.

I give consent to this copy of my thesis, when deposited in the University Library, being made available in all forms or media, now or hereafter known.

Islam Khamis Hassan

Acknowledgments

This project was begun on a sunny day and was completed on a sunny day. The two years in between saw both sunshine and rain. Much was learned. This project was begun with a smile and was completed with a smile.

There are many people whose time and effort helped see this work through. It has been an honor to work under the seasoned guidance of Professor Peter Blumbergs. Thank you for many hours spent in teaching me to appreciate the individual tunes of cells and the counterpoint of their harmonious interaction. It is a constant inspiration to learn from such a person whose spoken words bear the accuracy of written language.

I also consider myself fortunate to have worked under the supervision of Professor Robert Vink. Thank you for introducing me to experimental research and for your patience in teaching a beginner. I am always impressed by the magical ease with which you swiftly handle the most complicated of issues, both scientific and administrative. It demonstrates a beautiful coordination of wise action and wise patience.

Thank you to Mr. Jim Manavis, such a natural multi-tasker, for sectioning the human tissue used in this study and for teaching me many valuable laboratory techniques. It is a daily pleasure to see such a busy person keep a genuine smile on his face. I am especially grateful for your providing generously and tirelessly of your time to give technical advice, even over the phone on weeknights and weekends!

My deep appreciation goes to Dr. Ghafar Sarvestani for guiding me through the colorful world of confocal microscopy and for your extremely valuable advice and kind support.

Thank you to all the staff members of the Neuropathology Laboratory including Ms. Penny Leaney, Ms. Kathy Cash, Ms. Bernice Gutschmidt and Ms. Kathryn Rodgers, and also to Ms. Margaret Elemer, for always being available to make my life much easier with their technical expertise.

To my fellow students and friends whose company made the long hours bearable, thank you for being there for me. To Renée Turner (with an accent on the 'e', always!) goes all the credit for performing the rat middle cerebral artery occlusion surgery in this study. Beyond this formal recognition, thank you for being the fascinating combination of organization and fun that you are. You are a true team player. Happy days! To Tuyet Tran, thank you for countless dreams and laughs shared over coffee. Your bubbliness is contagious! To James Donkin, a paragon of calm efficiency, your clockwork discipline is an inspiration. And to Emma Thornton, your kind help and friendship are much appreciated.

To Dr. Felicity Johnson, Dr. Zhao Cai, Dr. Corinna Van Den Heuvel and Dr. Grace Scott, thank you for your valuable advice and continuous encouragement.

Finally, for my parents and my not-so-little sister, the thoughts and emotions between us are only for us to share.

Abbreviations

ACE	angiotensin-converting enzyme
APP	amyloid precursor protein
ARDS	adult respiratory distress syndrome
BBB	blood-brain barrier
°C	degree Celsius
CCA	common carotid artery
CGRP	calcitonin gene-related peptide
CNS	central nervous system
COPD	chronic obstructive pulmonary disease
CSF	cerebrospinal fluid
d	day
DAB	diaminobenzidine
DNA	deoxyribonucleic acid
ECA	external carotid artery
EDTA	ethylenediamene tetra-acetic acid
FBS	formal-buffered saline
FITC	fluorescein isothiocyanate
FPI	fluid percussion injury
g	gram
GABA	gamma-aminobutyric acid
GFAP	glial fibrillary acidic protein
H&E	hematoxylin and eosin
HIV	human immunodeficiency virus
hr	hour
ICA	internal carotid artery
ICAM	intercellular adhesion molecule
ICP	intracranial pressure
ID	identification
IHD	ischemic heart disease
IL	interleukin
IMVS	Institute of Medical and Veterinary Science
IR	immunoreactivity
IU	international unit
L	liter
Lt	left
μ	micron
MCA	middle cerebral artery
MCAO	middle cerebral artery occlusion
MHC	major histocompatibility complex
MI	myocardial infarction
min	minute
ml	milliliter
mm	millimeter

mRNA	messenger ribonucleic acid
mw	molecular weight
mW	milliwatt
N/A	not applicable
NA	numerical aperature
NEP	neutral endopeptidase
NH&MRC	National Health and Medical Research Council
NHS	normal horse serum
nm	nanometer
PBS	phosphate-buffered saline
pMCAO	permanent middle cerebral artery occlusion
PNS	peripheral nervous system
PPTA	preprotachykinin A
rMCAO	reperfused middle cerebral artery occlusion
Rt	right
SAH	subarachnoid hemorrhage
sec	second
SP	substance P
SUDEP	sudden unexplained death from epilepsy
TBI	traumatic brain injury
TNF	tumor necrosis factor
TRS	target retrieval solution
UPLAPO	universal positive low APO chromatic

List of Figures

List of Tables

List of Appendices

Chapter 1

INTRODUCTION

Contents

1.1 Cerebral infarction and contusion

1.1.1 Epidemiological significance of stroke and traumatic brain injury (TBI)

Cerebrovascular stroke is a clinical condition characterized by sudden onset of neurological symptoms due to ischemia or hemorrhage. These symptoms can be either focal or global but must, by definition, persist for more than 24 hours. Cerebrovascular disease is the commonest neurological disorder (Frosch *et al.* 2005) with the incidence rates of stroke estimated to be as high as 1 in 250 per year (Dirnagl *et al.* 1999). The incidence rate increases with age to reach 1 in 33 for individuals aged 85 years and above (Kalimo *et al.* 2001). Stroke carries a mortality rate of around 30% which makes it the third commonest cause of death in industrialized countries (Dirnagl *et al.* 1999). As with the incidence, the mortality rate increases dramatically with age; the age-specific death rate is doubled each time the age is increased by only 5 years (Millikan *et al.* 1987). Even for those patients who surivive, long-term disability is common. For example, in the United States about 4 million people are living with its debilitating complications (Taylor *et al.* 1996).

Traumatic brain injury (TBI) is the term used to refer to damage of the brain caused by head injury. TBI has been called, quite appropriately, the silent

epidemic (Goldstein 1990). With estimated annual incidence rates reaching 1 in 400 (Leon-Carrion *et al.* 2005), it is the leading cause of mortality and morbidity in people below 40 years of age (Fleminger & Ponsford 2005). Moreover, it is quite common for survivors to have long-term disabling neurological complications. A large survey conducted on cases of severe head injury in Europe showed that, 6 months after injury, only 31% of the patients had made what was described as a 'good recovery' (Murray *et al.* 1999).

1.1.2 Cerebral infarction

1.1.2.1 Definition

Cerebral infarction is the necrosis of brain tissue due to ischemia. Cerebral ischemia refers to a state in which blood supply to the brain is insufficient to sustain the normal metabolic activities of the cells. The cells in the brain differ in their vulnerability to ischemia. Neurons are the most vulnerable because their metabolism is extremely dependent on oxygen. Thus, ischemia might affect neurons without affecting any other cell type in the brain resulting in a condition known as selective neuronal necrosis. As the degree of ischemia increases, the other cell types in the brain are affected in the following order: oligodendrocytes, astrocytes and finally, being closest to the blood stream, vascular cells. The

irreversible affection of all tissue constituents is referred to as pan-necrosis (Kalimo *et al.* 2002).

1.1.2.2 Progressive damage and the concept of the evolving penumbra

It is important to appreciate that within a single lesion, the degree of ischemic damage observed tends to exhibit both temporal and spatial variation (Dirnagl *et al.* 1999). In terms of the temporal development, ischemic damage has been suggested to evolve at quite a slow pace based upon evidence from both experimental studies (Dereski *et al.* 1993) and studies using magnetic resonance imaging (MRI) in stroke patients (Baird *et al.* 1997). As for the spatial variation of ischemic damage, the pathophysiologic changes involved do not occur homogeneously throughout the entire territory of ischemia. In the center of the ischemic territory, commonly referred to as the core, cells are rapidly killed due to the severe reduction in perfusion (Siesjo *et al.* 1998).

However, between the core and the surrounding unaffected cerebral tissue lies a peripheral rim of tissue named the penumbra (Astrup *et al.* 1981). This is a term borrowed from astronomy where it refers to the halo of partial darkness that surrounds the completely dark central region in an eclipse. In the penumbra, although the blood flow is reduced, it has not decreased beyond the critical level where cellular metabolic activities cannot be sustained (Astrup *et al.* 1981, Hossmann 1994, Obrenovitch 1995). With the passage of time, the penumbra

can either recover if perfusion is restored or otherwise progress to infarction. Several studies provide evidence for the occurrence of the penumbra in human cases of stroke (Furlan *et al.* 1996, Read *et al.* 1998). Hence, acting within this therapeutic window to salvage the penumbra is a main target for neuroprotection.

1.1.2.3 Effects of reperfusion

A phenomenon of important bearing on the outcome of ischemia is reperfusion. Restoration of blood flow to an ischemic territory may occur spontaneously by enzymatic fibrinolysis or through the opening of collateral anastomotic channels or therapeutically by the use of thrombolytic agents or surgical intervention (Wardlaw & Warlow 1992, Wardlaw *et al.* 2000). Although reperfusion of an ischemic territory should logically salvage any affected tissue that has not yet been irreversibly injured, this is often not the case. In addition, in some cases reperfusion might actually contribute to the damage.

i. No- reflow phenomenon

The reason behind the possible failure of reperfusion to salvage the ischemic penumbra is that the restored flow of blood might not gain access to the penumbra. This is termed the no-reflow phenomenon and is primarily encountered in cases of global cerebral ischemia (Ames *et al.* 1968) although it is also believed to occur in focal ischemia. No-reflow occurs due to compromise

of the penumbral microvasculature by the inflammatory process through perivascular edema formation, endothelial swelling and, most importantly, the occlusion of microvessels by neutrophils (del Zoppo *et al.* 1991). This microvascular accumulation of neutrophils is due to their increased recruitment and also due to the upregulated expression of adhesion molecules on both the neutrophils and the microvascular endothelium (Mori *et al.* 1992, Okada *et al.* 1994).

ii. Injury by oxygen-derived free radicals

As for the explanation of how reperfusion might paradoxically increase the damage in the penumbra and cause its recruitment into the core of the infarct, the restored blood flow carries oxygen into the penumbra. Because ischemic cells in the penumbra are metabolically hypoactive, this fresh supply of oxygen may well be in excess of local demand leading to the formation of reactive oxygen species. These highly reactive free radicals cause the peroxidation of lipids, oxidation of structural and functional proteins and alteration in DNA structure (Chan 1994).

iii. Hemorrhagic transformation

Yet another hazard of reperfusion is that it may restore blood flow to necrotic, leaky vessels leading to hemorrhagic transformation of the infarct. These

hemorrhagic infarcts are associated with a more guarded prognosis (Kalimo *et al.* 2002).

1.1.3 Cerebral contusion

1.1.3.1 Definition

Cerebral contusions are among the various pathological changes that may result from blunt head injury. They are localized regions of vascular disruption and parenchymal damage that classically occur at the crests of cerebral gyri and extend to varying depths into the cortical gray matter and possibly into the subcortical white matter as well. Initially, the contusion is restricted to streaks of perivascular hemorrhage perpendicular to the cortical surface. With the passage of time, the blood extends more into the cortical tissue leading to ischemic change of the neurons and subsequent necrosis. The blood occasionally infiltrates the underlying white matter even if initially unaffected. Throughout the acute phase, tissue swelling commonly occurs around the contusion. Later still, the contusion shrinks, assumes a triangular shape with its base towards the cortical surface and acquires a brown color attributed to hemosiderin, which accumulates as a result of breakdown of red blood corpuscles (Graham *et al.* 2002).

1.1.3.2 Progressive damage and the concept of an evolving primary injury

The current understanding of the pathological mechanisms that come into play after brain injury has evolved quite remarkably over the past few decades. In 1975, Peter Reilly and his colleagues published their landmark article 'Patients with head injury who talk and die' (Reilly *et al.* 1975). This paper directed attention toward the concept of secondary injury. In contrast to primary injury, which was regarded as an instantaneous event occurring at the moment of impact as in hematoma formation, secondary injury was thought to involve mechanisms that were not directly related to the physical impact but rather came into play later, such as raised intracranial pressure (ICP) and brain swelling.

Over the following quarter of a century however, there was an accumulation of evidence that modified the previously existing appreciation of the pathophysiology of TBI, which led Reilly to revisit the area with another publication in 2001 (Reilly 2001). In this paper, he described that the understanding of primary injury had evolved from the concept of an isolated event occurring at the precise time of impact that could possibly be followed by secondary damage to the present appreciation of primary injury as an entire sequence of events that was only triggered by the impact and that could continue to develop over the following several days. This cascade of events, if unchecked, could lead to epiphenomena such as cerebral edema, which is a

major cause of brain swelling and increased ICP. The issue of paramount clinical significance is that this sequence of events, as opposed to what was previously thought of the effects of primary injury, is not entirely irreversible. The importance arises from the fact that cerebral edema and increased ICP are extremely significant in adversely affecting the prognosis of patients with head injury. This has naturally stimulated research into the development of pharmacologic agents that can alter the mechanisms of cellular damage before they proceed beyond the limit of reversibility (Doppenberg & Bullock 1997, Bullock *et al.* 1999).

1.2 Vasogenic edema

1.2.1 Edema associated with cerebral infarction and contusion

A pathological event that has an important influence on the pathology of both cerebral infarcts (Klatzo *et al.* 1967) and cerebral contusions (Marmarou *et al.* 2000) is edema. This effect is most pronounced in younger victims of TBI where edema was responsible for 50% of all death and disability (Feickert *et al.* 1999). The term cerebral edema refers to increased water content of the tissue and is a cause of brain swelling (Fishman 1975, Go 1997). Its physical presence around the zone of original injury adds to the mass effect of the entire lesion. A potentially fatal complication of cerebral edema is raised intracranial pressure

(ICP) which, if increased beyond systemic arterial pressure, leads to total cessation of cerebral blood flow. Severely increased ICP is also associated with cerebral herniation and fatal brainstem compression.

In cerebral contusion, within and surrounding the necrotic core, there is commonly a better preserved zone of cerebral edema extending into the white matter. This edema (vasogenic) is caused by increased permeability of the BBB and is best observed from 24 h to about 2 weeks after the injury (Bullock *et al.* 1990, Marmarou 1994). The microvasculature in this zone is affected such that capillaries exhibit increased permeability and arterioles lose their capacity to regulate blood flow (Dietrich *et al.* 1994).

In cerebral infarction, the severity of an ischemic insult appears to influence the degree of edema. More edema formation has been correlated with longer and more severe ischemia (Iannotti & Hoff 1983, Bell *et al.* 1985, Todd *et al.* 1986). Ischemia might also be involved in the cytotoxic edema observed with cerebral contusion (Bullock *et al.* 1991). It is surprising however that in absolute deprivation of blood supply, the progression of edema is halted. Thus, it seems that, for edema to develop, a certain amount of blood flow must be preserved (Iannotti & Hoff 1983, Crockard *et al.* 1980, Kogure *et al.* 1981).

There are two major types of edema that occur in the settings of infarction and contusion: cytotoxic edema and vasogenic edema.

1.2.1.1 Cytotoxic edema

The first type, cytotoxic edema, is an accumulation of water inside the cells, primarily astrocytes, due to excessive movement of water from the extracellular compartment to the intracellular compartment across a functionally-altered cell membrane. However, the total water content of the tissue remains unchanged and therefore, this type of edema does not significantly contribute to brain swelling or the associated delayed deterioration of the clinical condition (Klatzo 1967). Also, the mechanism of cytotoxic edema does not involve an alteration in BBB permeability or structure; an important distinction from the other type of edema, vasogenic edema.

1.2.1.2 Vasogenic edema

Vasogenic edema, is an accumulation of water in the extracellular space due to an altered BBB that allows excessive movement of water from the intravascular compartment to the extravascular compartment. The fluid tends to spread from the gray matter into the white matter in the extracellular space along the nerve tracts and its accumulation can be a major addition to the mass effect of the original causative lesion. It is important to note that the fluid that accumulates in vasogenic edema is rich in plasma proteins. This fact provides some help in the histopathological assessment of the extent of edema using markers for albumin

(Nakata *et al.* 1995). Otherwise, edema appears as vacuolation on routine hematoxylin and eosin staining or as regions of pallor with myelin stains. However, these stains offer a very crude indication of the amount of edema since both the vacuolation and the pallor are not appearances specific to edema and are also associated with several other conditions (Ironside & Pickard 2002).

Research into the mechanism of formation of vasogenic edema, with the ultimate goal of identifying a therapeutic inhibitor of the process, is of paramount importance. This is due to a combination of the adverse effect of edema on patient outcome and the limitations of clinical modalities used to manage these patients. Elevated ICP is potentially fatal and, unfortunately, the currently available protocols for managing raised ICP leave much to be desired in terms of improving patient survival rates and functional outcome. They include pharmacological regimens such as administration of hyperosmotic agents and barbiturates, induction of hyperventilation and hypothermia, and surgical procedures such as drainage of cerebrospinal fluid (CSF) and decompressive craniotomy (Graham *et al.* 2002).

1.2.2 The blood-brain barrier (BBB)

The blood within the cerebral capillaries and proximal venules does not freely communicate with the extracellular fluid in which the cellular elements of the brain are bathed. This separation is brought about by both structural

components and functional mechanisms that are collectively termed the blood-brain barrier (BBB). Pathological opening of the BBB plays a role in the formation of edema. This has been demonstrated in several studies using a rat models of TBI (Barzo *et al.* 1997; Go 1997; Beaumont *et al.* 2000, 2002; Ayata & Ropper 2002).

1.2.2.1 Organization of cerebral vasculature

Blood reaches the brain through two arterial systems: the internal carotid system (formed by a pair of internal carotid arteries and their branches) and the vertebrobasilar system (formed by a pair of vertebral arteries and their branches). The internal carotid system is more or less responsible for supplying the entire cerebrum except for the occipital lobe and the diencephalon. These structures, as well as the cerebellum and brainstem, are all supplied by the vertebrobasilar system. The major arteries of the two arterial systems course through the subarachnoid space. At the base of the brain, these two systems meet to form a ring of arteries known as the circle of Willis. This anastomosis provides alternative routes for blood to reach the brain in the event of occlusion of one of the major arteries.

Before entering into the substance of the brain, these large arteries successively divide giving rise to branches that become progressively smaller. The most distal, smallest branches of the arterial tree on the surface of the brain are known

as the pial arteries. Extensive anastomoses connect the different branches of the arterial tree on the cortical surface which allows another opportunity to redistribute blood across arterial territories in case of occlusion of one of the arteries (Edvinsson & MacKenzie 2002). As these small arteries penetrate the substance of the brain (with some exceptions in the basal ganglia), their elastic laminae disappear and they become arterioles (Standring *et al.* 2005a).

More distally along the course of the arteriole, the smooth muscle cells in the vascular wall disappear and the arteriole becomes a capillary. The capillaries and the immediately distal venules resemble each other structurally in that their walls lack smooth muscle and are formed of a layer of endothelial cells surrounded by occasional pericytes (Edvinsson *et al.* 1983a). On microscopic examination, the two are distinguished solely on the basis of the larger caliber of venules. Venules are relevant to the topic of edema because they are the main part of the microcirculation through which inflammatory exudation occurs. The formation of endothelial gaps in venules is the most common mechanism of inflammatory vascular leakage. This is elicited by several chemical mediators including histamine, bradykinin, leukotrienes and substance P (McDonald *et al.* 1999).

1.2.2.2 Anatomical organization of the BBB

Three cells contribute to its structure: capillary endothelial cells, pericytes and (end feet of) astrocytes (Reese & Kamovsky 1967). The capillary endothelial cells in the brain differ structurally from those in the rest of the body. These structural peculiarities include the presence of tight junctions without fenestrations (thus functioning as an intercellular barrier), the paucity of pinocytotic intracellular vesicles (Reese & Kamovsky 1967) (thus functioning as an intracellular barrier) and the abundance of mitochondria (which indicates high metabolic activity) (Oldendorf *et al.* 1977, Oldendorf *et al.* 1981, Dietrich *et al.* 1984).

The endothelium is ensheathed in a basement membrane that is, in turn, externally covered by the foot processes of nearby astrocytes. The basement membrane intermittently splits into two layers to enclose a pericyte. There is evidence that astrocytes play a role in the function of the BBB (Janzer & Raff 1987, Goldstein 1988, Shivers *et al.* 1988) whereas pericytes are thought to respond primarily when the barrier is disrupted by proliferating to give rise to new endothelial and connective tissue cells (Standring *et al.* 2005b).

1.2.2.3 Physiological control of the BBB

The function of BBB is physiologically modulated by neural (noradrenergic fibers from the locus ceruleus) and hormonal (atrial natriuretic peptide, aldosterone and adrenocorticotropic hormone) mechanisms, as well as by other chemical mediators that include histamine, serotonin, bradykinin, nitric oxide and arachidonic acid derivatives (Easton & Fraser 1998, Mayhan 2000).

1.2.2.4 Pathological opening of the BBB

When excessive water passes from the blood through the BBB into the cerebral tissue, this results in vasogenic cerebral edema. Water can diffuse relatively freely through the BBB along hydrostatic and osmotic gradients, and it is therefore the alteration of these gradients that plays a major role in the formation of vasogenic brain edema. This is thought to occur through changes in the permeability of the BBB to several ions and molecules. Water channels (aquaporins) in the BBB might also have a role in the formation of cerebral edema (Venero *et al.* 2001).

Opening of the BBB may theoretically occur at one or more of the following three sites:

1. interendothelial tight junctions: Experimental models of BBB disruption failed to demonstrate opening of the tight junctions (Rapoport 1976).

2. intracellular vesicles: Certain pathological conditions have been associated with an increase in pinocytotic activity (Westergaard 1975, Beggs & Waggener 1976, Westergaard *et al.* 1977, Povlishock *et al.* 1978, Westergaard *et al.* 1978, Nag *et al.* 1979) but such an increase was only short-lived and was not shown to generate any transendothelial channels.

3. endothelial cell membrane: Disturbance of the membrane is thought to result in activation of several intracellular pathways including the arachidonic acid cascade and synthesis of nitric oxide culminating in the generation of oxygen-derived free radicals which cause BBB damage (Wakai *et al.* 1982, Kontos 1985, Cazaubon & Couraud 1998, Povlishock 1998). Other substances that are produced include inflammatory cytokines (which contribute to vascular leakage and edema) (Schilling & Wahl 1999, Stanimirovic & Satoh 2000) and adhesion molecules which promote the recruitment of leukocytes from the bloodstream into the brain parenchyma and the activation of resident microglia (Abbott 2000).

Thus, although the exact mechanism of BBB opening is unknown, the above discussion suggests that inflammatory mediators might play a role, possibly thorough receptor mediated actions. The following section reviews this role in greater detail.

1.2.3 Inflammation associated with cerebral infarction and contusion

Inflammation is thought to contribute to the death of cells in the penumbral zone in infarction as well as to the delayed effects of primary traumatic injury in contusion. This is supported by data from several studies described below. In both conditions, the adverse effect of inflammation might be due to disruption of the BBB resulting in the accumulation of vasogenic edema.

In infarction, a distinct inflammatory cell reaction is well characterized on histological examination. At 24hr neutrophils are observed to infiltrate the lesion and at 3d the inflammatory infiltrate predominantly consists of macrophages (Kalimo *et al.* 2002). A similar reaction has been demonstrated in contusion (Hulmin *et al.* 1998, Hausmann *et al.* 1999, Engel *et al.* 2000). In lesions aged 24hr, the cellular component of inflammation was represented by margination of neurophils in the vessels. At 3-5d of survival, the inflammatory cell reaction also included monocytes/macrophages and T-lymphocytes, as well as an activation of resident microglia. The inflammatory cell response was paralleled by proliferation of capillaries and swelling of their endothelium and by the formation of perivascular edema (Bullock *et al.* 1991, Vaz *et al.* 1997).

Several studies have also demonstrated an association between inflammation and cerebral edema. In a rat percussive head injury model accumulation of polymorphonuclear leucocytes correlated with the development of post traumatic oedema with an initial phase explained by an increase in blood volume and subsequently followed by an acute inflammatory phase (Schoettle *et al.* 1990). Holmin *et al.* (Holmin *et al.* 1995) used a concussional rat model and found a biphasic pattern of oedema with the secondary peak at 5-7 days, a finding which correlates with the commonly observed clinical deterioration in patients with contusions. Cytokines, in particular interleukin-1 (IL-1) and tumor necrosis factors (TNFs), have been shown in vivo to contribute to intracerebral inflammation, cell death by apoptosis and increased BBB permeability leading to oedema (Holmin & Mathiesen 2000). IL-1 antagonists significantly reduce neuronal damage in rats following traumatic brain injury (Toulmond & Rothwell 1995; Tehranian *et al.* 2002).

1.3 Substance P (SP)

1.3.1 Neuropeptides and inflammation

Two classes of substances are used by neurons for chemical signaling in the nervous system. One category is that of the well-characterized small-molecule neurotransmitters, also known as the classical neurotransmitters, which includes

molecules such as acetylcholine, norepinephrine and glutamate. The other group consists of the neuropeptides which, as the name implies, are simply short polymers of amino acids. One of these neuropeptides, substance P (SP) is the focus of this section.

Neuropeptides have been implicated in the initiation and propagation of the inflammatory response. The constellation of inflammatory effects of neuropeptides is referred to as neurogenic inflammation. Among these effects are an increase in vascular permeability, stimulation of inflammatory cell migration, and several other effects involved in the process of inflammation (Campos & Calixto 2000).

1.3.2 An overview of SP

1.3.2.1 History

SP was the first neuropeptide discovered. It was discovered incidentally by Ulf von Euler and John Gaddum in London around 1930 while they were measuring the concentration of acetylcholine in different tissues (von Euler and Gaddum 1931). The letter P derives from the 'powder' they extracted that contained the active substance. Four decades were to pass, however, before Susan Leeman's team in Boston were able to identify the 11-amino acid structure of the SP molecule (Chang *et al.* 1971).

This enabled them to synthesize the compound (Tregear *et al.* 1971) and set up a radioimmunoassay (Powell *et al.* 1973). Such advances allowed the effects of SP to be tested in physiological models (Henry 1976; Takahashi *et al.* 1974). Also, antibodies could be used to monitor SP with radioimmunoassay and immunohistochemical studies (Takahashi & Otsuka 1975; Hokfelt *et al.* 1975; Nilsson *et al.* 1975; Cuello & Kanazawa., 1978; Ljungdahl *et al.* 1978; Schultzberg *et al.* 1980; Costa *et al.* 1980).

1.3.2.2 Distribution

SP has been demonstrated in neurons of both the central (CNS) and peripheral (PNS) nervous systems. SP is widely distributed in the CNS. SP immunoreactivity has been demonstrated in the rhinencephalon, telencephalon, basal ganglia, hippocampus, amygdala, septal areas, diencephalon, hypothalamus, midbrain, pons, medulla and spinal cord (Shults *et al.* 1984). SP is also present in many components of the PNS. SP immunoreactivity has been observed in trigeminal (Lee *et al.* 1985) and dorsal root ganglia (Gibbins *et al.* 1987), and intrinsic neurons of the gut (Sternini *et al.* 1995). Nerve fibres containing SP-like immunoreactivity are also common in most autonomic ganglia (Helke *et al.* 1982; Helke & Hill 1988; Bergner *et al.* 2000).

Other cell types have been shown to contain SP including astrocytes and microglia (Too *et al.* 1994, Lai *et al.* 2000). In addition, endothelial cells *in vitro* have been stimulated to synthesize SP (Catalan *et al.* 1989).

1.3.2.3 Synthesis and degradation

The formation of the peptide bonds of neuropeptides necessitates that they be synthesized on ribosomes. The mRNA encoding SP is transcribed from the preprotachykinin A (PPTA) gene. The PPTA gene can express four different forms of mRNA through alternative splicing, two of which (the β and γ forms) encode synthesis of both SP and neurokinin A (NKA) (Kotani *et al.* 1986).

As for degradation of SP, the enzymes involved include neutral endopeptidase (NEP) (Matsas *et al.* 1984), SP-degrading enzyme (Probert & Hanley 1987), angiotensin-converting enzyme (ACE) (Skidgel & Erdos 1987), dipeptidyl aminopeptide IV (Heymann & Mentlein 1978), post-proline endopeptidase (Blumberg *et al.* 1980), cathepsin-D (Azaryan & Galoyan 1988). These enzymes cleave SP *in vitro,* however due to their specific cellular localisation it is probably NEP and/or ACE which are commonly involved in the cleavage of SP *in vivo* (Nadel 1991). NEP has been demonstrated to be involved in the metabolism of SP in the brain (Hooper & Turner 1987), spinal cord (Sakurada *et al.* 1990) and peripheral tissues (Di Maria *et al.* 1998) while ACE has been reported to degrade SP in plasma (Wang *et al.* 1991), CSF and substantia nigra contributing in the degradation of fragments released from NEP (Skidgel & Erdos 1987).

1.3.2.4 Receptors

The biological actions of SP are mediated by neurokinin (NK) receptors (Harrison & Geppetti 2001), rhodopsin-like membrane structures, consisting of seven hydrophobic transmembrane domains, connected by extracellular and intracellular loops and coupled to G-proteins (Nakanishi 1991, Maggi & Schwartz 1997). There are three types of mammalian NK receptors that have been cloned: NK1, NK2, NK3 exhibiting preferences for SP, neurokinin A, neurokinin B respectively (Regoli *et al.* 1994). Endogenous tachykinins (the family of neuropeptides to which SP belongs) are not highly selective for any given receptor, and may act on all three receptors with varying affinities under certain conditions such as receptor availability or high peptide concentrations. For this reason SP activates not only NK1 receptors, but also NK2 and NK3 receptors in a number of tissues (Regoli *et al.* 1994). As described later, this review is predominantly concerned with one particular effect of SP: the induction of increased vascular permeability (Maggi 1995). This effect is mainly mediated by the NK1 subclass of receptors which have been demonstrated in endothelial cells (Shimizu *et al.* 1999), cortical nerve cell bodies (Tooney *et al.* 2000), astrocytes (Michel *et al.* 1986, Torrens *et al.* 1986, Kostyk *et al.* 1989, Mantyh *et al.* 1989), microglia (Lai *et al.* 2000), and also acute inflammatory cells such as neutrophils (Kido *et al.* 1999).

1.3.2.5 Functions

SP has been implicated in many biological actions including the transmission of pain signals, regulation of blood pressure, stimulation of secretion by endocrine cells and increasing vascular permeability (Harrison & Geppetti 2001). It also plays a role in memory and reinforcement processes (Hasenohrl *et al.* 2000). In addition, it is widely expressed in areas of the brain associated with fear and defense responses including including the amygdala, septum, hippocampus, hypothalamus and periaqueductal gray (Rupniak & Kramer 1999).

1.3.3 SP in inflammation outside the central nervous system (CNS)

Responses produced at the peripheral level by SP are particularly prominent on the vasculature where it causes plasma protein extravasation in post-capillary venules and leukocyte adhesion to endothelial cells of venules. Additional tissue-specific responses produced by neurogenic inflammatory mechanisms include smooth muscle relaxation/contraction in the urinary bladder, ureter and iris, inotropic and chronotropic effect on the heart and bronchoconstriction in the airways (Geppetti *et al.* 1995).

Studies conducted on spinal afferent nerves suggests that the role of SP is primarily related to the changes in vascular permeability and the edema

associated with neurogenic inflammation (Brain 1997). For example, in the bronchi, activation of sensory neurons leads to increased vascular permeability. This effect was reduced by pretreatment with capsaicin, an agent that causes neuropeptide depletion. The increased vascular permeability was also reduced after treatment with an SP antagonist (Lundberg *et al.* 1983). In addition, SP induced neuroinflammation has been implicated in ischemic injury models. Post ischemic blockade of neurokinin receptors inhibited vascular permeability, neutrophil recruitment, intestinal hemorrhage and neutropenia following ischemia and reperfusion of the superior mesenteric artery in the rat (Souza *et al.* 2002).

1.3.4 SP in inflammation within the CNS

1.3.4.1 SP in perivascular nerve fibers

i. Cerebrovascular innervation

- Distribution of cerebrovascular innervation

Numerous studies over the past three and a half centuries have described the presence of nerve fibers intimately surrounding blood vessels of the cerebral circulation (Willis 1664, Benedikt 1874, Aronson l890, Hassin 1929, Purves 1972, Edvinsson 1975). These perivascular fibers were initially demonstrated around extraparenchymal arteries, and were later shown to invest the pial vessels and

enter with them into the substance of the brain to surround the intracortical arterioles and veins (Penfield 1932). The number of fibers innervating a given vessel was observed to correlate with the diameter of the vessel regardless of which lobe of the brain it was located in (Humphreys 1939).

- Pathways of cerebrovascular innervation

Extensive research has been carried out to trace the course of these perivascular nerves from the origins of their pathways in the central nervous system. This has led to the distinction of two classes of perivascular nerves depending on the course they run after their origin from the CNS (Goadsby & Edvinsson 2002). One class, known collectively as the extrinsic system, comprises neural pathways that arise in the CNS and then emerge from the CNS to course in peripheral nerves before returning to the brain to innervate its blood vessels. Thus, these pathways physically arise and terminate in the CNS but, in the intermediate portion of their course, run for some distance in the peripheral nervous system. Fibers of this extrinsic system can be further classified into somatic, sympathetic and parasympathetic fibers (Atalay *et al.* 2002). The other class of cerebral perivascular nerves, which form the intrinsic system, remain within the CNS throughout the entire length of their course from their origin to their termination.

1. Intrinsic system

Fibers of this intrinsic system are subdivided according to their site of origin in the CNS which can be in either the medulla (dorsal medullary reticular formation (Reis 1982) and rostroventrolateral medulla (Underwood 1992), pons (locus ceruleus (Raichle *et al.* 1976) and parabrachial nuclei (Mraovitch *et al.* 1985), midbrain (dorsal raphe nucleus (Edvinsson *et al.* 1983b)), cerebellum (fastigial nucleus (Nakai *et al.* 1983)) or forebrain (basal forebrain (Arneric 1989) and centromedian parafascicular thalamus (Mraovitch *et al.* 1986)).

2. Extrinsic system

a. Sympathetic nerves

The origin of the postganglionic fibers has been traced to the superior cervical sympathetic ganglion (Purves 1972). These fibers are the main source of noradrenergic innervation only to the extraparenchymal cerebral vessels whereas the noradrenergic fibers that supply the intraparenchymal vessels are believed to arise mainly from the locus ceruleus in the pons (part of the intrinsic system) (Cohen *et al.* 1997).

As for its functional role, the sympathetic innervation is vasoconstrictor to cerebral arteries and arterioles (Auer *et al.* 1981, Busija *et al.* 1985) and is thought to play a role in the autoregulation of cerebral blood flow (Bill & Linder 1976, Edvinsson *et al.* 1976, Edvinsson *et al.* 1985, Goadsby & Edvinsson 1993).

b. Parasympathetic nerves

This pathway has been demonstrated to arise from the superior salivatory nucleus, which is the parasympathetic nucleus of the facial nerve, in the pons (Chorobski & Penfield 1932). The preganglionic fibers run mainly in the greater superficial petrosal nerve (a branch of the facial nerve) and relay in the sphenopalatine and otic ganglia from which the postganglionic fibers emerge to supply the cerebral vessels (Walters *et al.* 1986).

Concerning its function, although the parasympathetic system has been shown experimentally to mediate a strong vasodilator effect on the cerebral vasculature, it does not seem to play a role in the autoregulation of cerebral blood flow (Forbes *et al.* 1937, Linder 1981). Thus, it does not take part in increasing local blood flow in response to changes in perfusion pressure or in response to hypoxia or hypercapnia (Hoff *et al.* 1977). Rather, this system might be significant

in the emergency reaction of the cerebral circulation to hazards such as ischemia (Goadsby *et al.* 1991). This is concordant with the fact that its vasodilatory effect produces an increase in blood flow that is unrelated to metabolic demand (Goadsby 1989).

c. Somatic nerves

The somatic component of the extrinsic system is entirely conducted through fibers of the trigeminal nerve. Thus, it is commonly referred to as the trigeminovascular system. It is this component of the cerebrovascular innervation that contains SP. The trigeminovascular system is described in greater detail in the following section.

ii. The trigeminovascular system

- *Anatomical pathway and released neurotransmitters*

The fibers of the trigeminovascular system are, in strict anatomical classification, afferent fibers. This means that these nerves should theoretically conduct nerve impulses from their peripheral terminal endings towards the CNS, and indeed they have been shown to transmit pain sensation from the dura mater and cranial vessels (Hüber 1899, Penfield 1932, Penfield 1934, Penfield & McNaughton 1940, Feindel *et al.* 1960). Therefore, it is somewhat of a peculiarity that the

peripheral endings of these fibers release transmitter molecules that are initially transported from the nerve cell body along the axon in a direction opposite to that of nerve signal conduction. The first order neurons of this pathway are bipolar neurons. The peripheral process of the neuron can be traced back from its endings (around cerebral vessels) traveling through the ophthalmic division of the trigeminal nerve to the cell body located in the trigeminal ganglion (Mayberg *et al.* 1981, Liu-Chen *et al.* 1983a, Liu-Chen *et al.* 1983b, Mayberg *et al.* 1984). From the cell body, the central process of the neuron passes to the ipsilateral spinal nucleus of the trigeminal nerve (located mostly in the medulla oblongata) where it synapses with the cell body of the second order neuron (Goadsby & Hoskin 1997). Axons of second order neurons leave the spinal nucleus, cross to the opposite side and ascend as part of the trigeminal lemniscus to relay in the posteromedial ventral nucleus of the thalamus. From here, third order neurons proceed to the sensory area in the postcentral gyrus of the cerebral cortex. This pathway applies to all trigeminovascular innervation with the exception of the innervation of the vessels caudal to the circle of Willis (Arbab *et al.* 1983). In these latter pathways, the first order neurons have their cell bodies in the dorsal root ganglia of the upper cervical spinal nerves. Nevertheless, the central processes of these neurons still relay in the spinal trigeminal nucleus and, from there onwards, this pathway joins the general trigeminovascular pathway to the cerebral cortex.

The perivascular endings of trigeminovascular fibers contain several neurotransmitters including SP (Edvinsson *et al.* 1989) as well as another neuropeptide that has been implicated in the inflammatory process: calcitonin gene-related peptide (CGRP) (Uddman *et al.* 1985, McCulloch *et al.* 1986). CGRP is briefly reviewed later in this section.

- *Functional significance*

Two types of studies have helped clarify the functional significance of the trigeminovascular system: lesioning studies and stimulation studies.

Lesioning studies

Lesioning of the trigeminal ganglion has no effect on resting cerebrovascular caliber (Edvinsson *et al.* 1986) nor does it impair the normal responsiveness of the cerebral circulation to stimuli such as hypercapnia (Moskowitz *et al.* 1988). However, the trigeminovascular system has been shown to mediate an important protective mechanism known as the trigeminovascular reflex (Edvinsson *et al.* 1986, McCulloch *et al.* 1986). This reflex involves the rapid restoration of normal vascular caliber within 1-2min following vasoconstriction such as occurs in the setting of subarachnoid hemorrhage (Edvinsson *et al.* 1990, Juul *et al.*

1990). Among the trigeminovascular transmitters, CGRP was identified as the major mediator of this reflex.

Stimulation studies

Experimental stimulation of the trigeminal ganglion produced vasodilation of both intracranial vessels (accompanied by increased cerebral blood flow) and extracranial vessels of the head (accompanied by cutaneous flushing, increased skin temperature and capillary pulsation) (Oka 1950, Sweet & Wepsic 1974, Onofrio 1975, Drummond *et al.* 1983). The cutaneous effects of trigeminal ganglion stimulation were accompanied by an increased level of the trigeminovascular transmitters SP and CGRP in blood from the ipsilateral external jugular vein but not in the peripheral circulation (Goadsby *et al.* 1988). It is worth noting that, in the cat, unilateral trigeminal ganglion stimulation increased blood flow bilaterally in the frontal and parietal cortical gray matter but not in the occipital cortex nor in the white matter, deep cerebral nuclei or brainstem. Surprisingly, these changes were demonstrated to be entirely mediated by the facial nerve, the sectioning of which totally abolished the effect of trigeminal ganglion stimulation on cortical blood flow (Goadsby & Duckworth 1987). The involvement of the facial nerve gives rise to an interesting issue which is discussed in the following paragraph.

Distinction between orthodromic and antidromic effects

When examining the effect of stimulation of the trigeminovascular system, an important distinction should be made. This is because the resultant vascular response might not only be due to direct release of transmitters from the peripheral endings of the trigeminal fibers, but they might also be a result of traveling of the nerve impulse through the trigeminal pathway in the afferent direction towards the CNS. These afferent trigeminal fibers represent the afferent limb of a reflex whose efferent limb returns to the cerebral circulation through the parasympathetic facial nerve fibers described earlier (Hoff *et al.* 1977). Thus, experimental stimulation of the trigeminal ganglion results in vascular effects that are due to:

1. conduction of nerve impulses along the central processes of the bipolar neurons in the normal afferent direction (orthodromic effect) subsequently activating the parasympathetic efferent fibers; and also due to
2. release of transmitters from the terminal endings of the peripheral processes of the bipolar neurons which is opposite to the direction of conduction of afferent nerve impulses along the fibers (antidromic effect).

In experiments that stimulated the trigeminal ganglion, distinguishing between the orthodromic and antidromic vascular effects was achieved by abolishing the orthodromic pathway. This was through sectioning the trigeminal root (afferent part of the reflex) or sectioning the greater superficial petrosal branch of the facial nerve (efferent part of the reflex). After this procedure, the effect of trigeminal ganglion stimulation was diminished to 20% of normal. This suggests that antidromic release of trigeminovascular transmitters is responsible for a portion of the vasodilatory response at least in the extracranial vessels. Experimental data from both animals and humans points towards CGRP as the main mediator of this vasodilation (Jansen *et al.* 1990, Edvinsson *et al.* 1995, Jansen-Olesen *et al.* 1996).

iii. The neuropeptide calcitonin gene-related peptide (CGRP)

CGRP is a 37 amino acid neuropeptide that was first identified in 1982 by Amara and co-workers (Amara *et al.* 1982). It derives its name from the fact that it is synthesized by alternative splicing from the primary transcript of same gene that encodes the hormone calcitonin (McCulloch *et al.* 1986, Jansen-Olesen *et al.* 1996).

CGRP is widely distributed in the nervous system. Nerve cell bodies and nerve fibers were demonstrated to contain CGRP in the trigeminal and dorsal root

ganglia (Uddman *et al.* 1986). With regard to the cerebrovascular innervation, CGRP is located in trigeminovascular nerve fibers associated with the arterial side of the circulation. This was shown in the anterior, middle and posterior cerebral arteries, the vertebral and basilar arteries, and also the pial and meningeal arterioles (Edvinsson *et al.* 1987, McCulloch *et al.* 1986, Moreno *et al.* 2002).

The actions of CGRP are mediated by binding to specific receptors that are present in many tissues including the brain (Aiyar *et al.* 1994, Wimalawansa & El-Kholy 1993). These receptors have been classified *in vitro* based on their varying affinities for peptide antagonists. However, the reliability of these classifications has been challenged due to the artificial settings of the experiments (Waugh *et al.* 1999). Molecular biology techniques suggest that the proper function of CGRP receptors requires the co-expression of three membrane protein complexes but the relationship of these molecules is not fully understood (Luebke *et al.* 1996, Chu *et al.* 2001, Moreno *et al.* 2002).

The biological actions of CGRP include inhibition of gastric secretion, increasing heart rate and the modulation of blood pressure and body temperature (Dennis *et al.* 1990, Aiyar *et al.* 1994). Its most significant action on the cerebral vasculature, however, as a result of its release from trigeminovascular nerve fibers, is vasodilation (Doods *et al.* 2000).

- Distinction between roles of CGRP and SP in neurogenic inflammation

The vascular action of CGRP differs from that of SP in several respects. Rather than acting on the endothelium, CGRP exerts its vasodilatory action through an effect on vascular smooth muscle (Sams *et al.* 2000). This concords with the facts that CGRP-immunoreactive perivascular nerve fibers are located in the vascular adventita and adventitial-medial border (McCulloch *et al.* 1986, Jansen-Olesen *et al.* 1996). Another contrast with SP is that CGRP does not dilate the venous side of the cerebral circulation (Edvinsson *et al.* 1986).

Research on spinal afferent nerves suggests that the vasodilation component of neurogenic inflammation is mediated mainly by CGRP while the role of SP is primarily related to the changes in vascular permeability and the edema associated with neurogenic inflammation (Brain 1997). The situation might be similar in the case of trigminovascular fibers, where vasodilation also appears to be largely due to CGRP (Edvinsson *et al.* 1982, Mejia *et al.* 1988, Stubbs *et al.* 1992, Edvinsson *et al.* 1995, Escott *et al.* 1995). Thus, in cerebral infarction and contusion, SP might be involved in the alteration of BBB permeability and the formation of cerebral edema while CGRP might not play a role in these processes.

iv. SP in cerebral ischemia and TBI

The evidence above points towards the potential significance of SP as a modulator of the inflammatory reaction in the brain (Catalan *et al.* 1989, Kennedy *et al.* 1997, 2003). This is especially relevant in the setting of ischemic brain injury (Stumm *et al.* 2001, Yu *et al.* 1997) and traumatic brain injury (Nimmo *et al.* 2004). This section reviews the few studies that have been conducted to date in this area.

- Cerebral ischemia

As mentioned earlier, SP-induced inflammation has been implicated in models of ischemic injury outside the CNS (Souza *et al.* 2002). In a rat model of cerebral ischemia, the use of an NK1 receptor antagonist reduced infarct volume after focal ischaemia (Yu *et al.* 1997). This suggested a role for SP in exacerbating ischemic damage. However, despite this positive finding, no similar studies have since been published in this area. Another study demonstrated increased SP immunoreactivity in gamma-aminobutyric acidergic (GABAergic) interneurons around regions of infarction and transient expression of SP immunoreactivity in cerebrovenular endothelium (Stumm *et al.* 2001). More recently, in human cases of both transient ischemic attack and completed stroke, serum levels of SP were found to be significantly elevated compared to controls (Bruno *et al.* 2003). The results of these studies collectively suggest that SP is involved in the progressive damage associated with the pathology of cerebral ischemia. Further

investigation is warranted in order to provide a better understanding of the exact role of SP and to explore possible targets of pharmacological intervention.

- *TBI*

Several published studies have investigated the role of classical inflammation in the formation of edema associated with TBI (Stahel *et al.* 1998, Lenzlinger *et al.* 2001, Besson *et al.* 2005). However, only one published study to date has examined the role of neurogenic inflammation in the setting of TBI (Nimmo *et al.* 2004). This study showed that the administration of capsaicin before TBI, which depletes the neuropeptide content of trigeminovascular fibers, significantly reduced edema formation and the development of motor and cognitive deficits. Yet, although this study demonstrated a role for neuropeptides in cerebral edema associated with TBI, it did not identify the particular neuropeptide responsible for this role. Unpublished work in our laboratory (Vink 2006) has recently demonstrated an almost complete resolution of edema in a rat model of TBI following the administration of an NK1 receptor antagonist. This implies that, among the many vasoactive mediators of inflammation, SP might play a central role in the production of edema in TBI. Further work is required to characterize the exact involvement of SP and to explore any potential therapeutic strategies.

1.3.4.2 SP in other cells

Apart from nerve fibers, several other cell types have been implicated in SP-mediated inflammation such as endothelial cells, astrocytes and microglia.

In addition to expressing the NK1 receptor, endothelial cells contain and release SP itself (Linnik & Moskowitz 1989, Gorelova *et al.* 1996, Cioni *et al.* 1998). Thus, the endothelial cells may have a capacity for autocrine stimulation (Brain 1997, Catalan *et al.* 1989, Annunziata *et al.* 1998, Stumm *et al.* 2001). *In vitro* studies have shown that inflammatory mediators such as the cytokines interleukin-1β (IL-1β) and tumor necrosis factor-α (TNFα) induce endothelial cells cultured from the rat brain to release SP (Catalan *et al.* 1989). Another stimulus, human immunodeficiency virus-1 (HIV-1) envelope protein gp120, not only induced the cultured cells to release SP, but also increased their permeability to albumin. This effect on permeability appeared to be SP-mediated because it was abolished by a SP antagonist and by SP antibodies (Annunziata *et al.* 1998). More recently, *in vitro* studies on endothelium stimulation have demonstrated that SP released from the cerebral endothelium mediated an increase in BBB permeability, an upregulation of major histocompatibility complex-II (MHC-II) molecules and an increased expression of intercellular adhesion molecule-1 (ICAM-1). Furthermore, SP antagonists neutralized all these inflammatory effects and also prevented the associated changes in cellular morphology (Annunziata *et al.* 2002).

Experimental evidence shows that SP can also be synthesized by astrocytes (Too *et al.* 1994) and microglia (Lai *et al.* 2000). Inasmuch as these two cell types can also express NK1 receptors, they might be involved in a local autocrine and paracrine loops as well. Indeed, *in vitro* studies demonstrated that SP stimulated astrocytes to produce IL-1 (Martin *et al.* 1992) and stimulated macrophages to produce IL-12 (Kincy-Cain & Bost 1997).

1.4 Hypothesis and aims

Hypothesis

Substance P (SP) plays a role in the cerebral edema associated with cerebral infarction and contusion and damage to SP-containing perivascular nerve fibers is involved in this process.

Aims

- For each of four groups (rat infarcts, rat contusions, human infarcts and human contusions) the core and margin of the lesion will be examined at several timepoints to:

1. Characterize and correlate SP-immunoreactivity (SP-IR) and albumin-IR using extravascular albumin-IR as a marker for vasogenic edema.
2. Identify damaged perivascular SP nerve fibers using SP-IR and amyloid precursor protein (APP) immunohistochemistry as a marker for damaged axons.

- To identify any differences and/or similarities that may exist between contusions and infarcts and between human and animal tissue as determined by addressing the previously mentioned aims.

Chapter 2

METHODOLOGY

Contents

2.1 Rat pathological models

Two experimental models were used in this study: the rat model of middle cerebral artery occlusion (MCAO) and the rat model of lateral fluid percussion injury (FPI).

2.1.1 Animals used and ethics approval

All animal experiments in this project were performed within the guidelines of the National Health and Medical Research Council (NH&MRC) and were approved by the animal ethics committees of the University of Adelaide and the Institute of Medical and Veterinary Science (39/04 and 37/04). Adult male Sprague-Dawley rats (weighing 265-295g for MCAO and 400-500g for FPI) were used. The animals were group-housed in a conventional rodent room on a 12h day-night cycle and provided with a standard diet of rodent pellets and water *ad libitum*. A summary of the experimental animals used in each model is provided in tables 2.1 and 2.2.

Table 2.1: Animals used in MCAO model

Group	Post-occlusior survival time	Number of animals
pMCAO	5h	1
	7h	1
	24h	2
	26h	1
rMCAO	2+5h	4
	2+24h	3
Sham	N/A	4
Naive	N/A	4

N/A: not applicable; pMCAO: permanent middle cerebral artery occlusion; rMCAO: reperfused middle cerebral artery occlusion

Table 2.2: Animals used in FPI model

Group	Post-injury survival time	Number of animals
FPI	30 min	3
	5h	3
	1d	3
	2d	1
	3d	1
Sham	N/A	4
Naive	N/A	4

N/A: not applicable; FPI: fluid percussion injury

2.1.2 Description of the models

2.1.2.1 Middle cerebral artery occlusion model

i. Selection of the model

This rat model of focal cerebral ischemia (Zea Longa *et al.* 1989) was chosen because it allows the production of both reperfused and non-reperfused lesions in the territory of the middle cerebral artery (MCA). Producing lesions in this particular part of the brain allowed for a direct comparison with tissue obtained from the rat model of lateral fluid percussion injury, described later in this section, which produces a contusion in the same anatomical region of the rat brain. Furthermore, these two models allowed for a direct comparison with the human infarct and contusion tissue used in this study which was generally situated, as described later in this section, in the human MCA territory. This is an advantage of using rat tissue because the anatomical distribution of the MCA in rats is analogous to that in humans (Coyle 1975).

ii. Basic principle

The basic principle of the procedure is blocking blood flow into the MCA by occluding the lumen of the artery at its origin from the internal carotid artery (ICA). The lumen is blocked using a 4-0 intraluminal nylon suture that is introduced into the ICA in the neck and advanced distally through its lumen to

occlude the origin of the MCA. In addition, collateral blood flow to the MCA territory is reduced by ligation or cautery of all branches of the external carotid artery (ECA) and all extracranial branches of the ICA.

iii. Procedure

- Preparation of nylon sutures

Nylon monofilament sutures (4-0 Nylon, Dynek #405) were straightened by mild heating using an electrocautery unit. The tip of each straightened suture was rounded in a flame. Then, the sutures were coated with poly-L-lysine (Sigma; mw = 70 000-150 000; 1mg/mL) and dried at 60°C for 1 hr.

- Pre-operative care and anesthesia

Each animal to be operated on was fasted the night before the operation and then, during the next 12hr light cycle, removed from the rodent room and placed in an anesthesia induction box. General anesthesia was induced by inhalation of 3% Halothane (1.5L/min oxygen). An endotracheal tube (Norton, USA) was then inserted using direct laryngoscopy and position was confirmed by equal bilateral chest expansion. Mechanical ventilation (95-100 breaths/min, tidal volume 2ml) was initiated using a Harvard rodent ventilator. 1.5-2% Halothane was used to maintain anesthesia (1L/min oxygen ratio). As soon as the paw reflex elicited no response, the animal was placed in the

supine position on a heating pad (37°C). The neck was shaved using electric clippers and 70% alcohol was used to swab the area.

- *Surgical procedure for occluding the MCA*

Under the operating microscope, an incision was made in the neck to the left of the midline. Blunt dissection of the superficial connective tissue and retraction of the muscles exposed the common carotid artery (CCA) at the level of its bifurcation into the ECA and ICA. The branches of the ECA were cauterized – reducing the ECA to a stump – and the pterygopalatine artery, an extracranial branch of the ICA, was ligated. An arterial clamp was then placed on the CCA and an incision was made in the ECA stump to insert the nylon suture. The ECA stump was mobilized such that it no longer formed an angle with the ICA and such that both vessels formed a straight line passing through the carotid bifurcation. The tip of the previously prepared nylon suture was then advanced through the ECA into the ICA. The tip was advanced further into the ICA to a distance of 17mm from the origin of the ECA (marked on the thread with Papermate liquid paper) or until resistance was encountered. This indicated that the suture had occluded the origin of the MCA. The suture was then held in place by ligation of the ECA and removal of the arterial clamp. A length of nylon suture was left protruding from the stump of the ECA so that it could be withdrawn at later timepoint to allow reperfusion if desired. Finally, Lignocaine was applied to the field and the surgical wound was closed using wound clips (9mm Autoclip wound clips, Becton Dickinson).

- *Sham procedure*

The same procedure as described above was performed on sham animals with the exception of advancing the thread into the ICA.

- *Post-operative care and monitoring*

The animal was weaned off mechanical ventilation and left on the heating pad till recovery from anesthesia. Before full recovery from anesthesia, the animal was injected with saline (5ml subcutaneously) to prevent post-stroke dehydration. Once awake, the animal was moved to the cooling box. The animal was then monitored for an increase in temperature and for clockwise circling (as a sign of right hemiparesis) which both typically occur with this model. From this stage onwards, the protocol differed according to which group of study the animal belonged to. The procedure for animals belonging to the reperfused MCAO (rMCAO) is discussed in the next paragraph. Each animal in the permanent MCAO (pMCAO) group was left for the specified post-occlusion survival time without further surgery and provided with rodent pellets and water *ad libitum*. For animals in both the pMCAO and rMCAO groups, several post-occlusion survival times were chosen – as detailed in table 2.1 – to allow comparative histological analysis of neuropeptide expression and edema at various timepoints following arterial occlusion.

- Surgical procedure for reversing the MCA occlusion

Each animal belonging to the reperfused MCAO (rMCAO) group was once again anesthetized as detailed above within the second hour post-occlusion. The wound was re-opened by removing the wound clips and the carotid arteries were exposed as described earlier. At exactly 2h post-occlusion, reperfusion was initiated by withdrawing the nylon suture from the MCA into the ICA. As described above, the wound was then closed and the animal was allowed to recover from anesthesia upon which it was returned to the cooling box.

2.1.2.2 Lateral fluid percussion injury model

i. Selection of the model

This rat model of lateral fluid percussion injury (FPI) (McIntosh *et al.* 1989) was chosen because it produces a focal lesion large enough to be differentiated into several pathological zones on histological examination. In addition, the resulting lesion occurs in the MCA territory which provided a common anatomical background against which the pathological changes could be compared with those resulting from the previously described rat model of MCAO. Also, the use of this model allowed for a more direct comparison with the human pathological tissue used in this study which was generally situated, as described later in this section, in the human MCA territory.

ii. Basic principle

The basic principle of this model is to generate a reproducible localized contusion on the surface of the cerebrum by applying a constant force onto a constant surface area of cerebral tissue. This is achieved by injecting a given volume of saline under a constant pressure onto a given area of dura mater. The area of dura mater is defined by the area of overlying skull bone that is removed to expose it.

iii. Fluid percussion injury device

A device specifically designed (Biomedical Engineering, University of Virginia, USA) for inducing this injury was used. As shown in figure 2.1, the device consisted of a pendulum, a horizontal fluid column and a distal outflow nozzle. The horizontal column was completely filled with normal saline and it was ensured before every usage that there were no air bubbles in the fluid. When the pendulum is released, it swings down (from an adjustable preset height) under the effect of gravity to strike the piston at the proximal end of the horizontal fluid column. The pressure of the impact is transmitted through the horizontal fluid column such that a certain amount of saline is driven out of the distal outflow nozzle. The saline is forced directly onto the exposed dura mater of the rat.

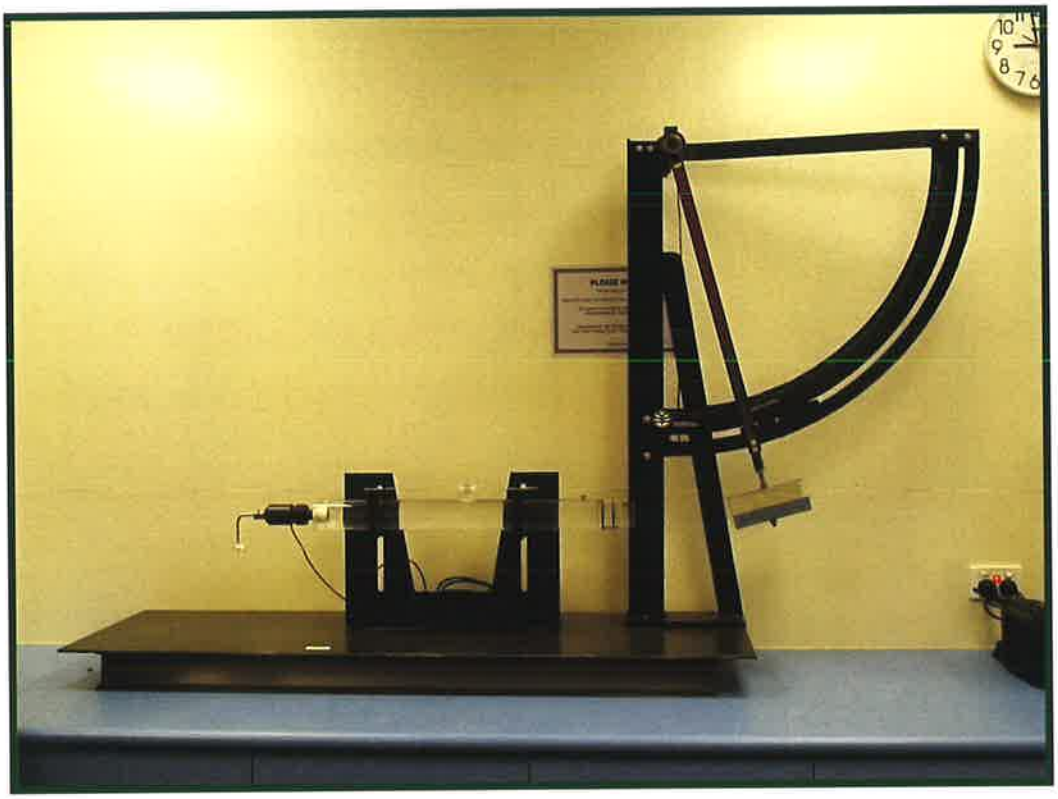

Figure 2.1: Fluid percussion injury device

iv. Procedure

- Pre-operative care and anesthesia

The steps of this procedure are depicted in figure 2.2. Each animal was taken from the rodent room and general anesthesia was induced as described with the MCAO model. As soon as the paw reflex was lost, the animal was removed from the induction box and placed prone on a 37°C heat pad. Halothane anesthesia was promptly maintained using a nose cone without endotracheal intubation or mechanical ventilation. The scalp was shaved and local anesthesia was induced in this area by infiltrating 0.5 ml of Lignocaine.

- Surgical procedure for craniotomy

A midline incision was made in the scalp and the edges were retracted to expose the sagittal, coronal and lambdoid sutures of the skull. At a point exactly midway between the coronal and lambdoid sutures and 2mm to the left of the sagittal suture, a bur hole (5mm diameter) was drilled using an electric high-speed microdrill (Fine Science Tools Inc., Vancouver, Ca.) with a 5mm craniotomy drill bit (Fine Science Tools Inc., Vancouver, Ca.). Care was taken during drilling in order to expose the dura mater without breaching it.

- Sham procedure

The sham animals underwent the same details of the craniotomy procedure. However, upon exposure of the dura mater, the scalp wound was immediately closed using surgical wound clips.

- *Connection of the animal to the FPI device*

After exposing the dura, each of the animals to be injured underwent the following procedures. A plastic Luer-Loc connector (5mm diameter) was then fitted snugly onto the edges of the bur hole using cyanoacrylate adhesive and fixed in position using quick drying dental cement (Glass Ionomer Luting Cement, 3M ESPE Ketac Cem μ, Seefeld, Ge.). Once the dental cement was dry, normal saline was instilled into the Luer-Loc such that it contained no air bubbles. The animal was then disconnected from the nose cone and the Luer-Loc was connected to the distal outflow nozzle of the fluid percussion device.

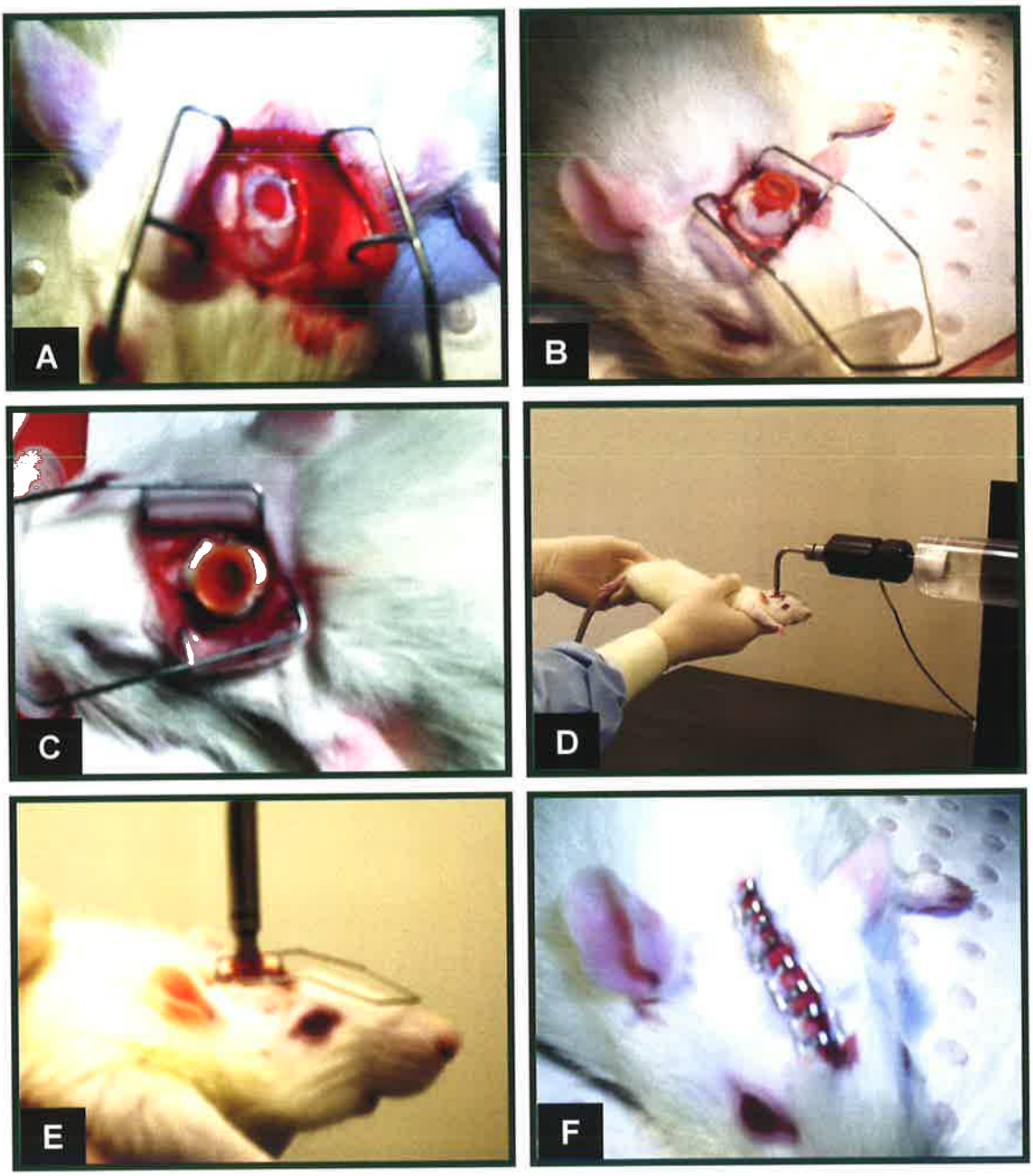

Figure 2.2: Steps of the lateral fluid percussion injury procedure

- *Delivery of the impact*

The device was tested immediately before each usage to ensure that it would function properly when the rat was connected. The impact was delivered by means of releasing the pendulum, which had been preset to exert a pressure of 2.7 atmospheres.

- *Post-operative care and monitoring*

Immediately following the impact, the animal was returned to the heating pad and examined to detect the cessation of spontaneous ventilatory effort. The occurrence of apnea was typical following the impact and resuscitation was performed using a manual pump connected to the nose of the rat. When spontaneous ventilation resumed, the Luer-Loc connector was detached from the skull and the scalp wound was closed with surgical wound clips (9mm Autoclip wound clips, Becton Dickinson). The animal was left on the heating pad until it recovered from anesthesia. The animal was subsequently monitored for right hemiparesis as manifested by clockwise circling. After the impact, the injured animals were isolated from the uninjured animals, returned to conventional rodent room housing on a 12hr day-night cycle and provided with rodent pellets and water *ad libitum*. Each injured animal was subsequently sacrificed after the specified post-injury survival time. As detailed in table 2.2, several post-injury survival times were chosen to allow comparative histological analysis of neuropeptide expression and edema at various timepoints following the injury.

2.1.3 Brain fixation and extraction

At the time of sacrifice, each animal was anesthetized with halothane as previously described and the anesthesia was maintained via a nose cone. The animal was placed in the supine position and a transverse incision was made in the upper abdomen to expose the undersurface of the diaphragm. This was followed by an incision in the diaphragm to expose the thoracic cavity and allow rapid access to the heart. A blunt 9-gauge needle was inserted into the ascending aorta and the right atrium was incised. Through the needle, the animal was given 5000 IU/mL of heparin and then transcardial perfusion of 10% formal-buffered saline (FBS) was commenced. After perfusion, decapitation and extraction of the brain from the skull were delayed by 1 hour to allow the brain to become firmer and thus make its extraction easier. Following extraction, the brain was kept in 10% FBS for 7 days before being processed for histological examination.

2.1.4 Tissue processing

Following fixation, the whole brain was placed into the concavity of a rat brain blocker (PA 00145 0-600gm type, David Kopf Instruments, Tujunga, California, USA). Razor blades were used to coronally section serial tissue blocks at 2mm intervals from the rostral to the caudal end of the brain. Each block was placed in a tissue cassette labeled to indicate the position of the block and was impregnated with wax overnight. This standardized procedure allowed the precise identification of anatomical location in any section from any rat using a

stereotactic rat brain atlas (Paxinos *et al.* 1998). Furthermore, the accumulation of these standardized tissue blocks has formed a rat 'brain bank' from which more tissue can be taken for future studies. Following overnight processing, each block was embedded in paraffin wax and sectioned, using the rotary microtome, into serial sections, each 5μ thick, as required for staining.

2.1.5 Staining methods: hematoxylin and eosin (H&E) and immunohistochemistry

1. Each tissue section was stained with hematoxylin and eosin (H&E) and stained immunohistochemically for SP, albumin, APP, NK1 and CGRP. In addition, for examination with laser scanning confocal microscopy, selected tissue was immunostained for glial fibrillary acidic protein (GFAP). Staining for the neuropeptides SP and CGRP was intended to characterize their relationship with cerebral edema. This was assisted by staining for the SP receptor, NK1. Staining for the CGRP receptor was not possible due to the unavailability – at the time of conducting the experiment – of a specific antibody that could be applied to formalin-fixed paraffin-embedded tissue. Staining for extravascular albumin is well-established as a marker of edema in studies of the BBB (Nakata *et al.* 1995). Immunostaining for APP is a sensitive method for detecting axoplasmic flow impairment (Blumbergs *et al.* 1995) and was used to identify injured perivascular nerve fibers. GFAP is well-established marker for astrocytes (Eng *et al.* 2000). Routine H&E staining was used to identify general cellular pathology and provide a frame of reference

against which the observations from the other staining methods could be assessed.

Details of the procedures for H&E staining and immunohistochemical staining as well as details of the primary antibodies and fluorophores used are indicated in appendices 1 and 2. To avoid the confounding effect of technique-dependent variability in immunostaining, all tissues to be compared were stained in the one session. As a standard procedure, each session of staining included – for each antibody – standard control tissue of known IR that was processed with and without the primary antibody to serve as a positive and negative control respectively.

2.1.6 Tissue selection and microscopic analysis

Regions of particular interest in brains were the cortex and subcortical white matter in the MCA territory. As previously described, this was the location of the lesions produced by both the MCAO model and FPI model. This allowed for comparative analysis of both pathologies against a common anatomical background. This also allowed for a more direct comparison with the human pathological tissue used in this study which was generally situated, as described later in this section, in the human MCA territory. All tissue was examined under a light microscope with a camera attachment (Olympus DP-12, Japan). Selected tissue was examined using a laser scanning confocal microscope (BioRad Microscience Ltd., UK) equipped with three lasers, Argon ion 488nm (14mW);

Green HeNe 543nm (1.5mW); Red Diode 637nm (5mW) outputs and Olympus IX70 inverted microscope. The objective used was a 10-60x universal positive low APO chromatic (UPLAPO) with numerical aperture (NA)=1.4 oil. Images were analyzed using Confocal Assistant software (Todd Clark Brelje, USA).

2.2 Human pathological tissue

2.2.1 Case selection

2.2.1.1 Pathological tissue

Post mortem tissue was selected from the archives of the Institute of Medical and Veterinary Science (IMVS), Adelaide, South Australia. The material was obtained from cases of fatal cerebral infarction (n=9) and cerebral contusion (n=8). An effort was made to select lesions that involved the MCA territory. This allowed the comparison of pathological features between the lesions against a common anatomical background. This also allowed a more direct comparison with the animal lesions used in this study which, as mentioned earlier, involved the rat MCA territory. This is an advantage of using rat tissue because the anatomical distribution of the MCA in rats is analogous to that in humans (Coyle 1975). Also, cases were selected from various age groups and from both genders to minimize any possible effect of age and sex on the results. In addition, a wide distribution of post-insult survival times was selected to allow

comparative histological analysis of neuropeptide expression and edema at various timepoints following the injury.

An inherent limitation of using human tissue is that the pathological changes often do not only reflect the investigated pathological conditions. In many cases, the histological features of the tissue are affected by treatment received before death, by co-existing pathological conditions and by complications of the initial lesion. To minimize this effect as much as possible, the selection of cases was based on an examination of both histopathological reports and clinical records. Furthermore, any unavoidable confounding factors were indicated in the results section.

2.2.1.2 Control tissue

Control tissue was selected from the IMVS archives. Tissue was obtained from a cohort of cases (n=10) of known past medical history in which the post mortem neuropathological examination had detected no abnormality. Examination of clinical data allowed selection of cases with illnesses unrelated to cerebral edema, cerebral infarction or cerebral contusion. Furthermore, in order to avoid a possible relationship between a particular cause of death and any of the studied molecules, control tissue was obtained from a range of cases with a variety of fatal conditions (indicated in the results section). These cases were further classified according to cause of death into two groups. In one group the cause of death was neurological (sudden unexplained death from epilepsy,

SUDEP) (N=4) and in the other the causes of death were several non-neurological conditions (N=6). The cases represented various age groups and both genders. Also, the examined tissue was obtained from the MCA territory for direct anatomical comparison with pathological tissue.

2.2.2 Staining methods: H&E and Immunohistochemistry

Paraffin-embedded tissue blocks from the tissue archives were sectioned using the rotary microtome to produce serial sections, each 5μ thick. The sections were stained as described above for the rat tissue.

2.2.3 Microscopic analysis of tissue

This was the same as mentioned earlier for the rat tissue.

2.3 Descriptive terminology

The description of certain histological features of the examined tissue required the use of specific terms and ranking systems. An explanation of this terminology is given below.

2.3.1 Defining the different zones of lesions

Both pathological processes - infarction and contusion – were associated with lesions that could be differentiated into two distinct zones. Each lesion consisted of a central mass of damaged tissue termed the core (either ischemic area or contusion) surrounded by a rim of less affected tissue termed the margin (Figure 2.3).

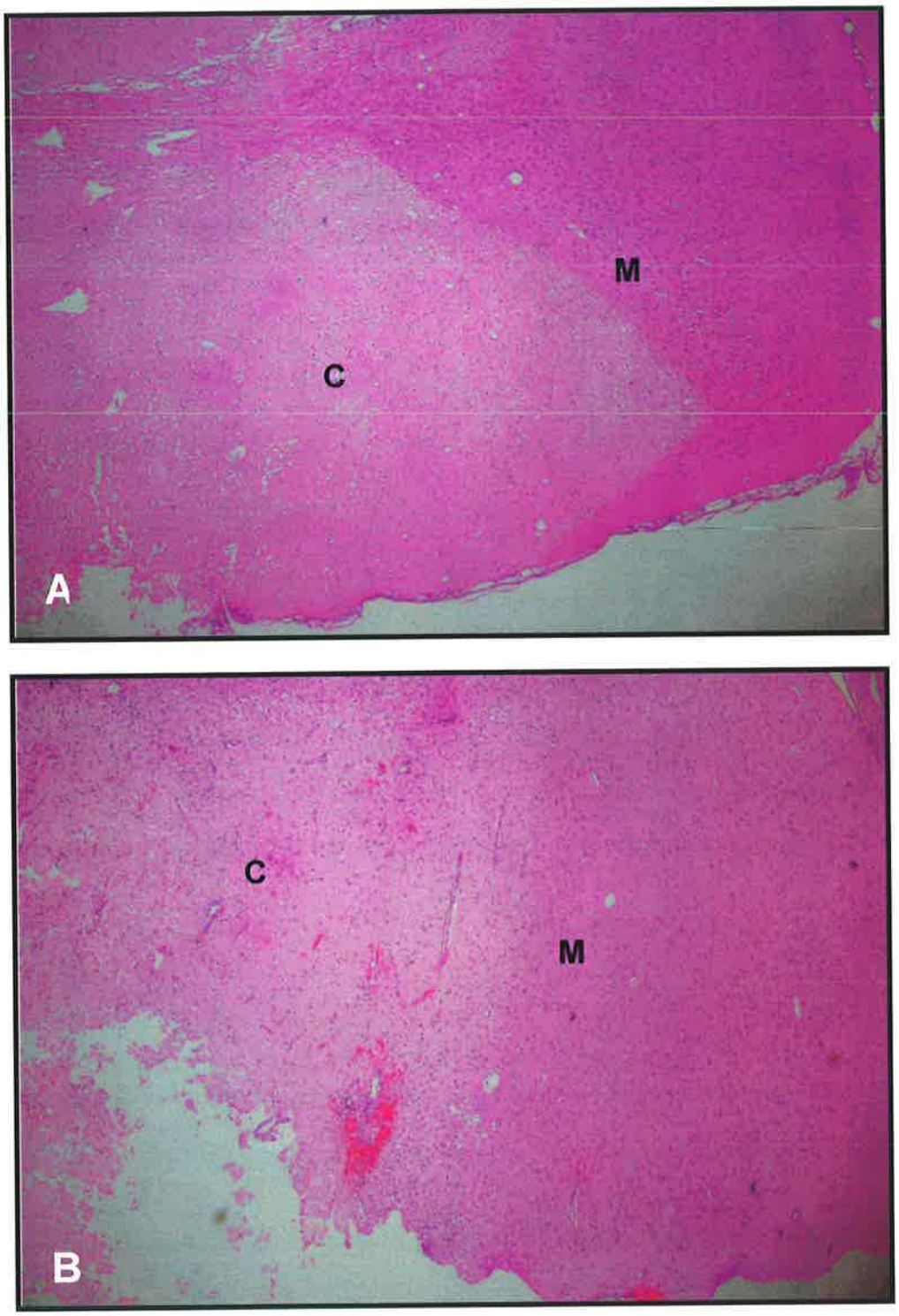

Figure 2.3: Zonal character of infarct (A) and contusion (B) in rat cerebrum. Each lesion consists of a core (C) surrounded by a margin (M) of better-preserved tissue. (H&E staining, x40)

2.3.2 Morphological types of neuronal damage

H&E staining was used to identify several types of neuronal damage (Auer *et al.* 2002, Graeber *et al.* 2002):

1. Red cell (acute ischemic cell) change: This describes intense cytoplasmic eosinophilia often associated with a shrunken, triangular nucleus. It is commonly associated with neuronal ischemia and is believed to represent irreversible neuronal damage.
2. Dark cell change: This refers to a purple appearance of the cytoplasm due to affinity for both acidic and basic dyes. The dendrites often acquire a characteristic corkscrew appearance which aids in differentiating dark cell change from the red cell change mentioned above. Dark cell change is also commonly encountered in neuronal ischemia but, contrary to red cell change, is believed to represent reversible neuronal damage. These two tinctorial changes are thought to represent the opposite ends of a continuum along which cells may progress from reversible to irreversible damage. However, the credibility of dark cell change as a marker of reversible injury is confounded by the fact that it is also known to occur as an artefact in several settings including delayed tissue fixation. This effect was minimzed in this study by perfusion fixation of experimental animals and by delaying extraction of the brain from the skull to allow more time for fixation of the tissue before its manipulation.

3. Necrosis: This is considered a morphological correlate of cell death. It generally refers to cytoplasmic fragmentation with any of several nuclear alterations (karyolysis, pyknosis and karyorrhexis).
4. Apoptosis (programmed cell death): This is attended by the disintegration of nuclear material into several apoptotic bodies.

2.3.3 Semi-quantitative grading of SP-immunoreactivity (SP-IR) and albumin-IR

Histological examination of the tissues revealed different degrees of perivascular SP-IR and different degrees of extravascular albumin-IR. A semi-quantitative grading system was used to describe these different degrees of IR (Figures 2.4 and 2.5). For perivascular SP-IR, grading was based on the percentage of the circumference of a vessel that was surrounded by immunoreactive profiles. The grade demonstrated by the majority of the vessels in a given area of tissue was used to represent that area of tissue. For albumin-IR, the grade used to describe a particular area of tissue was based on the intensity of IR in that area. It is well recognized in technical practice that the intensity of immunohistochemical staining might vary slightly from one staining session to the other. This would affect the accuracy of the grading system used in his study. Therefore, this limitation was avoided by staining all the tissue to be compared for each stain – including both study tissue and control tissue as well as standard tissue of known immunoreactivity – in one single session.

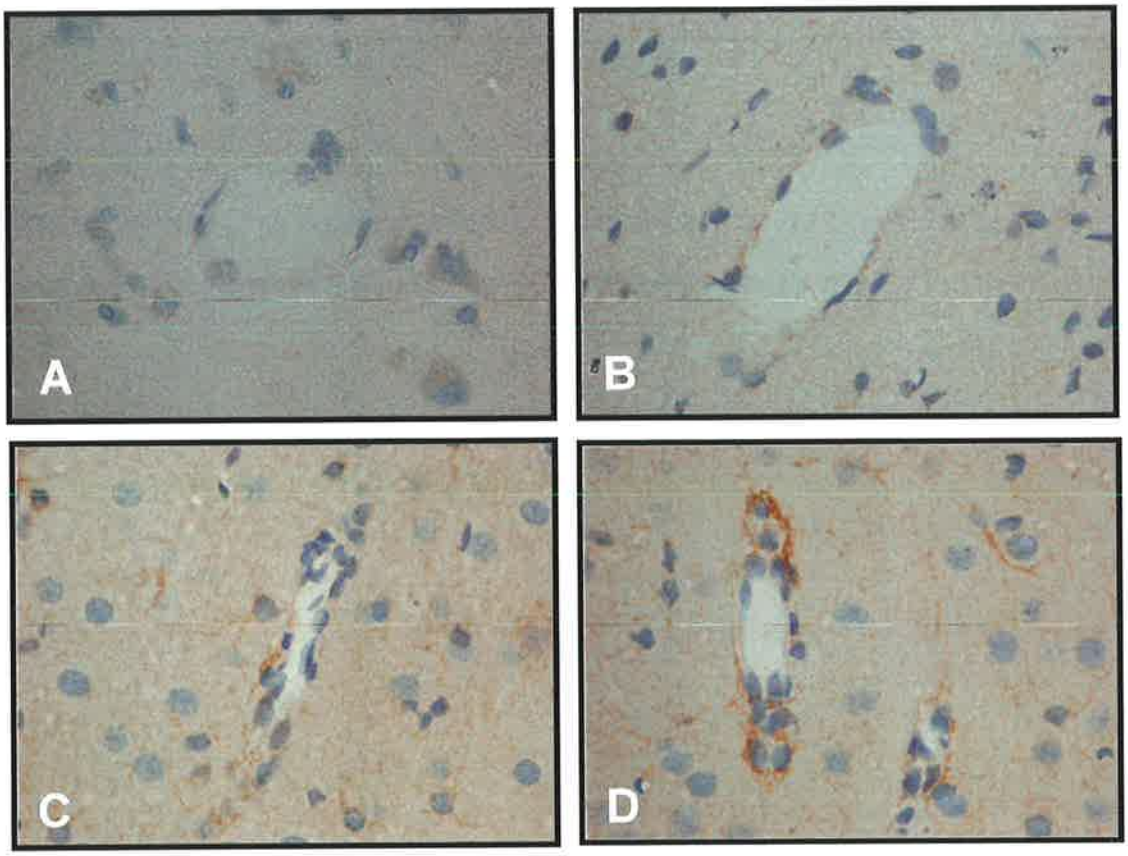

Figure 2.4: Semi-quantitative grading of perivascular SP-IR. (A-D: x400) As indicated in the results tables, the grades are:

0 : not visible (A)
\+ : minimal (B); occasional IR profiles
++ : moderate (C); IR profiles around < 25% of the circumference of the vessel
+++ : severe (D); IR profiles around > 25% of the circumference of the vessel

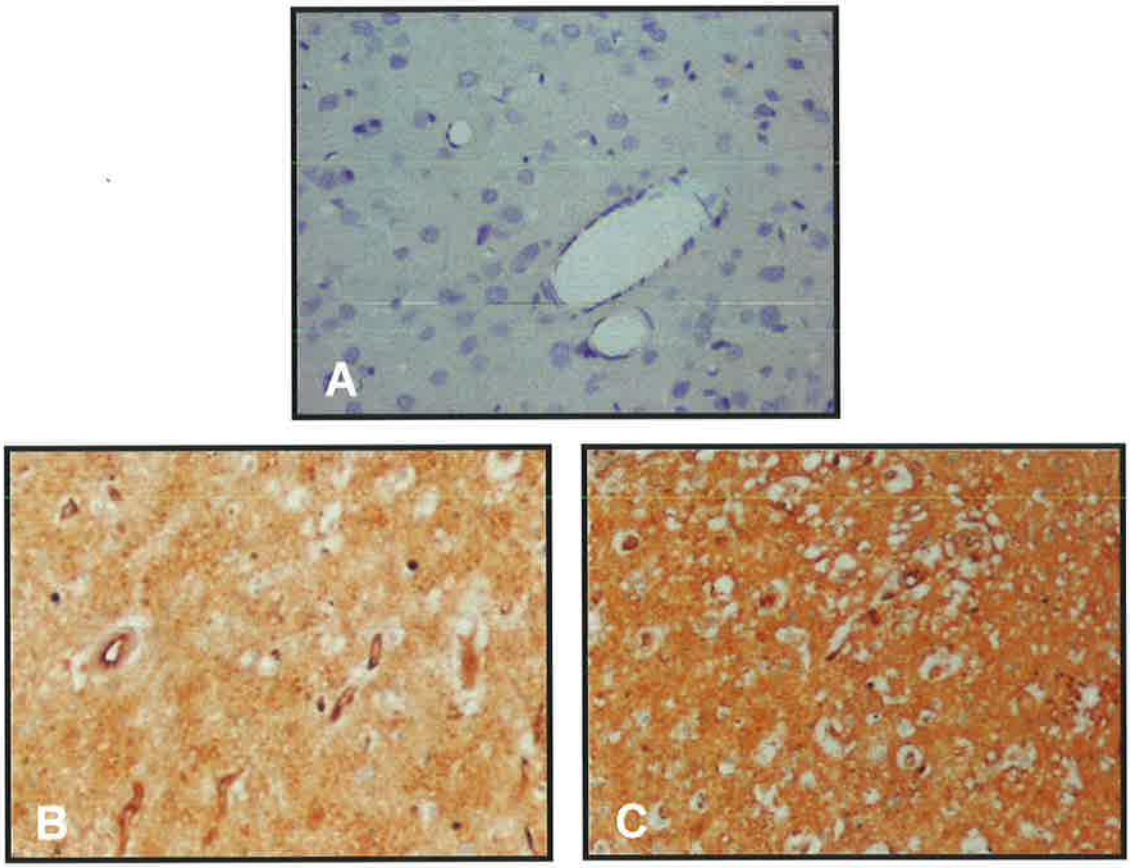

Figure 2.5: Semi-quantitative grading of albumin-IR. (A: x200; B and C: x100) As indicated in the results tables, the grades are:
0 : not visible (A)
P(m) : Present (moderate) (B)
P(s) : Present (severe) (C)

Chapter 3

RESULTS

Contents

3.1 Perivascular SP-IR

In all the tissue examined in this study, from both rats and humans, perivascular SP-IR was observed in astrocytic processes and not in nerve fibers (Figures 3.1 and 3.2). On light microscopy, the SP-immunoreactive processes were often seen along the full length of astrocytic processes extending from the vessel wall to the astrocytic cell body. One such astrocytic process is presented under high magnification in Figure 3.1. The astrocytic location of SP-IR was confirmed with the aid of laser scanning confocal microscopy which demonstrated perfect colocalization between GFAP-IR and SP-IR. An example of this colocalization is presented in Figure 3.2. The perivascular astrocytic SP-IR was mainly concentrated around thin-walled venules.

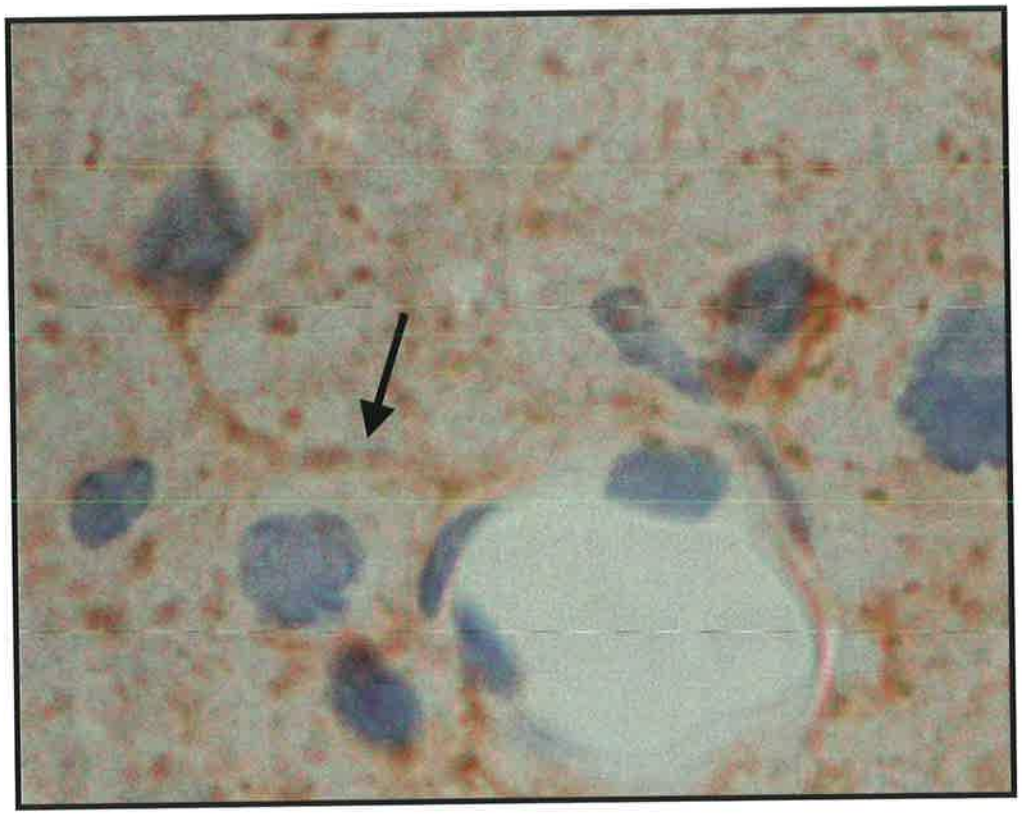

Figure 3.1: Perivascular SP-IR in astrocytic process (x1000, oil immersion lens). Cortical vessel in rat following reperfused MCAO showing perivascular astrocytic SP-IR. Some SP-IR (arrow) can be followed along the full length of the astrocytic process till the cell body.

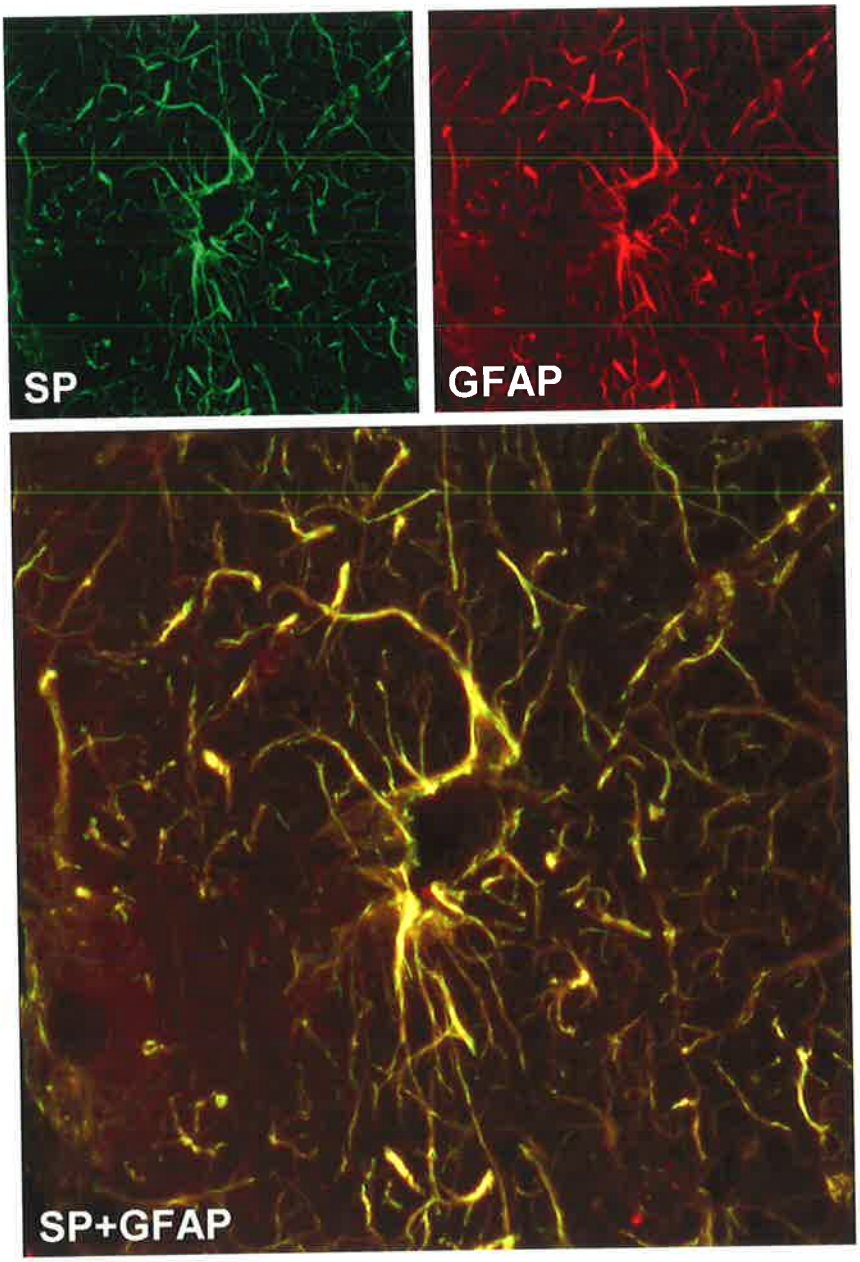

Figure 3.2: Perivascular SP-IR in astrocytic processes – confocal micrographs (x600). Cortical venule from rat following FPI. **SP**: SP-IR (green) is present around the venule. **GFAP**: GFAP-IR (red) specifically marks astrocytic processes around the venule. **SP+GFAP**: Merging the two previous images shows complete colocalization (yellow) of SP-IR and GFAP-IR; all the SP-IR colocalizes with the GFAP-IR.

3.2 Naïve (control) rat cerebral tissue

The histological features of naïve (control) rat cerebral tissue are presented in Table 3.1 and Figure 3.3.

Table 3.1: Naïve (control) rat cerebral tissue. Perivascular SP-IR was normally present in astrocytic processes.

Rat ID	H&E		Perivascular SP-IR		Albumin-IR	Perivascular nerve fiber APP-IR
	Neurons	Astrocytes	Nerve fiber IR	Astrocytic processes IR		
N 1	normal	normal	0	++	0	0
N 2	normal	normal	0	++	0	0
N 3	normal	normal	0	++	0	0
N 4	normal	normal	0	++	0	0

0: not visible; +: minimal; ++: moderate; +++: severe

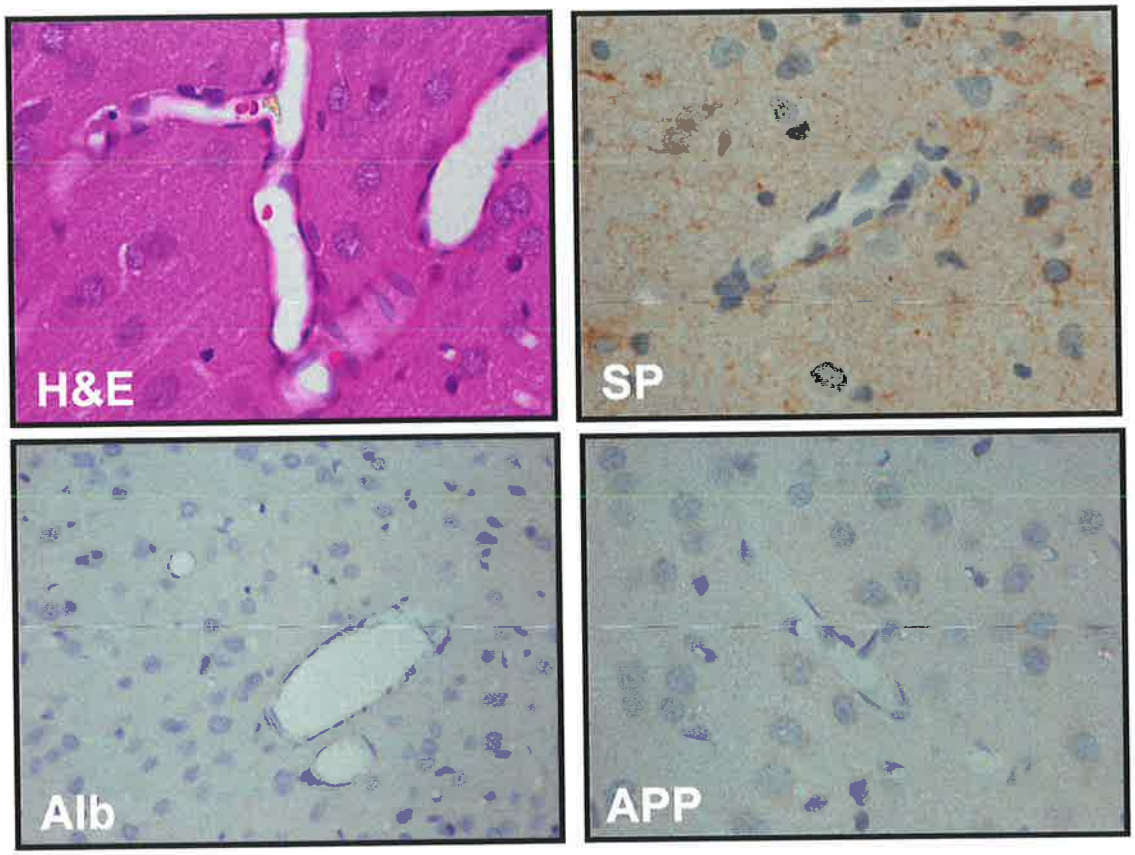

Figure 3.3: Naïve (control) rat cerebral tissue. **H&E**: Cortical tissue shows normal H&E staining (x400). **SP**: SP-IR is seen in perivascular astrocytic processes. (x400). **Alb**: Albumin-IR is not visible (x200). **APP**: No APP-immunoreactive perivascular nerve fibers are seen (x400).

3.3 Pathological features of rat cerebral tissue following MCAO

3.3.1 Model mortality and morbidity

The overall mortality from the MCAO model was 24% with the major cause of death being intracranial hemorrhage due to perforation of the ICA by the intraluminal suture. All animals suffered right hemiparesis manifested by clockwise circling.

3.3.2 Sham (control) MCAO

The histological features of rat cerebral tissue following sham (control) MCAO are presented in Table 3.2 and Figure 3.4.

Table 3.2: Sham (control) MCAO. Perivascular SP-IR was observed in astrocytic processes.

Rat ID	H&E		Perivascular SP-IR		Albumin-IR	Perivascular nerve fiber APP-IR
	Neurons	Astrocytes	Nerve fiber IR	Astrocytic processes IR		
MCAO-S 1	normal	normal	0	++	0	0
MCAO-S 2	normal	normal	0	++	0	0
MCAO-S 3	normal	normal	0	++	0	0
MCAO-S 4	normal	normal	0	++	0	0

0: not visible; +: minimal; ++: moderate; +++: severe

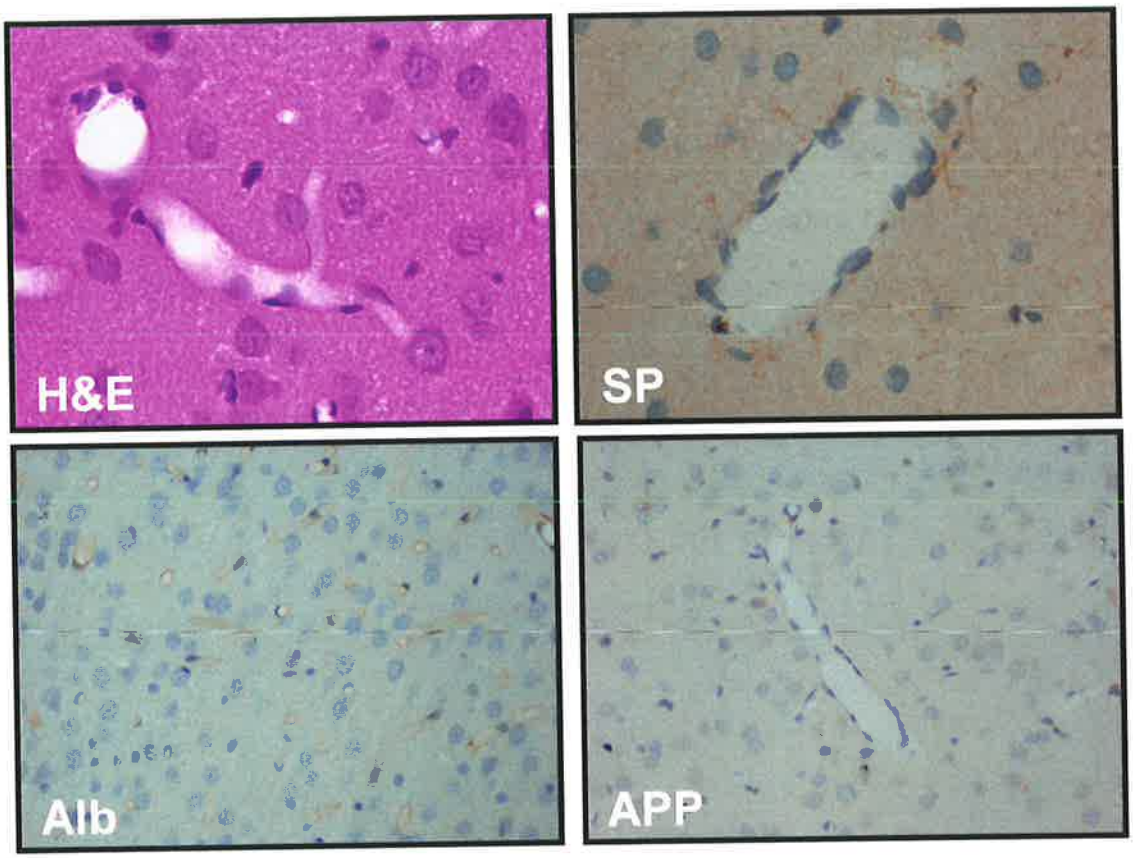

Figure 3.4: Sham (control) MCAO. H&E: Cortical tissue shows normal H&E staining (x400). **SP**: SP-IR is seen in perivascular astrocytic processes (x400). **Alb**: Albumin-IR is not visible in the extracellular space (x200). **APP**: No APP-immunoreactive perivascular nerve fibers are seen (x400).

3.3.3 Permanent MCAO (pMCAO)

The histological features of rat cerebral tissue following pMCAO are presented in Tables 3.3 and 3.4 and Figures 3.5 and 3.6.

Table 3.3: pMCAO – H&E staining. The later timepoints showed a sharper demarcation between the ischemic area and its margins and a loss of astrocytes in the ischemic area.

Rat ID	Post-occlusion survival time	Ischemic area			Margins				Distant area		
		Neurons	Astrocytes	Inflammatory cells	Demarcation	Neurons	Astrocytes	Inflammatory cells	Neurons	Astrocytes	Inflammatory cells
pMCAO 1	5hr	D, fewer N	swollen	0	ill-defined, patchy	D	swollen	0	0	normal	0
pMCAO 2	7hr	D, fewer N	swollen	0	ill-defined, patchy	D-R	swollen	0	0	normal	0
pMCAO 3	24hr	D-R, N, A	decreased	0	well-defined	D-R	normal	0	0	normal	0
pMCAO 4	24hr	D-R, N, A	decreased	0	well-defined	D-R	normal	0	0	normal	0
pMCAO 5	26hr	D-R, N, A	decreased	0	well-defined	D	normal	0	0	normal	0

A: apoptosis; D: dark cell change; D-R: dark to red cell change; N: necrosis

Table 3.4: pMCAO – immunohistochemical staining. Margins showed increased perivascular astrocytic SP-IR at all timepoints. In the ischemic area, perivascular astrocytic SP-IR was increased at earlier timepoints and decreased at later timepoints. At all timepoints, albumin-IR was severe in the ischemic area and moderate in the margins.

Rat ID	Post-occlusion survival time	Ischemic area				Margins				Distant area			
		Perivascular SP-IR		Albumin-IR	Perivascular nerve fiber APP-IR	Perivascular SP-IR		Albumin-IR	Perivascular nerve fiber APP-IR	Perivascular SP-IR		Albumin-IR	Perivascular nerve fiber APP-IR
		Nerve fiber IR	Astrocytic processes IR			Nerve fiber IR	Astrocytic processes IR			Nerve fiber IR	Astrocytic processes IR		
pMCAO 1	5hr	0	+++	P(s)	0	0	+++	P(m)	0	0	++	0	0
pMCAO 2	7hr	0	+++	P(s)	0	0	+++	P(m)	0	0	++	0	0
pMCAO 3	24hr	0	+	P(s)	0	0	+++	P(m)	0	0	++	0	0
pMCAO 4	24hr	0	+	P(s)	0	0	+++	P(m)	0	0	++	0	0
pMCAO 5	26hr	0	+	P(s)	0	0	+++	P(m)	0	0	++	0	0

0: not visible; +: minimal; ++: moderate; +++: severe; P(m): present (moderate); P(s): present (severe)

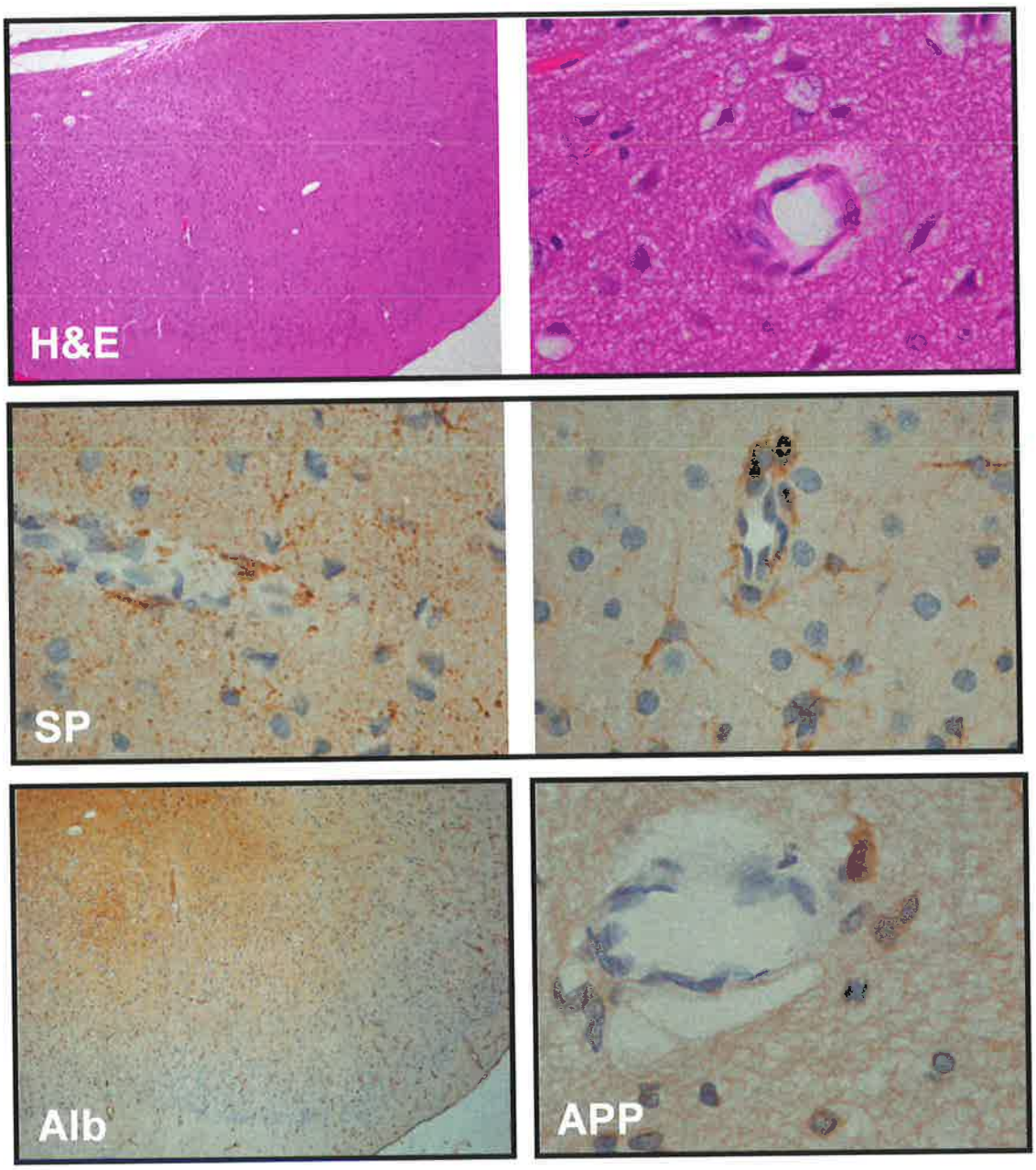

Figure 3.5: 7hr post-pMCAO. **H&E**: H&E staining shows ill-defined demarcation between the ischemic area and its margins (Lt) as well as neuronal dark cell change in the ischemic area (Rt) (Lt: x40; Rt: x400). **SP**: Increased SP-IR is seen in perivascular astrocytic processes and neuropil in both the ischemic area (Lt) and its margins (Rt) (x400). **Alb**: Extravascular albumin-IR is seen in the ischemic area and its margins respectively (x40). **APP**: No APP-IR is seen in association with the microvasculature in the ischemic area (x400).

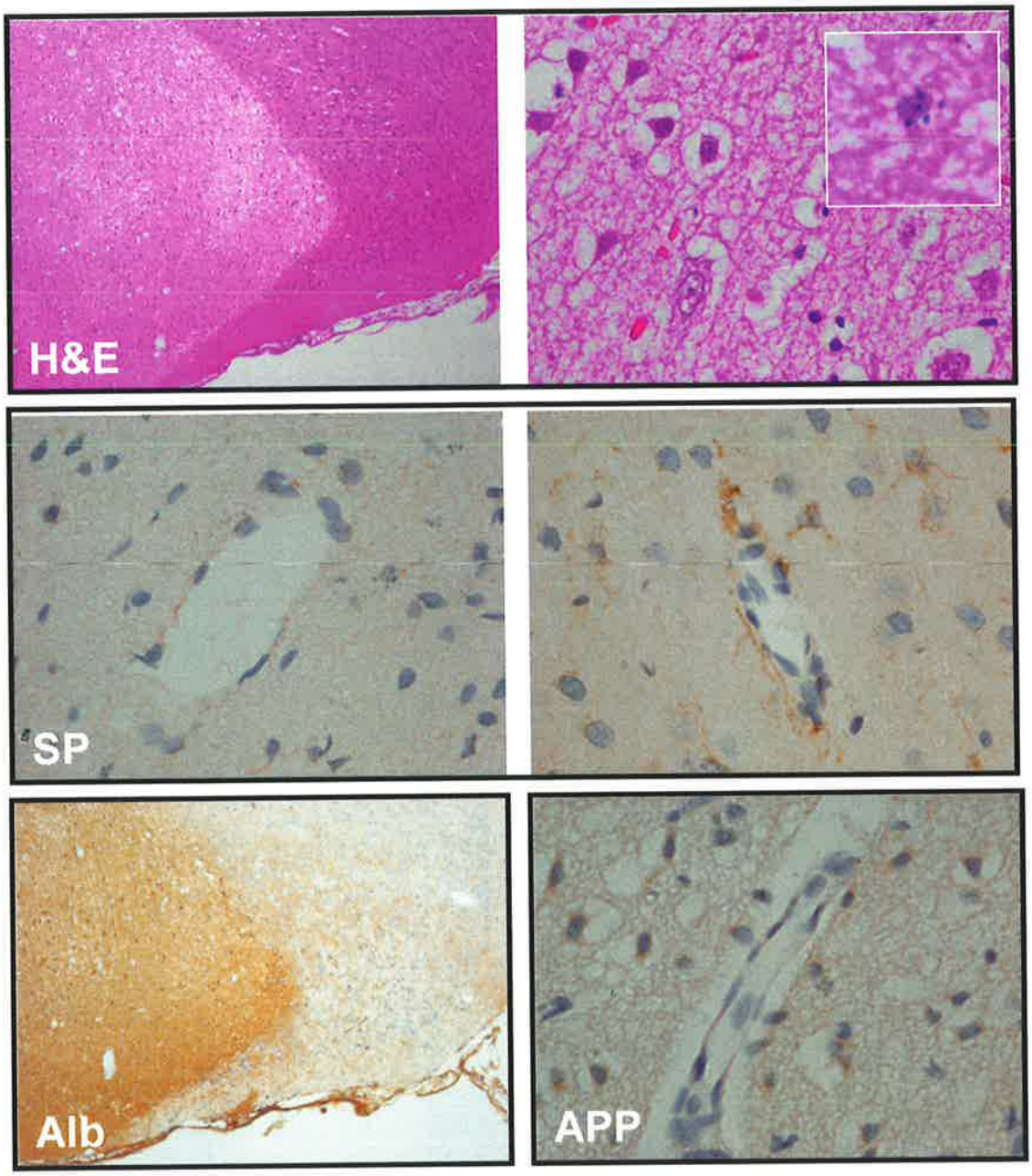

Figure 3.6: 24hr post-pMCAO. H&E: H&E staining shows well-defined demarcation between the ischemic area and its margins (Lt) as well as neuronal dark to red cell change, necrosis (arrow) and apoptotic bodies (inset) in the ischemic area (Rt) (Lt: x40; Rt: x400; inset: x1000 oil immersion). **SP**: Perivascular astrocytic processes show minimal SP-IR in the ischemic area (Lt) and severe SP-IR in its margins (Rt) (x400). **Alb**: Extravascular albumin-IR is seen in the ischemic area and its margins respectively (x40). **APP**: No APP-IR is seen in association with the microvasculature in the ischemic area (x400).

3.3.4 Reperfused MCAO (rMCAO)

The histological features of rat cerebral tissue following rMCAO are presented in Tables 3.5 and 3.6 and Figures 3.7 and 3.8.

Table 3.5: rMCAO – H&E staining. The later timepoints showed a sharper demarcation between the ischemic area and its margins.

Rat ID	Occlusion time + reperfusion time	Ischemic area			Margins				Distant area		
		Neurons	Astrocytes	Inflammatory cells	Demarcation	Neurons	Astrocytes	Inflammatory cells	Neurons	Astrocytes	Inflammatory cells
rMCAO 1	2+5hr	D, few N	normal	0	ill-defined, patchy	D	normal	0	0	normal	0
rMCAO 2		D, few N	normal	0	ill-defined, patchy	D-R	normal	0	0	normal	0
rMCAO 3		D	normal	0	ill-defined, patchy	D	normal	0	0	normal	0
rMCAO 4		D, few N	normal	0	ill-defined, patchy	D	normal	0	0	normal	0
rMCAO 5	2+24hr	D-R, few N	normal	0	well-defined, patchy	D-R	normal	0	0	normal	0
rMCAO 6		D-R, few N	normal	0	well-defined, patchy	D-R	normal	0	0	normal	0
rMCAO 7		D-R, few N	normal	0	well-defined	D-R	normal	0	0	normal	0

D: dark cell change; D-R: dark to red cell change; N: necrosis

Table 3.6: rMCAO – immunohistochemical staining. Increased perivascular astrocytic SP-IR was observed in both the ischemic area and its margins at both timepoints. At both timepoints, albumin-IR was severe in the ischemic area and moderate in the margins. At the later timepoint, moderate albumin-IR extended beyond the margins of the ischemic area into the surrounding cerebral tissue (referred to as "distant area").

Rat ID	Occlusion time + reperfusion time	Ischemic area				Margins				Distant area			
		Perivascular SP-IR		Albumin-IR	Perivascular nerve fiber APP-IR	Perivascular SP-IR		Albumin-IR	Perivascular nerve fiber APP-IR	Perivascular SP-IR		Albumin-IR	Perivascular nerve fiber APP-IR
		nerve fiber IR	astrocytic processes IR			nerve fiber IR	astrocytic processes IR			nerve fiber IR	astrocytic processes IR		
rMCAO 1	2+5h	0	+++	P(s)	0	0	+++	P(m)	0	0	++	0	0
rMCAO 2		0	+++	P(s)	0	0	+++	P(m)	0	0	++	0	0
rMCAO 3		0	+++	P(s)	0	0	+++	P(m)	0	0	++	0	0
rMCAO 4		0	+++	P(s)	0	0	+++	P(m)	0	0	++	0	0
rMCAO 5	2+24h	0	+++	P(s)	0	0	+++	P(m)	0	0	++	P(m)	0
rMCAO 6		0	+++	P(s)	0	0	+++	P(m)	0	0	++	P(m)	0
rMCAO 7		0	+++	P(s)	0	0	+++	P(m)	0	0	++	P(m)	0

0: not visible; +: minimal; ++: moderate; +++: severe; P(m): present (moderate); P(s): present (severe)

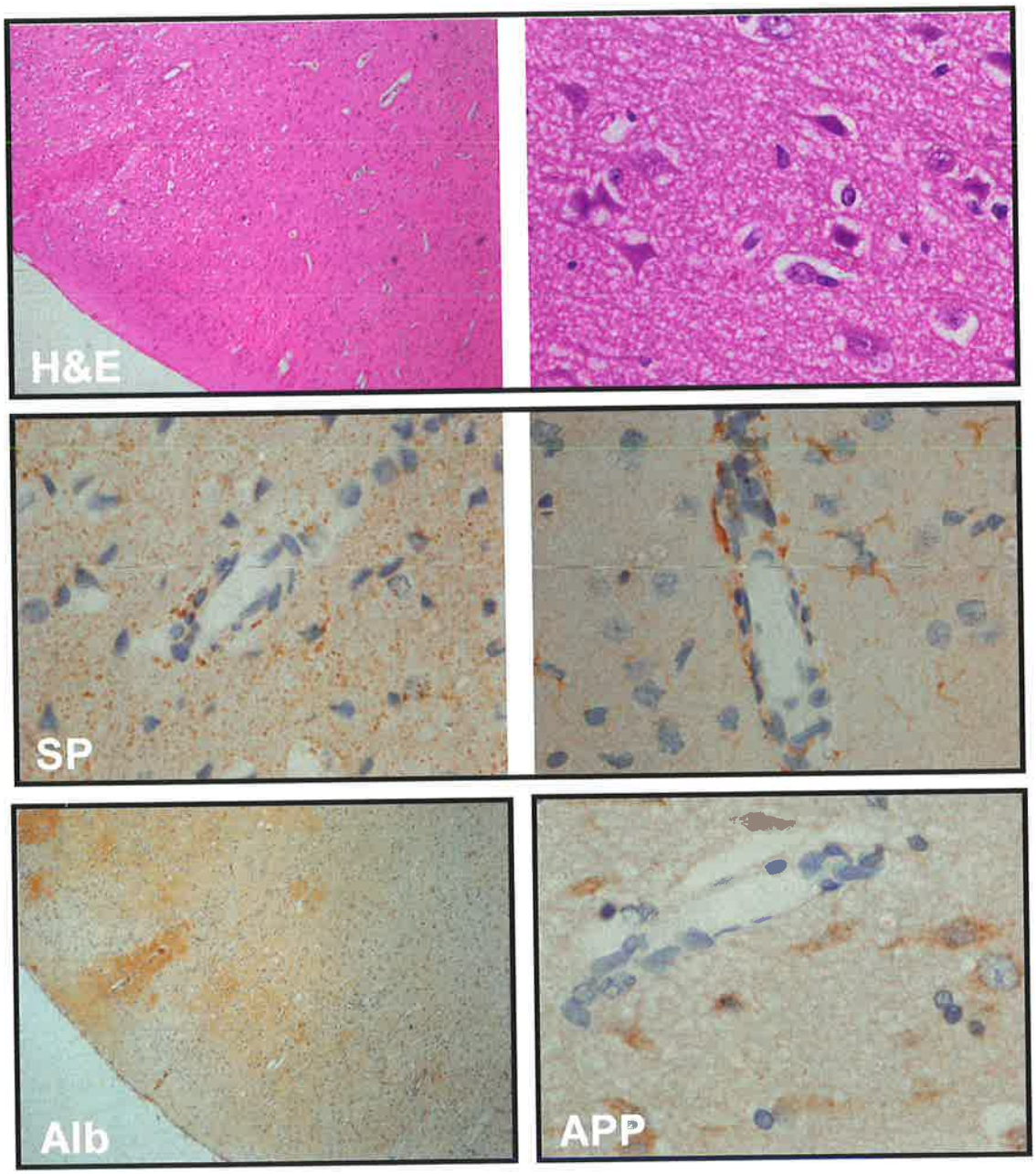

Figure 3.7: 2+5hr post-rMCAO. **H&E**: H&E staining shows ill-defined demarcation between the ischemic area and its margins (Lt) as well as neuronal dark cell change in the ischemic area (Rt) (Lt: x40; Rt: x400). **SP**: Increased SP-IR is seen in perivascular astrocytic processes and neuropil in both the ischemic area (Lt) and its margins (Rt) (x400). **Alb**: Extravascular albumin-IR is seen in the ischemic area and its margins respectively (x40). **APP**: No APP-IR is seen in association with the microvasculature in the ischemic area (x400).

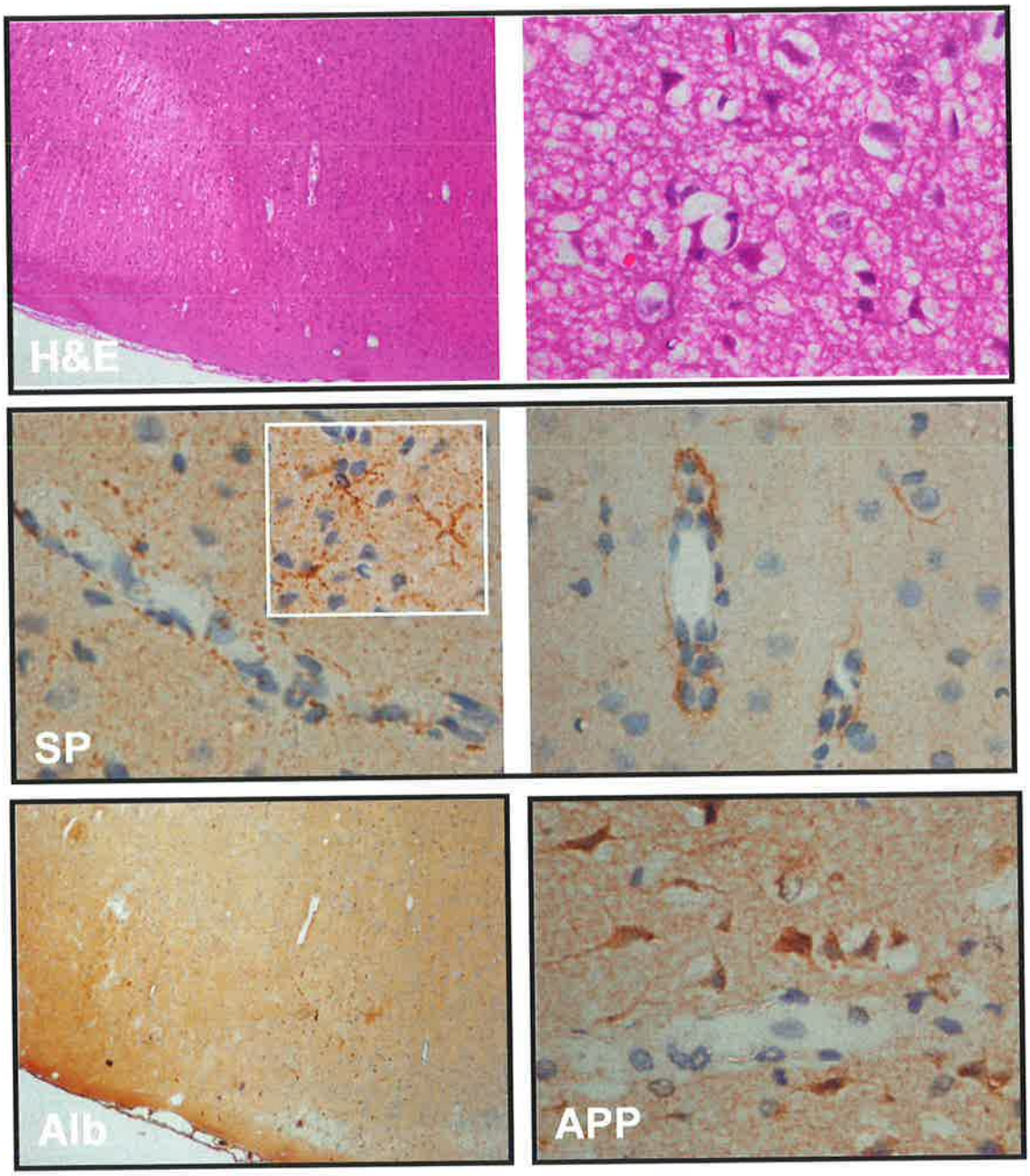

Figure 3.8: 2+24hr post-rMCAO. **H&E**: H&E staining shows well-defined demarcation between the ischemic area and its margins (Lt) as well as neuronal dark and red cell change in the ischemic area (Rt) (Lt: x40; Rt: x400). **SP**: Increased SP-IR is seen in perivascular astrocytic processes and neuropil in both the ischemic area (Lt) and its margins (Rt). The inset shows intense SP-IR in cortical astrocytes (x400). **Alb**: Extravascular albumin-IR is seen in the ischemic area and its margins respectively (x40). **APP**: Intense APP-IR is observed in nerve cell bodies while no APP-IR is seen in association with the microvasculature in the ischemic area (x400).

3.4 Pathological features of rat cerebral tissue following FPI

3.4.1 Model mortality and morbidity

The overall mortality from the FPI model was 15% with post-traumatic apnea as the major cause of death. Post-traumatic apnea was also a common morbidity in the animals that survived, usually lasting less than 5 minutes.

3.4.2 Gross pathological features

The gross pathological features of rat cerebral hemispheres following FPI are presented in Table 3.7 and Figures 3.9 and 3.10.

Table 3.7: FPI – Gross pathological features. All rats showed a left hemispheric contusion with an overlying subarachnoid hemorrhage. Some animals also demonstrated a laceration in the left hemisphere.

Rat ID	Post-injury survival time	Contusion	SAH
FPI 1	30min	C	+
FPI 2		C	+
FPI 3		C	+
FPI 4	5hr	C	+
FPI 5		C	+
FPI 6		C	+
FPI 7	24hr	C, L	+
FPI 8		C, L	+
FPI 9		C, L	+
FPI 10	48hr	C, L	+
FPI 11	72hr	C	+

+: present; C: contusion; L: laceration; SAH: subarachnoid hemorrhage

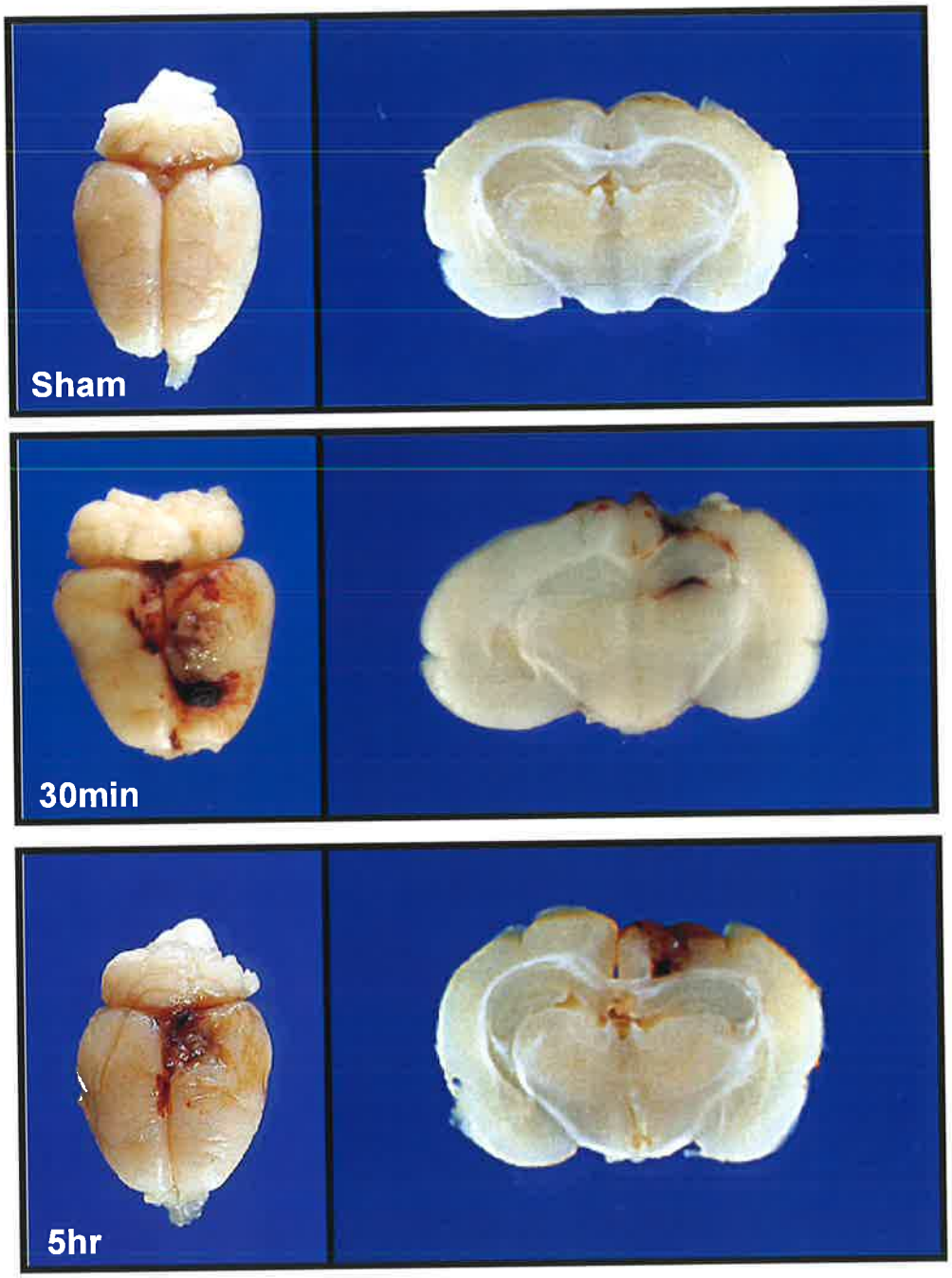

Figure 3.9: Gross pathological features of rat cerebral hemispheres following sham FPI and at 30min and 5hr post-FPI. Sham: Superior aspect (Lt) and coronal section (Rt): Cerebrum following sham FPI shows normal morphology. **30min**: Superior aspect (Lt) and coronal section (Rt): Cerebrum at 30min post-FPI shows left parieto-occipital subarachnoid hemorrhage and underlying contusion. **5hr**: Superior aspect (Lt) and coronal section (Rt): Cerebrum at 5hr post-FPI aspect shows left parieto-occipital subarachnoid hemorrhage and underlying contusion.

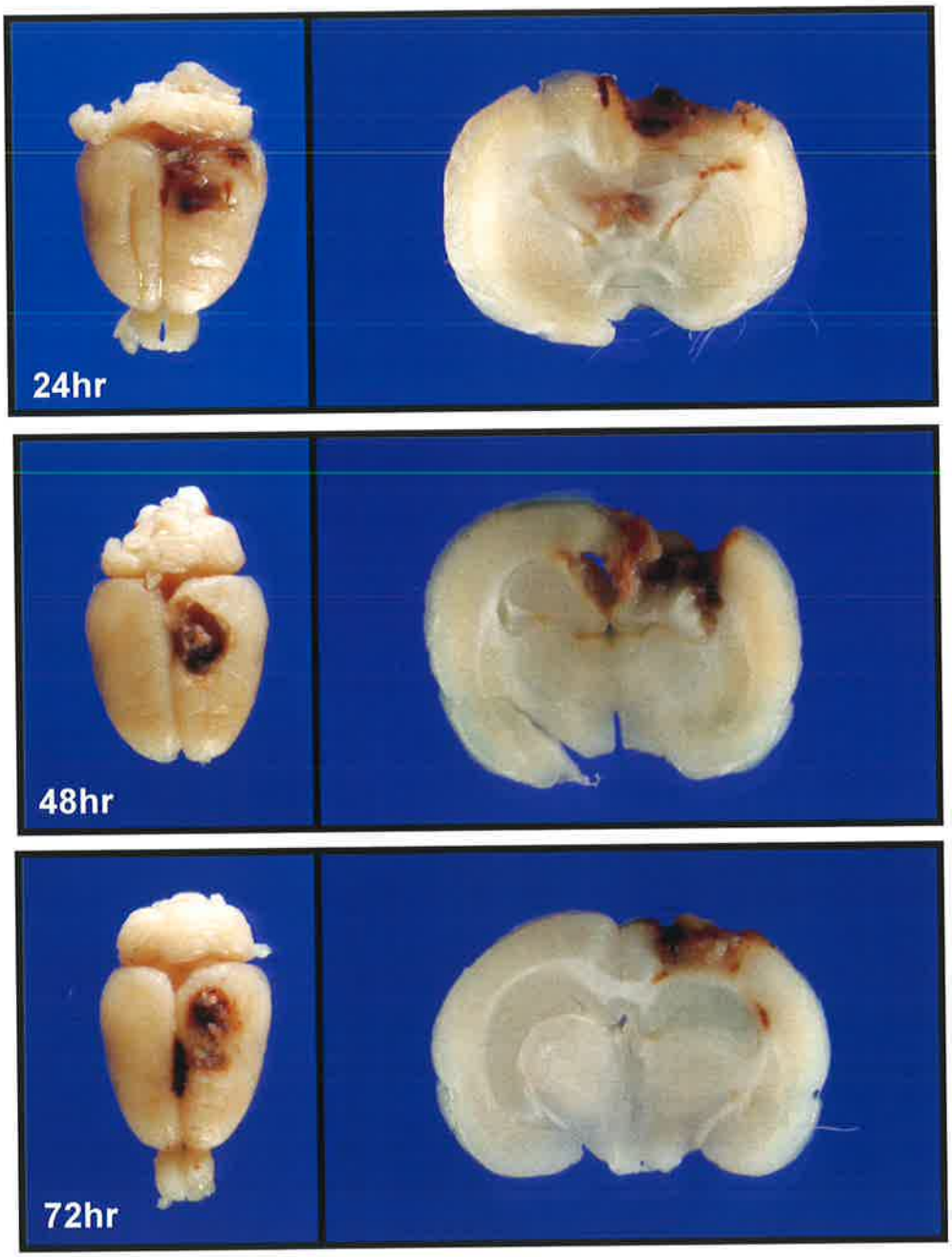

Figure 3.10: Gross pathological features of rat cerebral hemispheres at 24, 48 and 72hr post-FPI. 24hr: Superior aspect (Lt) and coronal section (Rt): Cerebrum at 24hr post-FPI shows left parietal subarachnoid hemorrhage, laceration and underlying contused tissue. **48hr**: Superior aspect (Lt) and coronal section (Rt): Cerebrum at 48hr post- FPI shows left parietal subarachnoid hemorrhage, laceration and underlying contused tissue. **72hr**: Superior aspect (Lt) and coronal section (Rt): Cerebrum at 72hr post-FPI shows left parietal subarachnoid hemorrhage and underlying contusion.

3.4.3 Sham (control) FPI

The histological features of rat cerebral tissue following sham (control) FPI are presented in Table 3.8 and Figure 3.11.

Table 3.8: Sham (control) FPI. Perivascular SP-IR was observed in astrocytic processes.

Rat ID	H&E		Perivascular SP-IR		Albumin-IR	Perivascular nerve fiber APP-IR	Remarks
	Neurons	Astrocytes	Nerve fiber IR	Astrocytic processes IR			
FPI-S 1	normal	normal	0	++	0	0	
FPI-S 2	normal	normal	0	++	0	0	
FPI-S 3	normal	normal	0	++	0	0	
FPI-S 4	D	normal	0	+++	P(s)	0	minimal contusion due to faulty surgical technique – animal excluded from analysis

0: not visible; +: minimal; ++: moderate; +++: severe; P(m): present (moderate); P(s): present (severe)

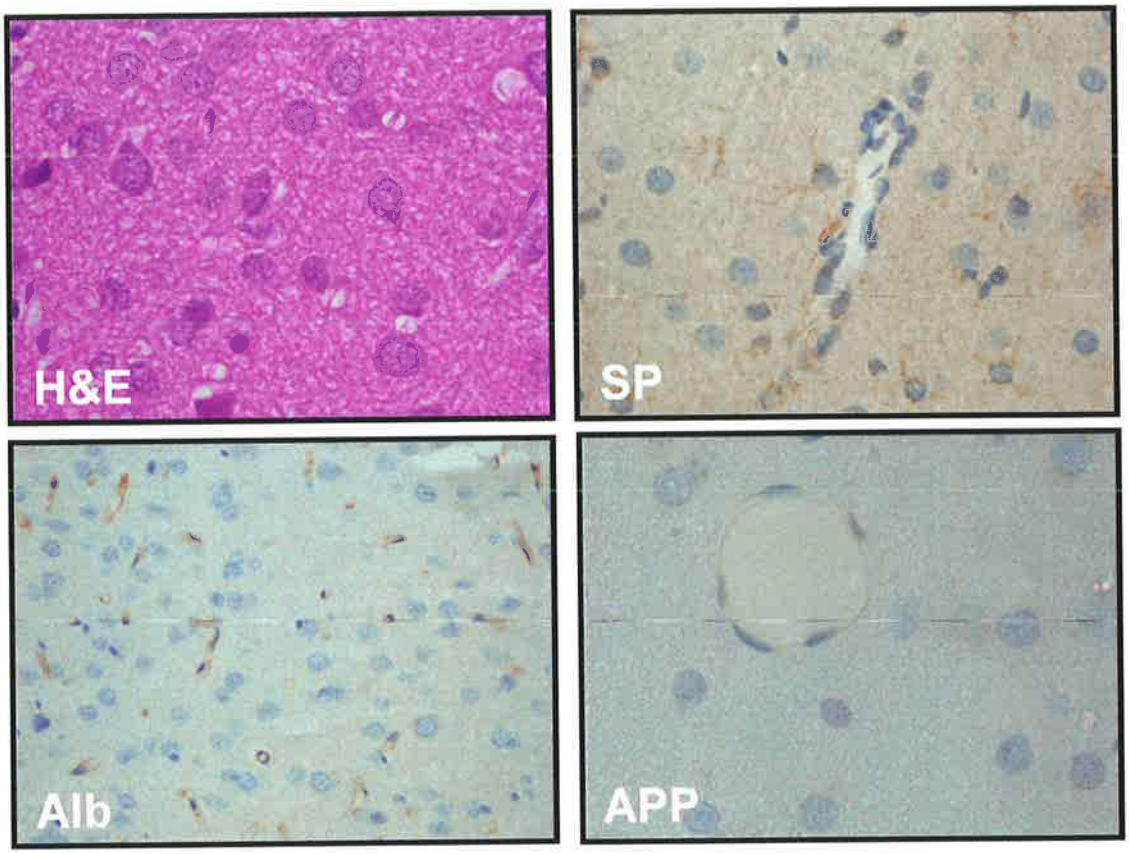

Figure 3.11: Sham (control) FPI. **H&E**: Cortical tissue shows normal H&E staining (x400). **SP**: SP-IR is seen in perivascular astrocytic processes (x400). **Alb**: No extravascular albumin-IR is seen and some albumin-IR is seen in vessels (x200). **APP**: No APP-immunoreactive perivascular nerve fibers are seen (x400).

3.4.4 FPI

The histological features of rat cerebral tissue following FPI are presented in Tables 3.9 and 3.10 and Figures 3.12-3.14.

Table 3.9: FPI – H&E staining. The later timepoints showed a sharper demarcation between the contusion and its margins as well as inflammatory cell infiltration in both zones.

Rat ID	Post-injury survival time	Contusion			Margins				Distant area			Remarks
		Neurons	Astrocytes	Inflammatory cells	Demarcation	Neurons	Astrocytes	Inflammatory cells	Neurons	Astrocytes	Inflammatory cells	
FPI 1	30min	D	normal	0	ill-defined, patchy	D	normal	0	normal	normal	0	
FPI 2		D	normal	0	ill-defined, patchy	D	normal	0	normal	normal	0	
FPI 3		D	normal	0	ill-defined, patchy	D	normal	0	normal	normal	0	
FPI 4	5hr	R, N	normal	0	ill-defined	R	normal	0	normal	normal	0	
FPI 5		D-R	normal	0	ill-defined	D-R	normal	0	normal	normal	0	
FPI 6		D-R	normal	0	ill-defined	D-R	normal	0	normal	normal	0	
FPI 7	24hr	R, N, A	normal	P	well-defined	R, A	normal	P	normal	normal	0	
FPI 8		R, N, A	normal	P	well-defined, patchy	R, A	normal	P	normal	normal	0	
FPI 9		N/A				R	normal	P	normal	normal	0	contused tissue lost during processing
FPI 10	48hr	R, N, A	swollen	P,M	well-defined	normal, few R	normal	P,M	normal	normal	0	
FPI 11	72hr	R, N, A	decreased	M	well-defined	normal	swollen	M	normal	normal	0	neuronal and astrocytic loss in contusion

A: apoptosis; D: dark cell change; D-R: dark to red cell change; M: macrophages; N: necrosis; N/A: not applicable; P: polymorphonuclear leukocytes; R: red cell change

Table 3.10: FPI – immunohistochemical staining. Increased perivascular astrocytic SP-IR was observed in both the contusion and its margins at all timepoints except at 72hr in the contusion where it was minimal. At all timepoints, Albumin-IR was severe in the contusion. In the margins, albumin-IR was not visible at 30min post-FPI, moderate at 5hr post-FPI and severe at 24, 48 and 72hr post-FPI. At 24, 48 and 72hr post-FPI, moderate albumin-IR was present beyond the margins of the ischemic area in the surrounding cerebral tissue (referred to as "distant area").

Rat ID	Post-injury survival time	Contusion				Margins				Distant area				Remarks
		Perivascular SP-IR		Albumin-IR	Perivascular nerve fiber APP-IR	Perivascular SP-IR		Albumin-IR	Perivascular nerve fiber APP-IR	Perivascular SP-IR		Albumin-IR	Perivascular nerve fiber APP-IR	
		Nerve fiber IR	Astrocytic processes IR			Nerve fiber IR	Astrocytic processes IR			Nerve fiber IR	Astrocytic processes IR			
FPI 1	30min	0	+++	P(s)	0	0	+++	0	0	0	++	0	0	
FPI 2		0	+++	P(s)	0	0	+++	0	0	0	++	0	0	
FPI 3		0	+++	P(s)	0	0	+++	0	0	0	++	0	0	
FPI 4	5hr	0	+++	P(s)	0	0	+++	P(m)	0	0	++	0	0	
FPI 5		0	+++	P(s)	0	0	+++	P(m)	0	0	++	0	0	
FPI 6		0	+++	P(s)	0	0	+++	P(m)	0	0	++	0	0	
FPI 7	24hr	0	+++	P(s)	0	0	+++	P(s)	0	0	++	P(m)	0	
FPI 8		0	+++	P(s)	0	0	+++	P(s)	0	0	++	P(m)	0	
FPI 9		N/A				0	+++	P(s)	0	0	++	P(m)	0	contused tissue lost during processing
FPI 10	48hr	0	+++	P(s)	0	0	+++	P(s)	0	0	++	P(m)	0	
FPI 11	72hr	0	+	P(s)	0	0	+++	P(s)	0	0	++	P(m)	0	neuronal and astrocytic loss in contusion

0: not visible; +: minimal; ++: moderate; +++: severe; P(m): present (moderate); P(s): present (severe)

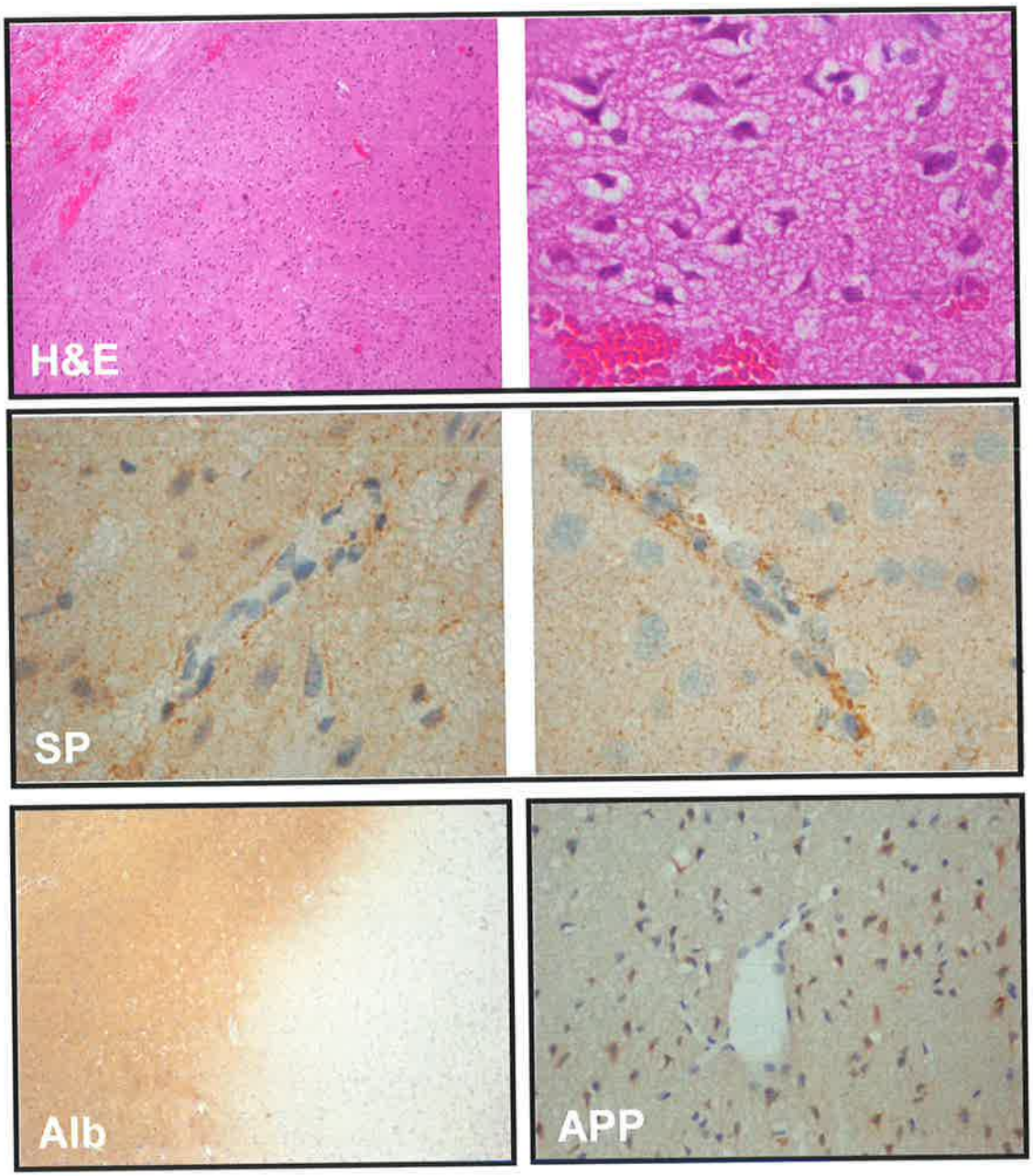

Figure 3.12: 30min post-FPI. **H&E**: H&E staining shows ill-defined demarcation between the contusion and its margins (Lt) as well as neuronal dark cell change in the contusion (Rt) (Lt: x40; Rt: x400). **SP**: Increased SP-IR is seen in perivascular astrocytic processes and neuropil in both the contusion (Lt) and its margins (Rt) (x400). **Alb**: Extravascular albumin-IR is severe in the contusion but not visible in the margins (x40). **APP**: No APP-immunoreactive perivascular nerve fibers are seen (x400).

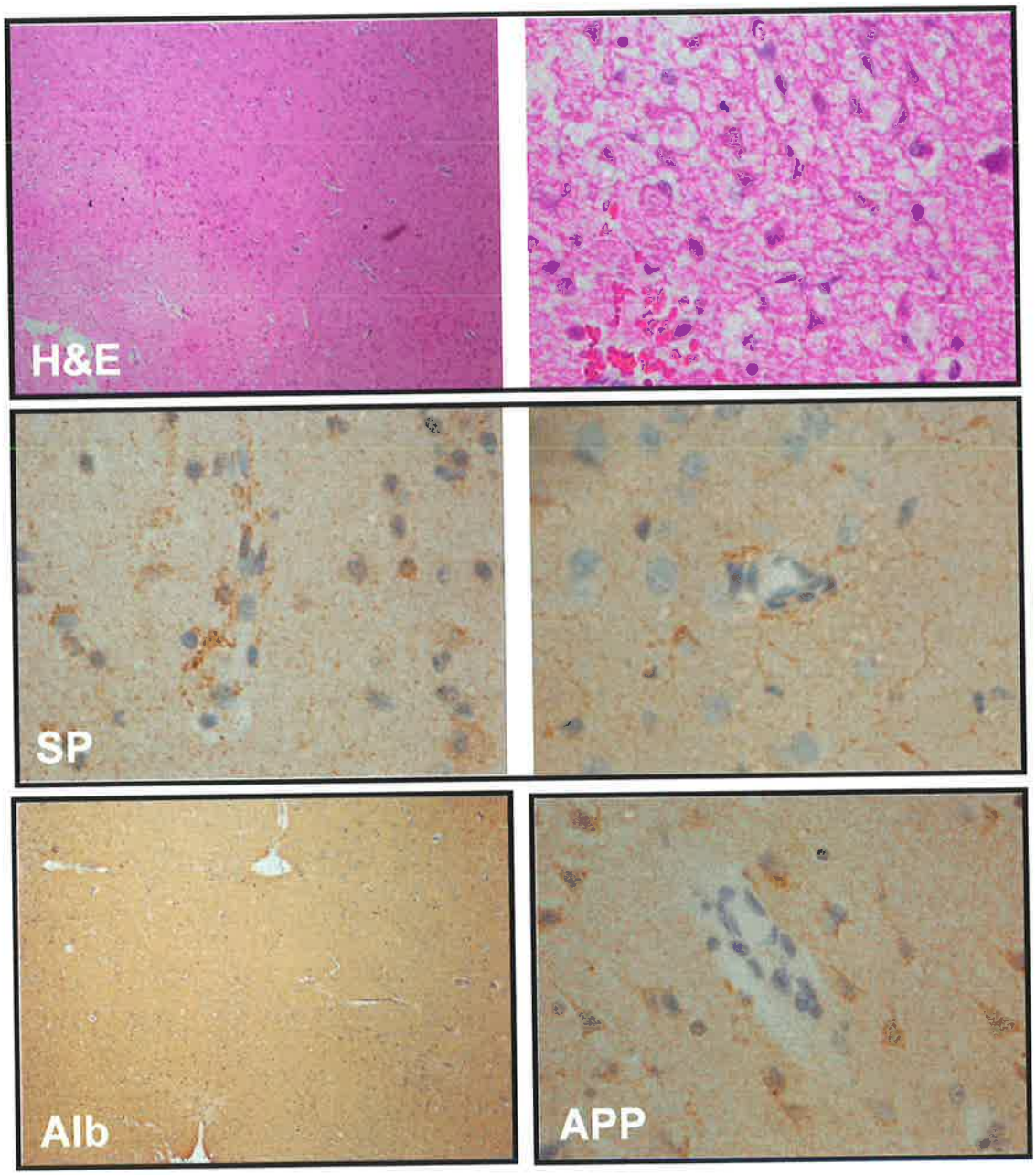

Figure 3.13: 24hr post-FPI. **H&E**: H&E staining shows well-defined demarcation between the contusion and its margins (Lt) as well as neuronal red cell change in the contusion (Rt) (Lt: x40; Rt: x400). **SP**: Increased SP-IR is seen in perivascular astrocytic processes and neuropil in both the contusion (Lt) and its margins (Rt) (x400). **Alb**: Extravascular albumin-IR is present in both the contusion and in the margins (x40). **APP**: No APP-immunoreactive perivascular nerve fibers are seen (x400).

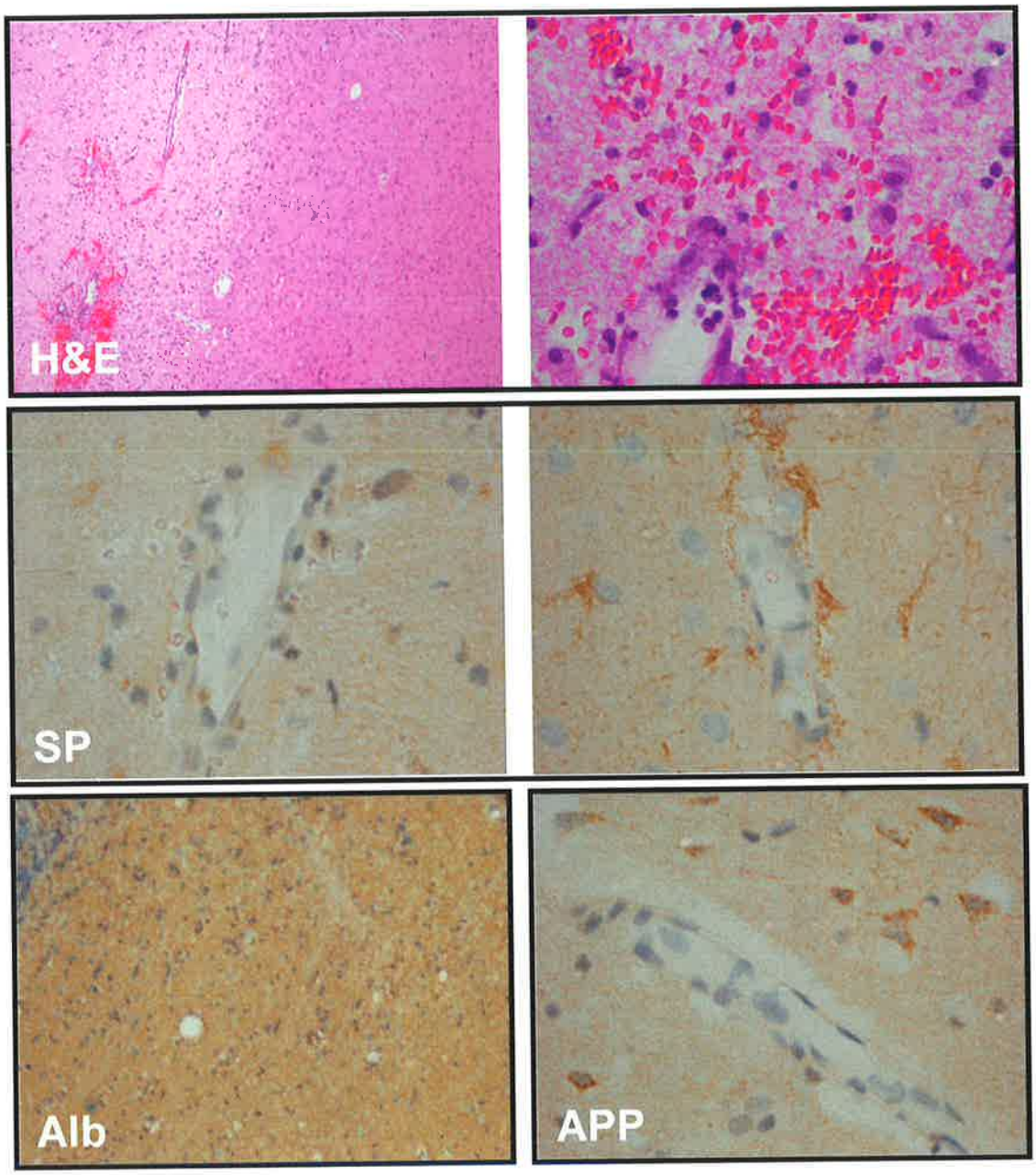

Figure 3.14: 72hr post-FPI. **H&E**: H&E staining shows well-defined demarcation between the contusion and its margins (Lt). In the contusion, there is loss of neurons and astrocytes and infiltration with macrophages (Rt) (Lt: x40; Rt: x400). **SP**: SP-IR in perivascular astrocytic processes is decreased in the contusion (Lt) but increased in its margins (Rt) (x400). **Alb**: Extravascular albumin-IR is present in both the contusion and in the margins (x100). **APP**: No APP-immunoreactive perivascular nerve fibers are seen (x400).

3.5 Perivascular APP-IR

In all the tissue examined, both rat and human, immunostaining for APP demonstrated no APP-IR in perivascular nerve fibers. APP-IR was observed, however, in rat pericytes in control and sham animals and following FPI but not in the ischemic area following MCAO (Figure 3.15).

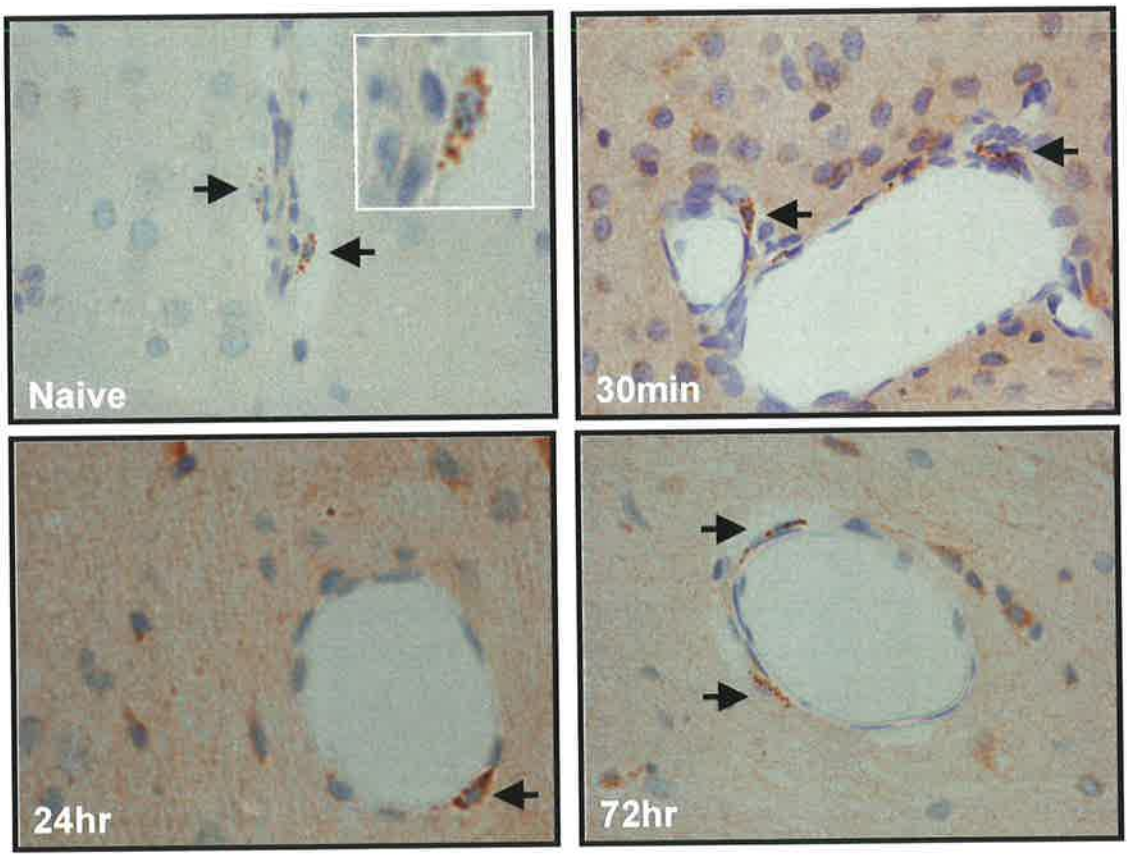

Figure 3.15: APP-IR in rat pericytes. Pericytic APP-IR (arrows) is seen in pericytes in a naive rat and at 30min, 24hr and 72hr following FPI (x400; inset: x1000, oil immersion). The APP-IR closely surrounds the nucleus of each pericyte. Endothelial cells are present between the pericytes and the vascular lumen.

3.6 Perivascular NK1-IR in rats

No perivascular NK1-IR was visible in any of the rat cerebral tissue examined in the study. This applies to all naïve and sham animals as well as all areas of the cerebral hemispheres examined following pMCAO, rMCAO and FPI at all timepoints. All these tissues, however, demonstrated NK1-IR in a subset of cortical neurons. Figure 3.16 shows these histological features in selected examples of control and pathological rat tissue.

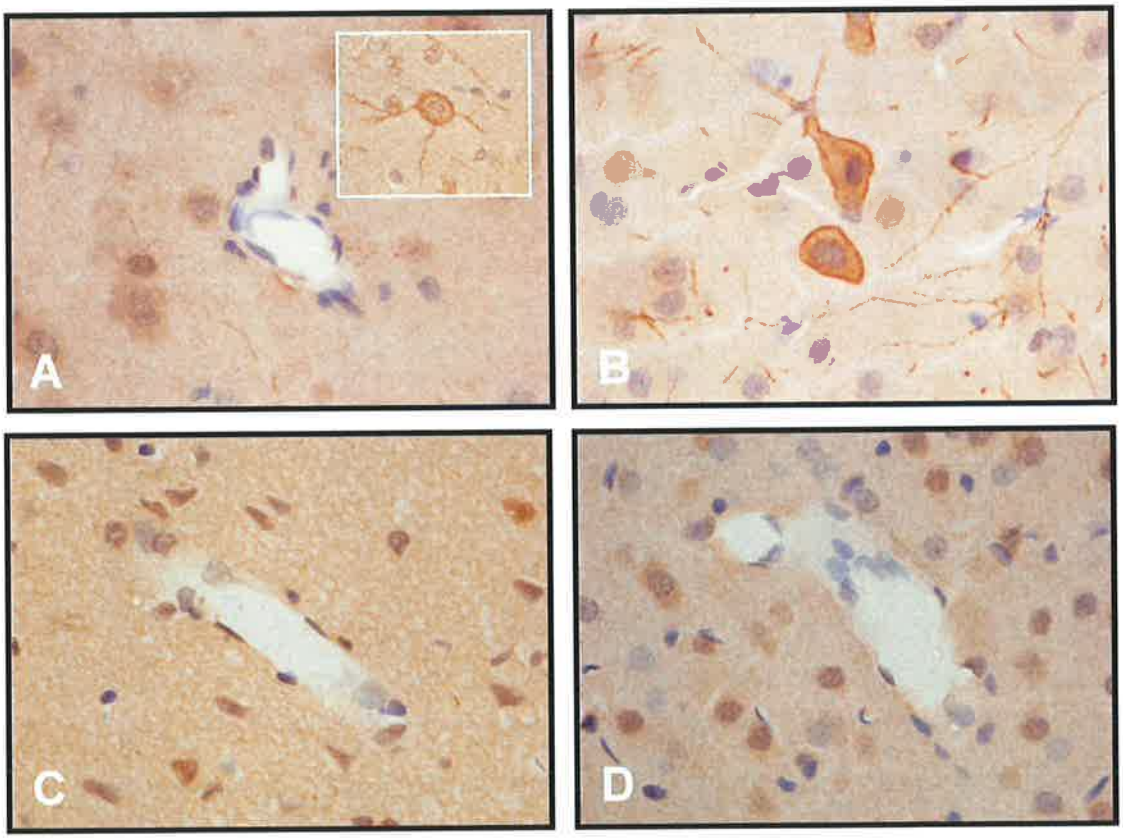

Figure 3.16: Naïve and pathological (post-MCAO and -FPI) rat cerebral tissue immunostained for NK1. **A**: Naïve rat tissue shows no perivascular IR and prominent IR in dendrites, some of which can be traced back to their nerve cell body (inset) (x400). **B**: Several neurons in the naïve rat tissue show a concentration of IR on the cell membrane (x400). **C**: At 2+24hr post-rMCAO there is no perivascular IR in the margins of the ischemic area (x200). **D**: At 24h post-FPI there is no perivascular IR in the margins of the contusion (x400).

3.7 Perivascular CGRP-IR in rats

No perivascular CGRP-IR was visible in any of the rat cerebral tissue examined in the study. This applies to all naïve and sham animals as well as all areas of the cerebral hemispheres examined following pMCAO, rMCAO and FPI at all timepoints. All these tissues, however, demonstrated CGRP-IR in a subset of cortical neurons. Figure 3.17 shows these histological features in selected examples of control and pathological rat tissue.

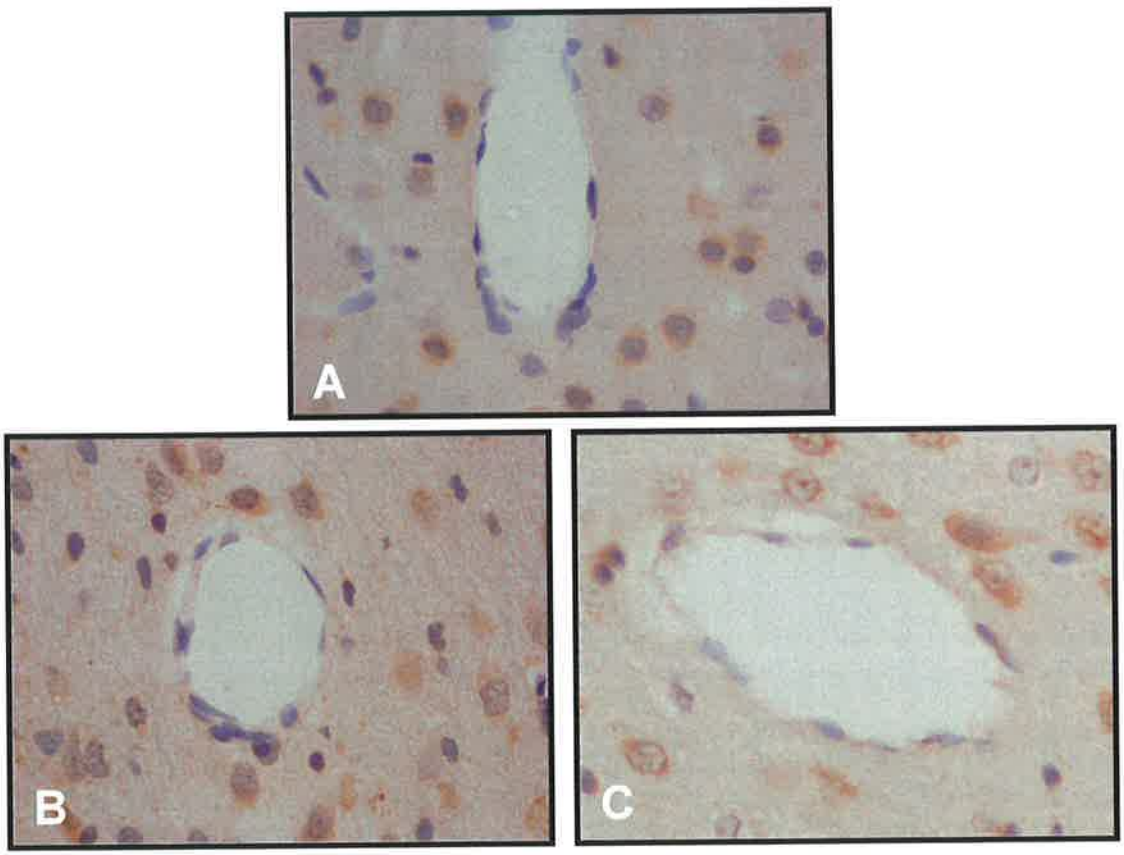

Figure 3.17: Naïve and pathological (post-MCAO and -FPI) rat cerebral tissue immunostained for CGRP. **A**: Naïve rat tissue shows no perivascular IR and some IR in a subset of neurons (x400). **B**: At 26hr post-pMCAO there is no perivascular IR in the margins of the ischemic area (x400). **C**: At 24h post-FPI there is no perivascular IR in the margins of the contusion (x400).

3.8 Human controls

The histological features of cerebral tissue from human controls are presented in Tables 3.11 and 3.12 and Figures 3.18 and 3.19.

Table 3.11: Human controls – neurological cause of death (SUDEP). A minimal to moderate degree of perivascular SP-IR was observed in astrocytic processes.

Case ID	H&E		Perivascular SP-IR		Albumin-IR	Perivascular nerve fiber APP-IR	Remarks
	Neurons	Astrocytes	Nerve fiber IR	Astrocytic processes IR			
Control 1	normal	normal	0	++	0	0	14♀
Control 2	normal	normal	0	++	0	0	26♂
Control 3	normal	normal	0	+	0	0	31♂
Control 4	normal	normal	0	+	0	0	33♂

0: not visible; +: minimal; ++: moderate; +++: severe; SUDEP: sudden unexplained death from epilepsy

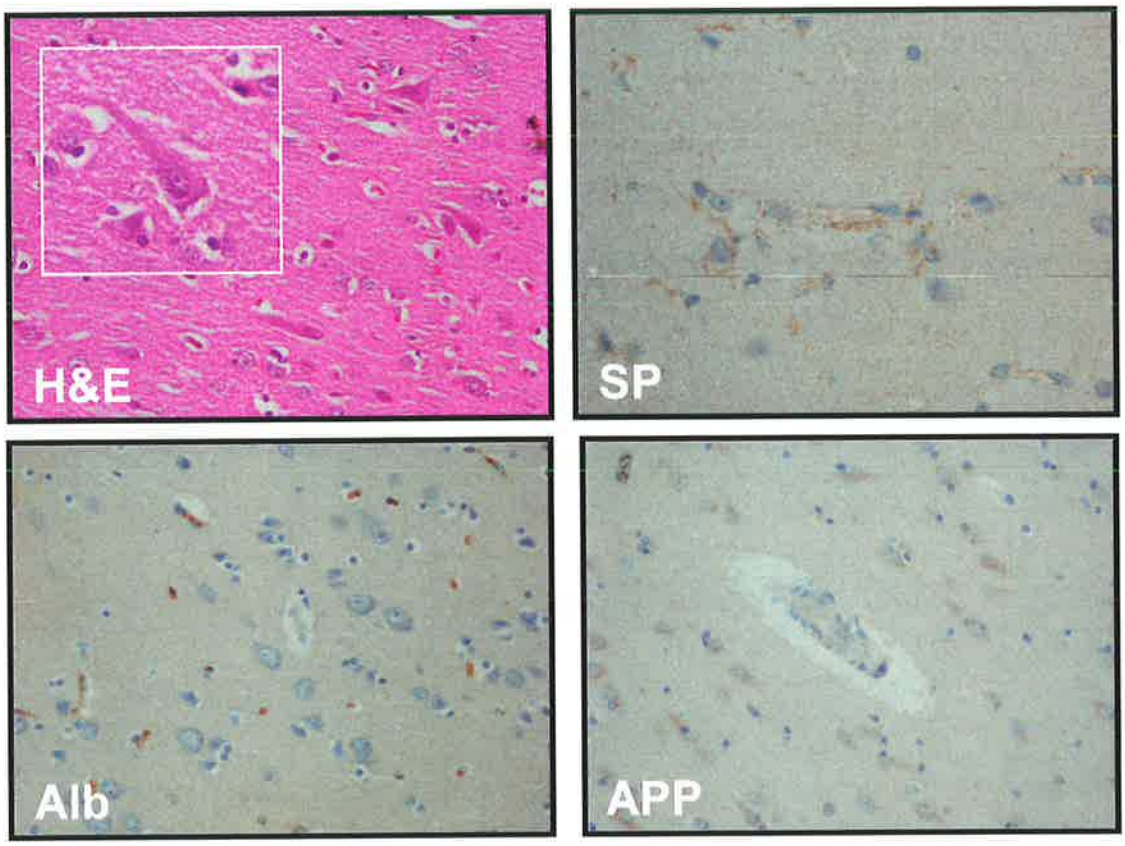

Figure 3.18: Human control – neurological cause of death (SUDEP). **H&E**: Cortical tissue shows normal H&E staining. Inset shows neuron of normal tinctorial character (x400; inset: x1000). **SP**: SP-IR is seen in perivascular astrocytic processes (x400). **Alb**: No extravascular albumin-IR is seen (x200). **APP**: No APP-IR is seen in association with the microvasculature (x400).

Table 3.12: Human controls – non-neurological causes of death. A minimal to moderate degree of perivascular SP-IR was observed in astrocytic processes.

Case ID	H&E		Perivascular SP-IR		Albumin-IR	Perivascular nerve fiber APP-IR	Remarks
	Neurons	Astrocytes	Nerve fiber IR	Astrocytic processes IR			
Control 5	normal	normal	0	++	0	0	39♀; generalized sepsis with pneumonia
Control 6	normal	normal	0	+	0	0	45♂; acute MI on top of chronic IHD
Control 7	normal	normal	0	+	0	0	56♀; acute MI
Control 8	normal	normal	0	++	0	0	66♂; metastatic bronchogenic carcinoma
Control 9	normal	normal	0	++	0	0	67♂; pneumonia
Control 10	normal	normal	0	++	0	0	79♀; COPD

0: not visible; +: minimal; ++: moderate; +++: severe; COPD: chronic obstructive pulmonary disease; IHD: ischemic heart disease; MI: myocardial infarction

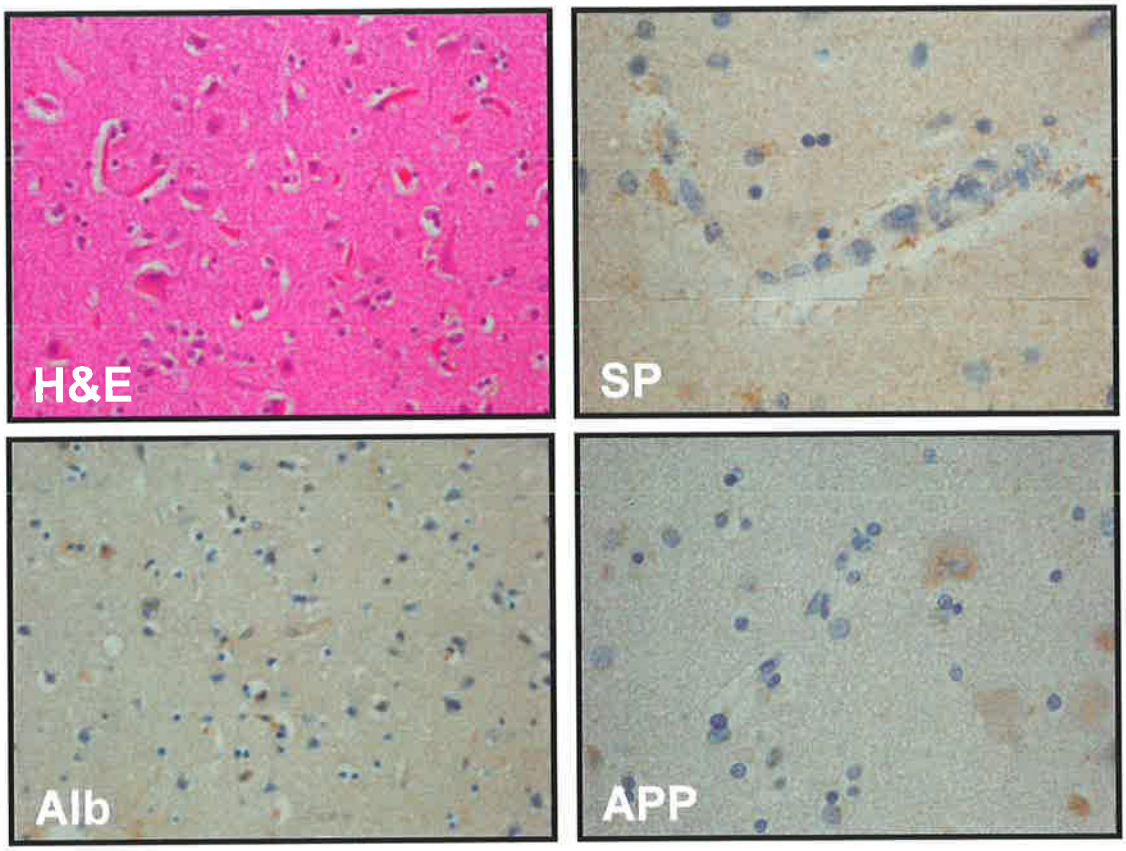

Figure 3.19: Human control – non-neurological cause of death (COPD). H&E: Cortical tissue shows normal H&E staining (x400). **SP**: SP-IR is seen in perivascular astrocytic processes (x400). **Alb**: No extravascular albumin-IR is seen (x200). **APP**: No APP-IR is seen in association with the microvasculature (x400).

3.9 Human cerebral infarct tissue

The histological features of human cerebral infarct tissue are presented in Tables 3.13 and 3.14 and Figures 3.20 and 3.21.

Table 3.13: Human cerebral infarct tissue – H&E staining. The timepoints examined generally showed neuronal injury and inflammatory cell infiltration in both the contusion and its margins.

Case ID	Post-occlusion survival time	Ischemic area			Margins				Remarks
		Neurons	Astrocytes	Inflammatory cells	Demarcation	Neurons	Astrocytes	Inflammatory cells	
I 1	1d	R	normal	P	N/A				65♀; hgic component; tissue block consisted only of ischemic area without margin
I 2	1-2d	R	normal	no	well-defined	R	normal	0	15♂
I 3	1-2d	R	normal	P	N/A				60♂; tissue block consisted only of ischemic area without margin
I 4	2d	R	normal	no	well-defined	R	normal	0	66♂
I 5	2d	D-R, N	normal	no	well-defined	D-R	normal	0	16♂
I 6	3-5d	R	normal	M, few P	N/A				32♀; tissue block consisted only of ischemic area without margin
I 7	~10d	R	normal	M, few P	well-defined	R	normal	M, few P	65♂; hgic component
I 8	10d	R	swollen	M	well-defined	R	swollen	M	38♀; hgic component
I 9	19d	R, G	decreased	M	well-defined	R	swollen	M	71♂; hgic component

D: dark cell change; D-R: dark to red cell change; G: ghost cells; hgic: hemorrhagic; M: macrophages; N: necrosis; N/A: not applicable; P: polymorphonuclear leukocytes; R: red cell change

Table 3.14: Human cerebral infarct tissue – immunohistochemical staining. At the examined timepoints, perivascular astrocytic SP-IR was decreased in the ischemic area and was similar to controls in the margins. At all timepoints, albumin-IR was severe in the ischemic area and moderate in the margins.

Case ID	Post-occlusion survival time	Ischemic area				Margins				Remarks
		Perivascular SP-IR		Albumin-IR	Perivascular nerve fiber APP-IR	Perivascular SP-IR		Albumin-IR	Perivascular nerve fiber APP-IR	
		Nerve fiber IR	Astrocytic processes IR			Nerve fiber IR	Astrocytic processes IR			
I 1	1d	0	0	P(s)	0	N/A				65♀; hgic component; tissue block consisted only of ischemic area without margin
I 2	1-2d	0	0	P(s)	0	0	++	P(m)	0	15♂
I 3	1-2d	0	0	P(s)	0	N/A				60♂; tissue block consisted only of ischemic area without margin
I 4	2d	0	0	P(s)	0	0	+	P(m)	0	66♂
I 5	2d	0	0	P(s)	0	0	++	P(m)	0	16♂
I 6	3-5d	0	0	P(s)	0	N/A				32♀; tissue block consisted only of ischemic area without margin
I 7	~10d	0	0	P(s)	0	0	+	P(m)	0	65♂; hgic component
I 8	10d	0	0	P(s)	0	0	++	P(m)	0	38♀; hgic component
I 9	19d	0	0	P(s)	0	0	+	P(m)	0	71♂; hgic component

0: not visible; +: minimal; ++: moderate; +++: severe; P(m): present (moderate); P(s): present (severe); hgic: hemorrhagic; N/A: not applicable

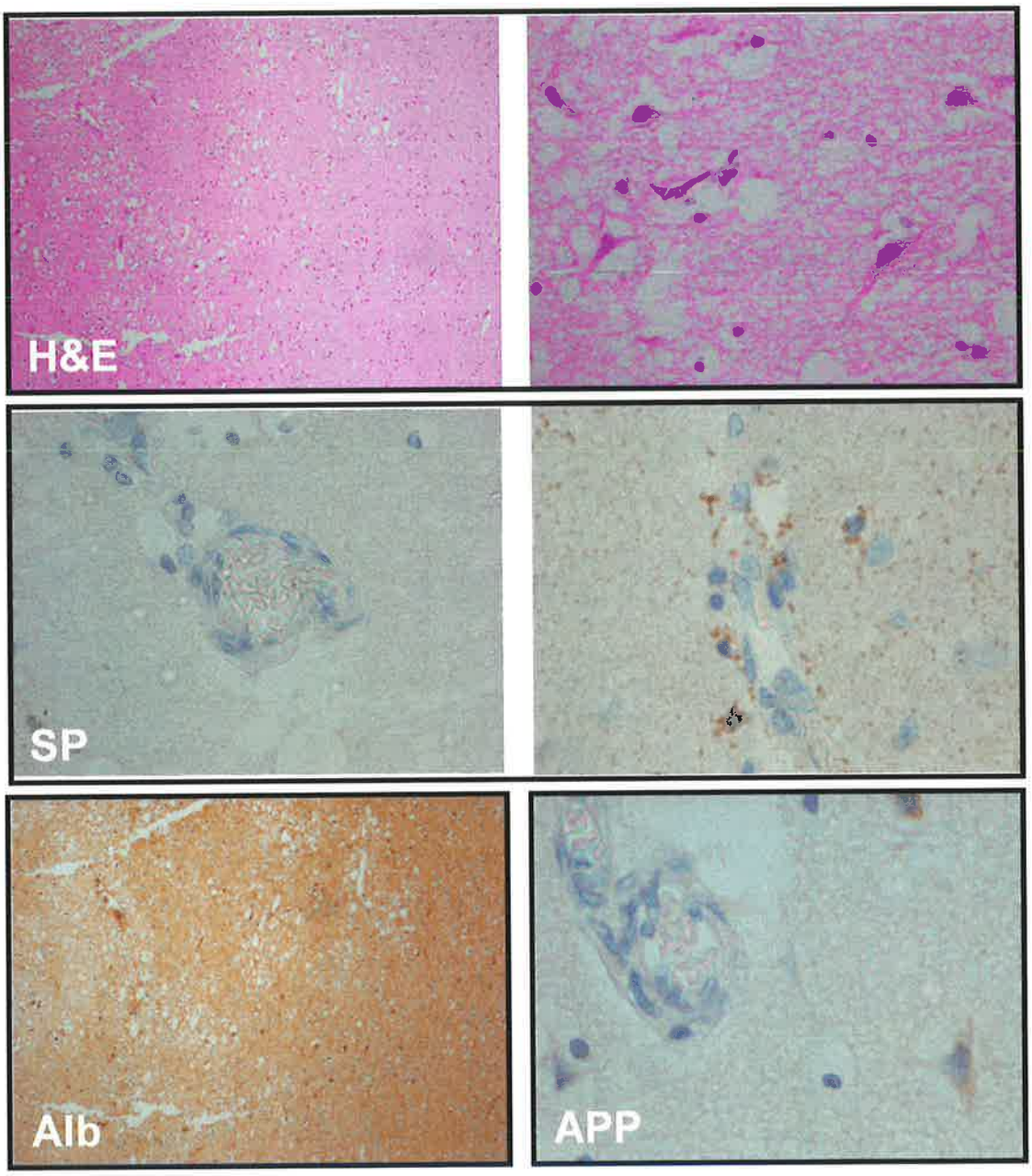

Figure 3.20: Human infarct at 1-2d post-occlusion. **H&E**: H&E staining shows well-defined demarcation between the ischemic area and its margins (Lt) as well as neuronal red cell change in the ischemic area (Rt). (Lt: x40; Rt: x400). **SP**: SP-IR in perivascular astrocytic processes is decreased in the ischemic area (Lt) but similar to controls in its margins (Rt) (x400). **Alb**: Extravascular albumin-IR is present in the ischemic area and the margins (x40). **APP**: No APP-IR is seen in association with microvasculature in the ischemic area (x400).

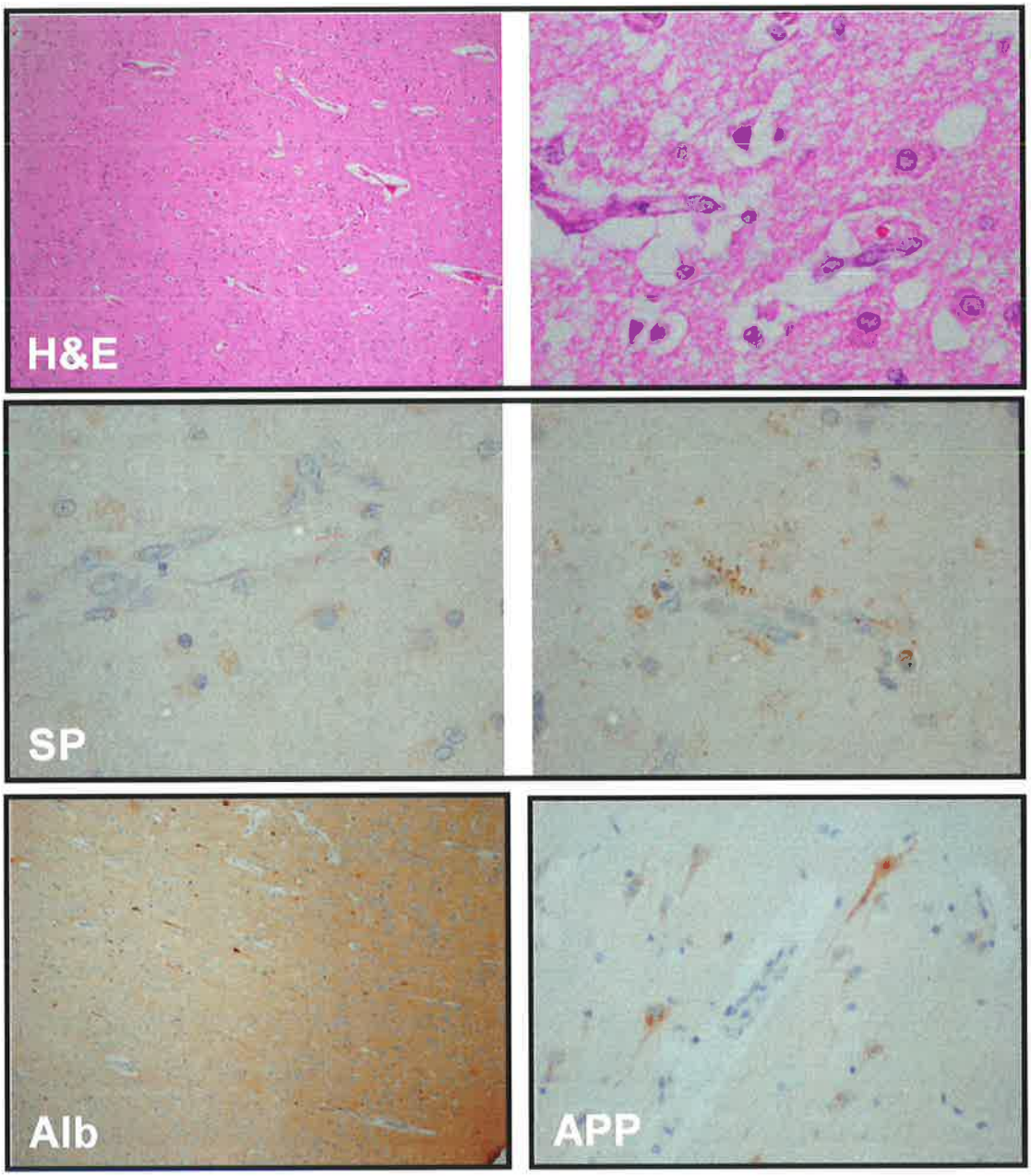

Figure 3.21: Human infarct at 10d post-occlusion. H&E: H&E staining shows the ischemic area and its margins (Lt) as well as neuronal red cell change and macrophage infiltration in the ischemic area (Rt). (Lt: x40; Rt: x400). **SP**: SP-IR in perivascular astrocytic processes is decreased in the ischemic area (Lt) but similar to controls in its margins (Rt) (x400). **Alb**: Extravascular albumin-IR is present in the ischemic area (x40). **APP**: Intense APP-IR is observed in some nerve cell bodies while no APP-IR is seen in association with the microvasculature in the ischemic area (x400).

3.10 Human cerebral contusion tissue

The histological features of human cerebral contusion tissue are presented in Tables 3.15 and 3.16 and Figures 3.22 and 3.23.

Table 3.15: Human cerebral contusion tissue – H&E staining. The timepoints examined showed neuronal injury and inflammatory cell infiltration in both the contusion and its margins.

Case ID	Post-injury survival time	Contusion			Margins				Remarks
		Neurons	Astrocytes	Inflammatory cells	Demarcation	Neurons	Astrocytes	Inflammatory cells	
C 1	1d	R	normal	P	ill-defined, patchy	R	normal	P	49♂; ↑ ICP
C 2	1d	R	normal	no	ill-defined, patchy	R	normal	no	23♂; ↑ ICP
C 3	2d	R	normal	P	well-defined, patchy	R	normal	P	28♂; ↑ ICP
C 4	2-3d	R	normal	P	well-defined	R	normal	P	82♀
C 5	4d	R	normal	P	well-defined	R	normal	P	17♂; ARDS; ↑ ICP; excluded from analysis due to severe autolysis
C 6	11d	R	swollen	M	well-defined	R	swollen	M	40♂; bronchopneumonia; ↑ ICP
C 7	12d	R	swollen	M	well-defined	R	swollen	M	41♂; ARDS; ↑ ICP
C 8	~3wk	R, G	decreased	M	well-defined	R	swollen	M	61♂; ↑ ICP

↑: increased; ARDS: adult respiratory distress syndrome; ICP: intracranial pressure; G: ghost cells; M: macrophages; N/A: not applicable; P: polymorphonuclear leukocytes; R: red cell change

Table 3.16: Human cerebral contusion tissue – immunohistochemical staining. At the examined timepoints, perivascular astrocytic SP-IR was decreased in the contusion and was either similar to controls or decreased in the margins. At all timepoints, albumin-IR was severe in the contusion and moderate in the margins.

Case ID	Post-injury survival time	Contusion				Margins				Remarks
		Perivascular SP-IR		Albumin-IR	Perivascular nerve fiber APP-IR	Perivascular SP-IR		Albumin-IR	Perivascular nerve fiber APP-IR	
		Nerve fiber IR	Astrocytic processes IR			Nerve fiber IR	Astrocytic processes IR			
C 1	1d	0	0	P(s)	0	0	+	P(m)	0	49♂; ↑ ICP
C 2	1d	0	0	P(s)	0	0	+	P(m)	0	23♂; ↑ ICP
C 3	2d	0	0	P(s)	0	0	0	P(m)	0	28♂; ↑ ICP
C 4	2-3d	0	0	P(s)	0	0	+	P(m)	0	82♀
C 5	4d	0	0	0	0	0	0	0	0	17♂; ARDS; ↑ ICP; excluded from analysis due to severe autolysis
C 6	11d	0	0	P(s)	0	0	0	P(m)	0	40♂; bronchopneumonia; ↑ ICP
C 7	12d	0	0	P(s)	0	0	+	P(m)	0	41♂; ARDS; ↑ ICP
C 8	~3wk	0	0	P(s)	0	0	0	P(m)	0	61♂; ↑ ICP

0: not visible; +: minimal; ++: moderate; +++: severe; P(m): present (moderate); P(s): present (severe) ↑: increased; ARDS: adult respiratory distress syndrome; ICP: intracranial pressure

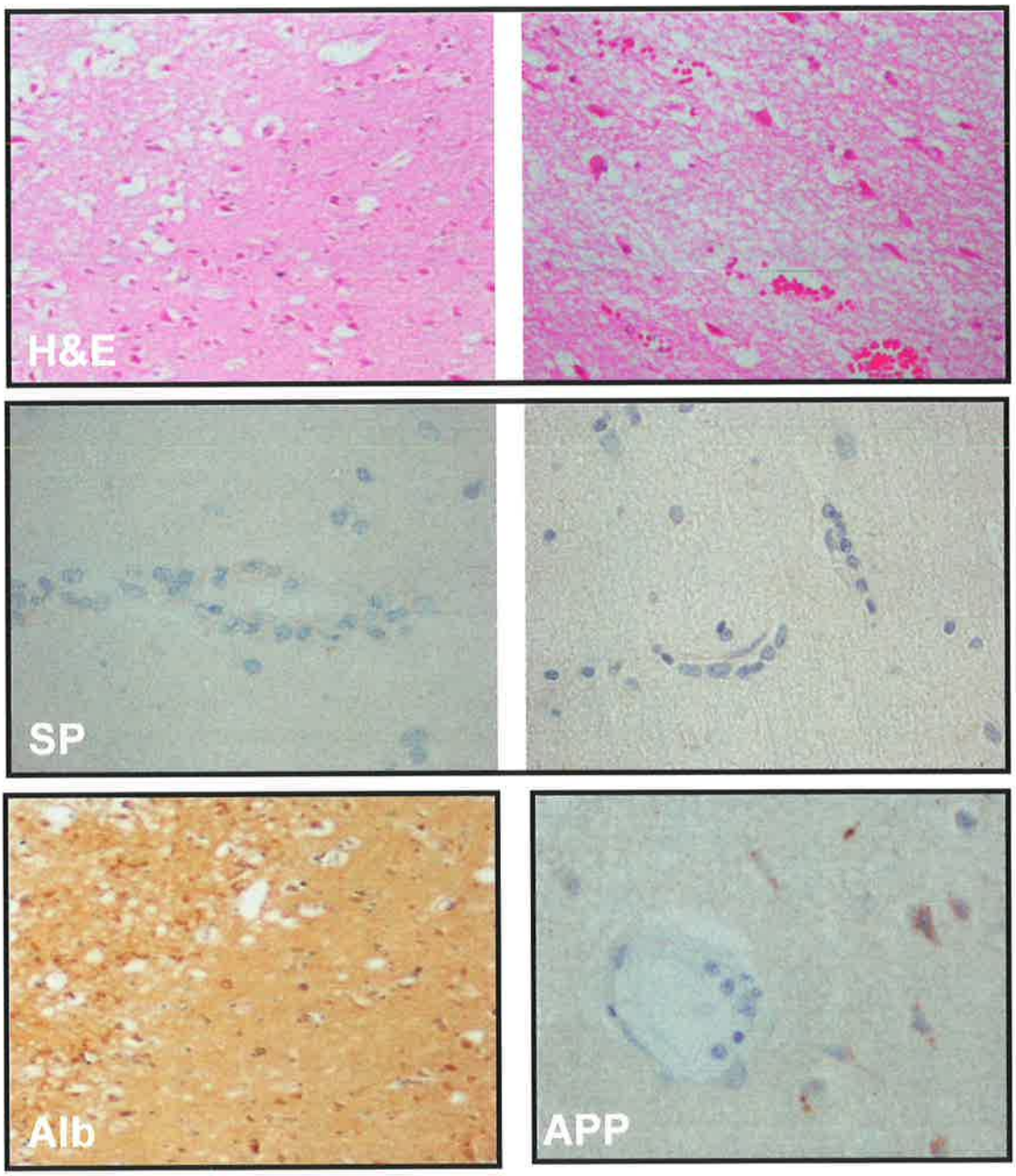

Figure 3.22: Human contusion at 2d post-injury. H&E: H&E staining shows demarcation between the contusion and its margins (Lt) as well as neuronal red cell change in the contusion (Rt). (Lt: x40; Rt: x400). **SP**: SP-IR in perivascular astrocytic processes is decreased in both the contusion (Lt) and its margins (Rt) (x400). **Alb**: Extravascular albumin-IR is present in the contusion and the margins (x40). **APP**: No perivascular APP-IR is in association with microvasculature (x400).

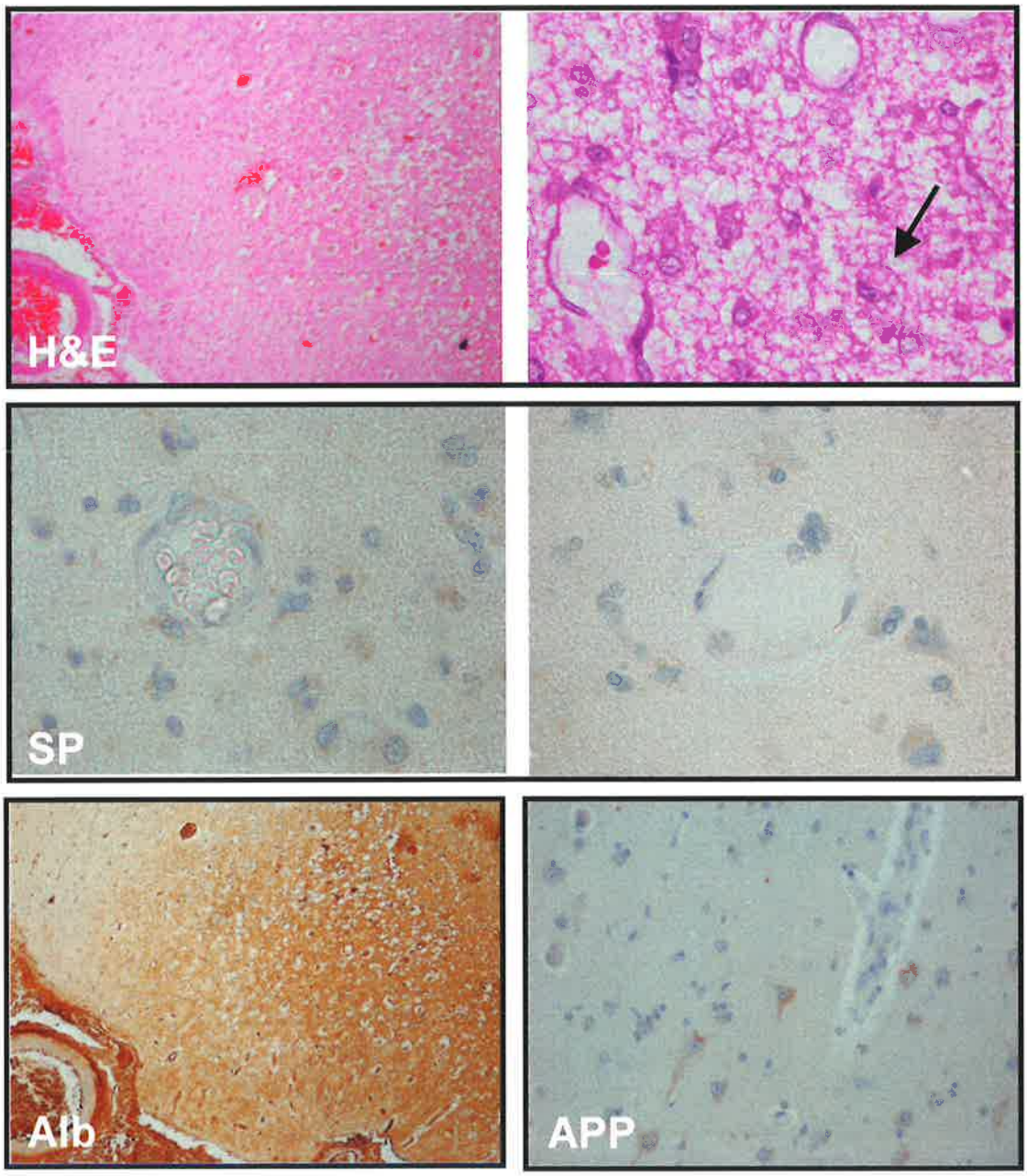

Figure 3.23: Human contusion at 11d post-injury. H&E: H&E staining shows demarcation between the contusion and its margins (Lt) as well as macrophage infiltration (arrow) in the contusion (Rt). (Lt: x40; Rt: x400). **SP**: SP-IR in perivascular astrocytic processes is decreased in both the contusion (Lt) and its margins (Rt) (x400). **Alb**: Extravascular albumin-IR is severe in the contusion and moderate in the margins (x40). **APP**: No perivascular APP-IR is in association with microvasculature in the contusion (x400).

Chapter 4

DISCUSSION

Contents

4.10.3 Limitations of the techniques applied to the tissue
4.10.3.1 Limitations of immunohistochemistry
4.10.3.2 Limitations of semi-quantitative grading system

4.11 **Conclusions**

4.1 Perivascular SP-IR

In all the tissue examined in this study, from both rats and humans, perivascular SP-IR was observed in astrocytic processes rather than in nerve fibers. This suggests that, at the examined timepoints, astrocytes might play a more important role than perivascular nerve fibers in the SP response in infarction and contusion. Perivascular astrocytic processes constitute part of the BBB and thus their SP content might be in an ideal location to exert an effect on the permeability of the barrier. In all the tissue examined, the perivascular astrocytic SP-IR was mainly concentrated around thin-walled venules which are the main site of inflammatory vascular leakage (McDonald *et al.* 1999).

Although the presence of SP in the nerve endings of perivascular fibers in the cerebral circulation has been reported in a large number of studies (Edvinsson *et al.* 1981, 1983c, Uddman *et al.* 1981, Edvinsson & Uddman 1982, Furness *et al.* 1982, Liu-Chen *et al.* 1983a, Yamamoto *et al.* 1983, Itakura *et al.* 1984, Jansen *et al.* 1992), these studies were primarily concerned with cerebral arteries, dural venous sinuses and pial arterioles rather than the intracerebral microvasculature. The presence of SP in intracerebral trigeminovascular nerve endings has mostly been inferred from these studies on extraparenchymal vessels. Little if any work has been done to anatomically characterize perivascular SP-IR in the intracerebral microcirculation. Thus, our inability to

detect SP-IR in perivascular nerve fibers related to the cerebral microvasculature does not contradict any anatomical evidence in the literature.

Our demonstration of SP-IR in perivascular astrocytic processes is supported by the findings of Barbato et al who also used confocal-based immunofluorescence to show an abundant presence of SP-IR in cultured human astrocytes (Barbato *et al.* 2005). Astrocytic SP-IR has also been demonstrated in normal human infants (Michel *et al.* 1986), around multiple sclerosis plaques in humans (Kostyk *et al.* 1989) and following carotid occlusion in the gerbil (Lin 1995).

4.2 Rat permanent MCAO

4.2.1 Characterization of SP-IR

In the control (naïve and sham) rats, moderate perivascular SP-IR was observed. Following pMCAO, perivascular SP-IR was increased in the margins of the ischemic area at all examined timepoints. In the ischemic area, pMCAO was associated with an increased perivascular SP-IR only at 5 and 7hr post-occlusion. At 24 and 26hr post-occlusion, perivascular SP-IR was decreased in the ischemic area. The early increase in SP-IR is in agreement with the findings of other studies conducted on rat models of focal cerebral ischemia (Yu

et al. 1997 and Stumm *et al.* 2001) although these studies did not explore the exact location of perivascular SP-IR. A possible explanation for the late decrease of perivascular SP-IR in the ischemic area is loss of astrocytes in this zone as seen on H&E staining. As mentioned earlier, perivascular SP-IR was observed in astrocytic processes rather than nerve fibers. Thus, a loss of astrocytes due to prolonged ischemia without reperfusion could deplete SP-IR in the tissue.

4.2.2 Characterization of albumin-IR

In the control (naïve and sham) rats, albumin-IR was not visible. At all examined timepoints following pMCAO, there was severe albumin-IR in the ischemic area and moderate albumin-IR in the margins. A possible explanation for the gradation of albumin-IR is that extracellular edema fluid accumulating in the lesion progressively spreads into the surrounding tissue with time. This pattern of edema fluid accumulation is well characterized in the literature (Iannotti and Hoff 1983, Bell *et al.* 1985, Todd *et al.* 1986).

4.2.3 Correlation of SP-IR and albumin-IR

In the margins, increased albumin-IR was associated with increased perivascular SP-IR at all timepoints following pMCAO. Similarly, in the ischemic area, at 5 and 7hr post-occlusion increased albumin-IR was

associated with increased perivascular SP-IR. However, in the ischemic area at 24 and 26hr post-occlusion increased albumin-IR was associated with decreased perivascular SP-IR. The decrease in perivascular SP-IR correlated with loss of astrocytes (see above).

4.3 Rat reperfused MCAO

4.3.1 Characterization of SP-IR

In the control (naïve and sham) rats, moderate perivascular SP-IR was observed. Following rMCAO, perivascular SP-IR was increased in both the ischemic area and its margins at both examined timepoints.

4.3.2 Characterization of albumin-IR

In the control (naïve and sham) rats, albumin-IR was not visible. At both examined timepoints following rMCAO, there was severe albumin-IR in the ischemic area and moderate albumin-IR in the margins. In addition, at 2+24hr post-occlusion, moderate albumin-IR extended beyond the margins of the ischemic area into the surrounding cerebral tissue. A possible explanation for the gradation of albumin-IR and its extension beyond the margins is that

extracellular edema fluid accumulating in the lesion progressively spreads into the surrounding tissue with time.

4.3.3 Correlation of SP-IR and albumin-IR

In the margins, increased albumin-IR was associated with increased perivascular SP-IR at both examined timepoints following rMCAO. Similarly, in the ischemic area, albumin-IR and perivascular SP-IR were concomitantly increased at both examined timepoints.

4.4 Rat FPI

4.4.1 Characterization of SP-IR

In the control (naïve and sham) rats, moderate perivascular SP-IR was observed.

Following FPI, perivascular SP-IR was increased in both the contusion and its margins at all timepoints except at 72hr where it was decreased in the contusion. The increase in SP-IR is concordant with the findings of Nimmo et al. in the rat (Nimmo *et al.* 2004). A possible explanation for the late decrease of perivascular SP-IR in the contusion is loss of astrocytes in this zone as seen on H&E staining. As mentioned above, perivascular SP-IR was observed in

astrocytic processes rather than nerve fibers. Thus, a loss of astrocytes at this timepoint might have possibly depleted SP-IR in the tissue.

4.4.2 Characterization of albumin-IR

In the control (naïve and sham) rats, albumin-IR was not visible. At all examined timepoints following FPI, there was severe albumin-IR in the contusion. In the margins, albumin-IR was not visible at 30min post-injury, moderate at 5hr post-injury and severe at 24, 48 and 72hr post-injury. In addition, at 24, 48 and 72hr post-injury, moderate albumin-IR was present beyond the margins of the contusion in the surrounding cerebral tissue. A possible explanation for this spatiotemporal evolution in the distribution and degree of albumin-IR is that extracellular edema fluid accumulating in the lesion progressively spreads into the surrounding tissue with time. Thus, at 30min post-injury the albumin-IR was localized to the contusion. After 5hr some albumin-IR might have spread to the margins and, within 24-72hr, some albumin-IR might have spread farther still beyond the margins into the surrounding tissue.

4.4.3 Correlation of SP-IR and albumin-IR

In the margins, increased perivascular SP-IR was associated with varying degrees of albumin-IR that increased with increasing post-injury survival time. In the contusion, increased albumin-IR was associated with increased perivascular SP-IR at all examined timepoints post-injury. At 30min post-injury, increased perivascular SP-IR in the contusion and margins was associated with increased albumin-IR in the contusion. At 5, 24, 48 and 72hr post-injury, increased perivascular SP-IR in the contusion and margins was associated with increased albumin-IR in both zones.

4.5 Human infarcts and contusions

4.5.1 Characterization of SP-IR

In the control tissue, moderate to equivocal/minimal perivascular SP-IR was observed. With ischemic insults as well as following blunt trauma, at all examined timepoints, perivascular SP-IR was decreased in the core (ischemic area or contusion) of the lesion and showed little change in the margins. It is not clear why perivascular SP-IR was decreased in the core of the lesion. As mentioned above, in all the tissue examined perivascular SP-IR was observed in astrocytic processes rather than in nerve fibers. Thus, a pathological loss of

astrocytes might possibly deplete SP-IR in the tissue. However, except for the latest examined timepoint (19d), all the examined timepoints revealed no apparent loss of astrocytes in the core of the lesion as most of the ischemic areas had selective neuronal necrosis and not pan-necrosis. The data from this study does not allow for an explanation of the observed depletion of perivascular SP-IR and further investigation is needed to gain a greater understanding of its mechanism.

Only one published study has quantified SP following human cerebral ischemia (Bruno *et al*, 2003). This study demonstrated that the levels of SP in serum drawn from human patients were increased at 12hr following the clinical onset of ischemia and increased to a lesser extent at 12-24hr. This does not conflict with our results since, as mentioned below with the limitations of the study, there was no tissue available in our *post mortem* tissue archives that represented these early timepoints within the first 24h following ischemia. Therefore, we were unable to make an assessment of SP-IR at these timepoints. Furthermore, the fact that Bruno *et al.* reported a decline in the level of serum SP beyond 12hr suggests that at the later timepoints examined in our study the serum SP might not be elevated. Furthermore, there is no data to indicate that the level of SP in the serum as measured by Bruno *et al.* is a direct correlate of SP-IR in neural tissue. Also, while our results are entirely derived from cases of clinical cerebrovascular stroke, Bruno *et al.* described that the levels of SP in the serum were significantly higher in transient ischemic

attack (lasting less than 24hr) than in completed stroke. Further work is required to characterize the serum levels of SP at later stages in the evolution of cerebral infarction.

4.5.2 Characterization of albumin-IR

In the control tissue, albumin-IR was not visible. With MCA territory ischemic insults as well as following blunt trauma to the MCA territory, at all examined timepoints, albumin was severe in the core (ischemic area or contusion) of the lesion and moderate in the margins. A possible explanation for the gradation of albumin-IR is that extracellular edema fluid accumulating in the lesion progressively spreads into the surrounding tissue with time.

4.5.3 Correlation of SP-IR and albumin-IR

In the margins, at all examined timepoints, increased albumin-IR was associated with little change in perivascular SP-IR. In the core, whereas albumin-IR was increased at all examined timepoints, perivascular SP-IR was decreased. There is no clear explanation for this discrepancy between albumin-IR and perivascular SP-IR in the two zones and further work is required to explore this.

4.6 Comparison of experimental and human findings

4.6.1 SP-IR

Comparing the groups of rat tissue following both MCAO and FPI revealed that the core and margins of the lesion, at all but the latest examined timepoints, showed increased perivascular SP-IR. At these later timepoints (24 and 26hr post-pMCAO and 72hr post-FPI) the core of the lesion demonstrated a decrease in perivascular SP-IR. The fact that this decreased SP-IR always coincided with a loss of astrocytes implies that these cells play an important role in the accumulation of perivascular SP-IR following MCAO and FPI. Furthermore, at 26hr post-occlusion, both the decreased perivascular SP-IR and the loss of astrocytes were observed following pMCAO but not rMCAO. This suggests that reperfusion of the ischemic area might be associated with a salvaging effect on astrocytes and a consequent accumulation of SP-IR.

In contrast to rat tissue, human tissue in the setting of both infarction and contusion showed no increase in perivascular SP-IR. However, the examined human tissue generally represented later timepoints than those of the rat tissue and therefore might not be directly comparable. Tissue from corresponding timepoints in both species was not available for technical reasons detailed in

the section on limitations of the study. It is also possible that the astrocytic SP response in both pathologies is different in humans compared to rats but further investigations are necessary to fully characterize astrocytic SP in both species in normal and pathological settings.

4.6.2 Albumin-IR

Rat and human control tissue both showed no extravascular albumin-IR. Following both blunt trauma and vascular occlusion, all the rat and human tissue examined in this study demonstrated extravascular albumin-IR. The albumin-IR was generally greater in the core of the lesion than in the margins. Furthermore, at the latest timepoints examined following rat rMCAO (2+24hr) and rat FPI (24, 48 and 72hr), albumin-IR was present beyond the margins of the lesion in the surrounding cerebral tissue. This suggests that with the passage of time following MCAO and FPI, extracellular edema fluid accumulating in the lesion spreads into the surrounding tissue. In addition, at 26hr post-occlusion, albumin-IR outside the margins of the lesion was observed following rMCAO but not pMCAO. This suggests that reperfusion of the ischemic area might be associated with an increased accumulation and spread of edema. This is supported by several studies demonstrating that the progression of edema is halted in absolute deprivation of blood supply which implies that a certain amount of blood flow must be preserved for edema to develop (Iannotti and Hoff 1983, Crockard *et al.* 1980, Kogure *et al.* 1981).

Additional studies using MRI at different timepoints are recommended to further explore effect of reperfusion on edema in this setting.

With human tissue, it was not possible in this study to assess the albumin-IR outside the lesion margins due to the use of previously sampled archival tissue as discussed in the section on limitations of the study. In the future, a cohort of *post-mortem* brain tissue could be specifically sampled to allow investigation of the extent of albumin-IR in greater detail.

4.6.3 Correlation of SP-IR and albumin-IR

In the setting of infarction and contusion, increased extravascular albumin-IR was associated with increased perivascular SP-IR only in rat tissue but not in human tissue at the timepoints examined. This implies that, in the rat, increased perivascular SP might play a role in the accumulation of edema with infarction and contusion. Although increased SP-IR was not observed in human tissue, this might be related to the unavailability of tissue from earlier timepoints and further investigation is warranted to provide greater detail on any possible involvement of SP with edema in these settings.

4.7 Perivascular APP-IR

In all the tissue examined, immunostaining for APP demonstrated no APP-IR in perivascular nerve fibers. APP-IR was observed, however, in rat pericytes in control and sham animals and following FPI but not in the ischemic area following MCAO.

The absence of visible APP-immunoreactivity in perivascular nerve fibers in the examined pathological tissue does not rule out that these fibers might be injured. Although APP is known to be a sensitive marker for axonal injury (Blumbergs *et al.* 1995), the sensitivity of APP as an indictor of damage in perivascular axons has never been assessed and there is no account in the literature of APP-IR in perivascular axons.

Although there is no evidence in the literature of the presence of APP-IR in rat pericytes, Verbeek *et al.* reported APP-IR in cultured human brain pericytes and used immunoelectron microscopy to demonstrate its presence in small intracellular vesicles that were characterized as lysosomes (Verbeek *et al.* 2002). Our results do not allow us to make any speculations about the functional significance of the observed pericytic APP-IR nor to explain its detection in rat tissue and not in human tissue.

4.8 Perivascular NK1-IR

In all the rat tissue examined, no perivascular NK1-IR was observed in relation to the intracerebral microvasculature. Although numerous *in vitro* studies have described the presence of NK1-IR in cultured endothelial cells and astrocytes, these findings have no parallel in *post mortem* tissue. However, the absence of visible perivascular NK1-IR in our study does not rule out a role for SP in influencing the BBB. It is possible that activation of the NK1 receptor at some distance from the BBB indirectly leads to the activation of other receptors near the BBB. Further investigation is required to characterize the exact anatomical and functional relationship of this receptor to the BBB.

4.9 Perivascular CGRP-IR

In all the rat tissue examined, no perivascular CGRP-IR was observed in relation to the intracerebral microvasculature. Our results lend further support to the belief that CGRP is not involved in altering vascular permeability in the setting of inflammation (Brain 1997). This is in agreement with the fact that the presence of CGRP has never been demonstrated around venules and capillaries in the literature. Moreover, although the presence of CGRP has been reported in perivascular nerve fibers related to arterioles in the cerebral

circulation, this has only been demonstrated in pial arterioles on the surface of the cerebrum and not in intracerebral arterioles (Edvinsson *et al.* 1995).

4.10 Limitations of the study

4.10.1 Limitations of human tissue

4.10.1.1 Restriction of observable timepoints

Human cerebral infarcts do not tend to cause death within the first day after onset. Consequently, there are no tissue samples available in our archives that represent this early interval and this limits any comparison with the short-surviving experimental groups. This limitation is quite important because an understanding of the early pathology would help to better evaluate the potential benefit of early pharmacologic intervention. It is hoped that, in the future, the resolution and magnification powers of imaging modalities will become greater to allow the examination of the brains of living patients at a microscopic level.

4.10.1.2 Pathological complexity

The results obtained from studying human tissue often do not only reflect the changes produced by the investigated pathological conditions. In many cases,

these results are confounded by treatment received before death, co-existing pathological conditions, and complications of the initial lesion. To minimize this effect as much as possible, the selection of cases for this study was based on an examination of both histopathological reports and clinical records in order to select cases that had as little confounding factors as possible. Furthermore, any unavoidable confounding factors were indicated in the results section.

4.10.1.3 Tissue fixation and *post mortem* delay

Because human tissue can only be fixed by immersion and not perfusion, this delays the penetration of the fixative into the tissue and decreases the quality of fixation. In addition, the logistics of hospital mortuary work make it impossible to standardize the time between the death of a patient and fixation. Therefore, the interval between death and tissue fixation – during which autolysis is delayed by refrigeration of the body is – is variable from case to case. Nevertheless, the post mortem interval generally did not exceed three days and within this time frame, this inevitable variability did not cause a notable difference in the level of staining in the control tissue for any of the stains used. Furthermore, none of the examined tissue showed histological evidence of marked autolysis except in one case and this was indicated in the results.

4.10.1.4 Pathological complexity

Although each post mortem tissue specimen used as a control was obtained from a patient who died due to an illness that was unrelated to cerebral edema, cerebral infarction or contusion, it still cannot be dismissed that the cause of death might have had an effect on any of the molecules examined in this study. In order to avoid the possible relationship between a particular cause of death and any of the studied molecules, control tissue was obtained from a range of cases with a variety of fatal conditions (indicated in the results section). The fact that the controls showed more or less similar levels of these molecules suggests that we managed to avoid any such confounding cause of death. However, it is still not possible to exclude that the actual process of death itself, regardless of the causative illness, might have an effect on any of the studied molecules. Further investigation is required to exclude any such relationship.

4.10.1.5 Previous sampling of archival tissue

Our human tissue archives consist of blocks of tissue that were routinely sampled over the years with a focus on sampling the actual lesions rather than the distant better-preserved tissue. For this reason, the blocks available to this study generally consisted of tissue from the core of the lesion and its margins with none of the immediately adjacent tissue of the brain. Thus, it was not possible to examine or comment on the parts of these brains away from the

lesions. With rat brains, this limitation was not encountered since it was intended to examine the entire brain and not only the lesions. Furthermore, the much smaller size of the rat brain allowed for a single tissue block to include a coronal section of the entire brain.

4.10.2 Limitations of rat tissue

4.10.2.1 Restriction of observable timepoints

Using rat models of infarction and contusion allowed the examination of earlier timepoints that could not be examined with the human tissue as previously discussed. However, it is a technical problem in the rat model of MCAO to extract the brain after one day post-occlusion because the infarcted tissue becomes too friable to handle. In the future, in order to overcome this difficulty, it would be worthwhile to attempt to modify the techniques of tissue extraction or design specific instruments for this particular task.

4.10.2.2 Number of animals used

This study was designed to allow the examination of several pathological settings at a large number of timepoints. Examining more timepoints meant that a relatively small number of animals were studied at each timepoint following MCAO and FPI. Furthermore, this study was intended to include a

quantitation of homogenized rat cerebral tissue using western blot analysis. A group of rats were processed for this purpose but there was technical difficulty in applying the western blotting technique using the antibodies available for SP. The rat brains intended for quantitation are currently stored in a freezer at -70°C and will be further studied as soon as quantitation becomes technically possible.

4.10.2.3 Reproducibly of the lesion

Although care was taken to perform the insult-resulting procedures in both animal models in a consistent manner, the lesions produced tended to vary in severity. This variation was minimized as much as possible by adhering to a strict protocol. In addition, inter-operator variability was not a concern since all the animals in each model were operated on by a single person. In any case, the fact that all the tissue was examined histologically provided an intrinsic control mechanism that correlated any changes in the investigated molecules with well-characterized general pathological changes seen on routine H&E staining.

4.10.2.4 Applicability of pathological model

In addition to the previously described possible difference between rat and human physiology, there is also the issue of applicability of the model of injury

induced in the rat to the actual injury that is encountered in humans. As discussed in the materials and methods section, great care has been taken in this study regarding both the choice of relevant experimental models and the interpretation of the results obtained from these models strictly within the limits of their applicability.

4.10.2.5 Possible differences between species

A limitation commonly associated with the use of experimental animal models – especially when investigating the function of a molecule such as SP – is that it is not certain that the function of the molecule in the animal is the same as its function in humans. Indeed, it was one of the aims of this study to compare the changes in SP between rats and humans. However, the unavailability of pathological tissue from comparable timepoints in both species, due to the technical reasons described above, limits our ability to comment on the differences between these species. Further investigations are necessary to fully characterize SP in both species in normal and pathological settings.

4.10.3 Limitations of the techniques applied to the tissue

4.10.3.1 Limitations of immunohistochemistry

i. Antibody recognition

The validity of immunohistochemical staining is directly related to the specificity and sensitivity of the antibodies used to recognize the studied antigens. In this study, care was taken to select well-tested antibodies from reliable commercial sources and to ensure that the antibodies are suitable for use with formalin-fixed paraffin-embedded tissue. In addition, before being used on study tissue, the antibodies were tested in our laboratory on control tissue containing anatomical structures of known immunoreactivity to ensure antibody specificity and to identify the optimal concentration of antibody that yields the best signal to noise ratio. Furthermore, the control tissue of known immunoreactivity was stained again with every batch of experimental tissue stained in order to validate the results obtained from each individual staining session. This control tissue was always stained both with and without the primary antibody to serve as both a positive and a negative control respectively.

However, one limitation that cannot be avoided is that we cannot exclude that the ability of an antibody to recognize an antigen might be affected by a change in the conformation of the antigen molecule if it is bound to another molecule in

the tissue. For example, there is no data currently available to guarantee that the antibody that recognizes the SP molecule will still recognize it if it is bound to the NK1 receptor. It is hoped that, with time, the increasing interest in neuropeptide research will lead to a more thorough characterization of the antibodies available against these molecules and their receptors.

ii. Potential variability in intensity of staining

It is common for the intensity of immunohistochemical staining to vary slightly from one staining session to the other even if the tissues stained in both sessions have the same content of antigen. This is because staining is affected by a large number of variables including the exact length of incubation time in the various solutions and the exact degree of freshness of solutions prepared throughout the procedure. For our semi-quantitative purposes, the effect of this variability was avoided by staining all the tissue to be compared for each stain – including both study tissue and control tissue as well as standard tissue of known immunoreactivity – in one single session.

4.10.3.2 Limitations of semi-quantitative grading system

A fundamental limitation of the methodology used in this study was the inability to quantitate SP using western blot analysis due to technical problems.

4.11 Conclusions

Our results demonstrated, in all examined rat and human tissue, that perivascular SP-IR was present in astrocytic processes rather than in nerve fibers. Furthermore, no APP-immunoreactive perivascular nerve fibers were observed. This implies that perivascular astrocytic processes might be more important than perivascular nerve fibers in any effect that SP may have on the BBB in the settings of infarction and contusion. In addition, the results generally showed, in rat infarcts and contusions, an increase in SP-IR and albumin-IR. This suggests that, in the rat, increased SP in the setting of infarction and contusion might contribute to vasogenic edema. Human tissue, however, showed no increase in SP-IR following infarction or contusion in spite of the presence of albumin-IR. These observations in human tissue might be related to the unavailability of tissue for examination at earlier timepoints post-insult and further investigation is warranted to provide greater detail on any possible involvement of SP with edema in these settings.

Chapter 5

REFERENCES

Abbott NJ. Inflammatory mediators and modulation of blood-brain barrier permeability. *Cell Mol Neurobiol* 2000; 20:131-47.

Aiyar N, Baker E, Nambi P et al. Characterisation of CGRP receptors in various regions of gerbil brain. *Neuropeptides* 1994; 26: 313-17.

Amara SG, Jonas V, Rosenfeld MG et al. Alternative Processing in calcitonin gene expression generates mRNAs encoding different polypeptide products. *Nature* 1982; 298: 240-44.

Ames A, Wright LW, Kowada M et al. Cerebral ischemia: II. The no-reflow phenomenon. Am J Pathol 1968; 52: 437-53

Annunziata P, Ciooi C, Toneatto S et al. HIV-1 gp120 increases the permeability of rat brain endothelium cultures by a mechanism involving substance P. *AIDS* 1998;12:2377-85.

Annunziata P, Cioni C, Santonini R et al. Substance P antagonist blocks leakage and reduces activation of cytokine-stimulated rat brain endothelium. *J Neuroimmunol* 2002; 131(1-2):41-9.

Arbab MAR, Delgado T, Wiklund L et al. Brain stem terminations of the trigeminal and upper spinal ganglia innervation of the cerebrovaecular system: WGA-HRP transganglionic study. *J Cereb Blood Flow Metab* 1983; 8:54-63.

Arneric SP. Basal forebrain neurons modulate cortical cerebral blood flow: increases by nicotinic cholinergic mechanisms. J *Cereb Blood Flow Metab* 1989; 9:502-9.

Aronson H. Über Nerven und Nervendigungen in der Pia Mater Z *Med Wissenschaft* I890;28:594-5.

Astrup I, Siesjo BK & Symon L. Thresholds in cerebral ischemia - the ischemic penumbra. *Stroke* 1981; 12: 723-5.

Atalay B, Bolay H, Dalkara T et al. Transcorneal stimulation of trigeminal nerve afferents to increase cerebral blood flow in rats with cerebral vasospasm: a noninvasive method to activate the trigeminovascular reflex. *J Neurosurg* 2002; 97(5):1179-83.

Auer LM, Johansson BB & Lund S. Reaction of pial arteries and veins to sympathetic stimulation in the cat. *Stroke* 1981; 12: 528-31.

Auer RN & Sutherland GR. Hypoxia and related conditions. In: Graham DI, Lantos PL, eds. *Greenfield's Neuropathology*, 7th ed. New York: Arnold, 2002: 233-80.

Ayata C & Ropper AH. Ischaemic Brain Oedema. *J Clin Neurosci* 2002; 9(2):113-24.

Azaryan AV & Galoyan AA. Substrate specificity of cerebral cathepsin D and high-MR aspartic endopeptidase. *J Neurosci Res* 1988; 19(2):268-71.

Baird AE, Benfield A, Schlaug G et al. Enlargement of human cerebral ischemic lesion volumes measured by diffusion-weighted magnetic resonance imaging. *Ann Neurol* 1997: 41(5): 581-9.

Barzo P, Marmarou A, Fatouros P et al. Acute blood-brain barrier changes in experimental closed head injury as measured by MRI and Gd-DTPA. *Acta Neurochir Suppl* 1997; 70: 243-6.

Beaumont A, Marmarou A, Hayasaki K et al. The permissive nature of blood brain barrier (BBB) opening in edema formation followingtraumaticbraininjury. *Acta Neurochir Suppl* 2000; 76:125-9.

Beaumont A, Marmarou A, Fatouros P et al. Secondary insults worsen blood brain barrier dysfunction assessed by MRI in cerebral contusion. *Acta Neurochir Suppl* 2002; 81:217-9.

Beggs JL & Waggener JD. Transendothelial vesicular transport of protein following compression injury to the spinal cord. *Lab Invest* 1976; 34: 428-39.

Bell BA, Symon L & Branston NM. CBF and time thresholds for the formation of ischemic cerebral edema, and effect of reperfusion in baboons. *J Neurosurg* 1985: 62(1): 31-41.

Benedikt M. Über die Innervation des Plexus Choriodeus Inferior. *Virchows Arch Pathol Anat Physiol* 1874; 59:395-400.

Bergner AJ, Murphy SM & Anderson CR. After axotomy, substance P and vasoactive intestinal peptide expression occurs in pilomotor neurons in the rat superior cervical ganglion. *Neuroscience* 2000; 96(3):611-8.

Besson VC, Chen XR, Plotkine M et al. Fenofibrate, a peroxisome proliferator-activated receptor alpha agonist, exerts neuroprotective effects in traumatic brain injury. *Neurosci Lett* 2005; 388(1):7-12.

Bill A & Linder J. Sympathetic control of cerebral blood flow in acute arterial hypertension. *Acta Physiol Scand* 1976; 96:114-21.

Blumberg S, Teichberg VI, Charli JL et al. Cleavage of substance P to an N-terminal tetrapeptide and a C-terminal heptapeptide by a post-proline cleaving enzyme from bovine brain. *Brain Res* 1980; 192(2):477-86.

Blumbergs PC, Scott G, Manavis J et al. Topography of axonal injury as defined by amyloid precursor protein and the sector scoring method in mild and severe dosed head injury. *J Neurotrauma* 1995; 12: 565-72.

Brain SD. Sensory neuropeptides: their role in inflammation and wound healing. *Immunopharmacology* 1997;37:133-52.

Bruno G, Tega F, Bruno A et al. The role of substance P in cerebral ischemia. *Int J Immunopathol Pharmacol* 2003; 16(1):67-72.

Bullock R, Statham P, Patterson J et al. The time course of vasogenic edema after focal human head injury-evidence from SPECT mapping of blood brain barrier deficit. Acta *Neurochir* 1990; 51 (Suppl): 286-8.

Bullock R, Maxwell WL, Graham DI et al. Glial swelling following human cerebral contusion: an ultrastructural study. *J Neurol Neurosurg Psychiatry* 1991; 54: 427-34.

Bullock MR, Lyeth BG & Muizelaar J. Current status of neuroprotection trials for traumatic brain injury: lessons from animal models and clinical studies. *Neurosurgery* P 1999; 45:207-17.

Busija DW, Leffier CW & Wagerle LC. Responses of newborn pig pial arterioles to sympathetic nerve stimulation and exogenous norepinephrine. *PediatrRes* 1985; 19:1210-14.

Campos, MM & Calixto JB. Neurokinin mediation of edema and inflammation. *Neuropeptides* 2000; 34(5): 314-22.

Catalan RE, Martinez AM, Aragones MD et al. Substance P stimulates translocation of protein kinase C in brain microvessels. *Biochem Biophys Res Commun* 1989;164: 595-600.

Cazaubon SM & Couraud PO. Nitric oxide and endothelin at the blood-brain barrier. In: Partridge WM ed. *Introduction to the blood-brain barrier*. Cambridge: Cambridge University Press, 1998: 338-44.

Chan PH. Oxygen radicals in focal cerebral ischemia. *Brain Pathol* 1994; 4: 59-65.

Chang MM, Leeman SE & Niall HD. Amino-acid sequence of substance P. *Nat New Biol* 1971; 232(29): 86-7.

Chorobski J & Penfield W. Cerebral vasodilator nerves and their pathway from the medulla oblongata. *Arch Neurol Psychiatry* 1932; 28:1257-89.

Chu DQ, Smith DM & Brain SD. Studies of the microvascular effects of adrenomedullin and related peptides. *Peptides* 2001; 22: 1881-86.

Cioni C, Renzi D, Calabro A et al. Enhanced secretion of substance P by cytokine-stimulated rat brain endothelium cultures. *J Neuroimmunol* 1998; 84:76-85.

Cohen Z, Molinatti G & Hamel E. Astroglial and vascular interactions of noradrenaline terminals in the rat cerebral cortex. *J Cereb Blood Flow Metab* 1997; 17:894-904.

Costa M, Cuello AC, Furness JB et al. Distribution of enteric neurons showing immunoreactivity for substance P in the guinea-pig ileum. *Neuroscience* 1980; 5(2):323-31.

Costa SK, Yshii LM, Poston RN et al. Pivotal role of endogenous tachykinins and the NK1 receptor in mediating leukocyte accumulation, in the absence of oedema formation, in response to TNF alpha in the cutaneous microvasculature. *J Neuroimmunol* 2006; 171(1-2):99-109.

Crockard A, Iannotti F, Hunstock AT et al. Cerebral blood flow and edema following carotid occlusion in the gerbil. *Stroke*, 1980: 11(5): 494-8.

Cuello AC & Kanazawa I. The distribution of substance P immunoreactive fibers in the rat central nervous system. *J Comp Neurol* 1978; 178(1):129-36.

del Zoppo GJ, Schmid-Schonbein GIN, Mori E et al. Polymorphonudear leukocytes occlude capillaries following middle cerebral artery occlusion and reperfusion in baboons. *Stroke* 1991; 22:1276-83.

Dennis T, Fournier A, Cadieux A et al. HCGRP 8-37, a calcitonin gene- related peptide antagonist revealing calcitonin gene-related peptide receptor heterogenity in brain and periphery. *The Journal of Pharmacology and Experimental Therapeutics* 1990; *254:* 123-28.

Dereski MO, Chopp M, Knight RA et al. The heterogeneous temporal evolution of focal ischemic neuronal damage in the rat. *Acta Neuropathol* (Berl), 1993: 85(3): 327-33.

Dietrich WD, Alonso 0 & Halley M. Early microvascular and neuronal consequences to traumatic brain injury: a light and electron microscopic study in rats. *J Neurotrauma* 1994; 11: 289-301.

Di Maria GU, Bellofiore S & Geppetti P. Regulation of airway neurogenic inflammation by neutral endopeptidase. *Eur Respir J* 1998; 12(6):1454-62.

Dirnagl U, Iadecola C & Moskowitz MA. Pathobiology of ischaemic stroke: an integrated view. *Trends Neurosci* 1999: 22(9): 391-7.

Doods H, Hallermayer G, Wu D et al. Pharmacological profile of BIBN4096BS, the first selective small molecule antagonist. *British Journal of Pharmacology.* 2000; 129: 420-23.

Doppenberg EMR & Bullock R. Clinical neuro-protection trials in severe traumatic brain injury: lessons from previous studies. *J Neurotrauma* 1997; 14: 71-80.

Drummond PD, Gonski A & Lance JW. Facial flushing after thermocoagulation of the gasserian ganglion. *J Neurol Neurosurg Psychiatry* 1983; 46:611-16.

Easton AS & Fraser PA. Arachidonic acid increases cerebral microvascular permeability by free radicals in single pial microvessels of the anaesthetized rat. *J Physiol* 1998; 507: 541-7.

Edvinsson L. Neurogenic mechanisms in the cerebrovascular bed. Autonomic nerves, amine receptors and their effects on cerebral blood *flow. Acta Physiol Scand* 1975; 427:1-35.

Edvinsson L, Owman C & Siesjo B. Physiological role of cerebrovascular sympathetic nerves in the autoregulation of cerebral blood flow. *Brain Res* 1976; 117:519-23.

Edvinsson L, McCulloch J & Uddman R. Substance P: Immunohistochemical localization and effect upon feline pial arteries in vitro and in situ. *J Physiol* 1981; 318: 251-58.

Edvinsson L, McCulloch J & Uddman R. Feline cerebral veins and arteries: comparison of autonomic innervation and vasomotor responses. *J Physiol* 1982; 325:161-73.

Edvinsson L & Uddman R. Immunohistochemical localization and dilatory effect of substance P on human cerebral arteries. *Brain Res* 1982; 232: 466-71.

Edvinsson L, Auer LM & Uddman R. Autonomic nerves and morphological organization of cerebral veins. In: Auer LM, Loew F, eds. *The cerebral veins. An experimental and clinical update.* Berlin: Springer-Verlag, 1983a: 73-9.

Edvinsson L, Degueurce A, Duverger D et al. Central serotonergic nerves project to the pial vessels of the brain. *Nature* 1983b; 306: 55-7.

Edvinsson L, Rosendal-Helgesen S & Uddman R. Substance P: localization, concentration and release in cerebral arteries, choroid plexus and dura mater. *Cell Tissue Res* 1983c; 234: 1-7.

Edvinsson L, MacKenzie ET, Robert JP et al. Cerebrovascular responses to haemorrhagic hypotension in anaesthetized cats Effects of α-adrenoceptor antagonists. *Acta Physiol Scand* 1985; 123:317-23.

Edvinsson L, McCulloch I, Kingman TA et al. On the functional role of the trigemino-cerebrovascular system in the regulation of cerebral circulation. In: Owman C, Hardebo JE, eds. *Neural regulation of the cerebral circulation.* Stockholm: Elsevier Science, 1986:407-18.

Edvinsson L, Ekman R, Jansen I et al. Calcitonin gene-related peptide and cerebral blood vessels: distribution and vasomotor effects. *J Cereb Blood Flow Metab.* 1987; 7: 720-8.

Edvinsson L, Gulbenkian S, Jansen I et al. Comparision of peptidergic mechanisms in different parts of the guinea pig superior mesenteric artery: immunocytochemistry at the light and ultrastructural levels and responses in vitro of large and small arteries. *J Auton Nerv Syst* 1989; 28:141-54.

Edvinsson L, Delgado-Zygmunt T, Ekman R et al. Involvement of perivascular sensory fibers in the pathophysiology of cerebral vasospasm following subarachnoid hemorrhage. *J Cereb Blood Flow Metab* 1990; 10:602-7.

Edvinsson L, Jansen-Olesen I, Kingman TA et al. Modification of vasoconstrictor responses in cerebral blood vessels by lesioning of the trigeminal nerve: possible involvement of CGRP. *Cephalalgia* 1995; 15.373-83.

Edvinsson L & MacKenzie ET. General and comparative anatomy of the cerebral circulation. In: Edvinsson L, Krause DN, ed. Cerebral *Blood Flow and Metabolism*, 2nd ed. Philadelphia: Lippincott Williams and Wilkins, 2002:3-29.

Eng LF, Ghirnikar RS & Lee YL. Glial fibrillary acidic protein: GFAP – thirty-one years (1969-2000). *Neurochem Res* 2000; 25: 1439-51.

Engel S, Schluesener H, Mittelbronn M et al. Dynamics of microglial activation after human traumatic brain injury are revealed by delayed expression of macrophage related proteins MRP8 and MRP14. Ada *Neuropathol* 2000; 100:313-22.

Escott KJ, Connor HE, Brain SD et al. The involvement of calcitonin gene-related peptide (CGRP) and substance P in feline pial artery diameter responses evoked by capsaicin. *Neuropeptides* 1995; 29: 129-35.

Feickert HJ, Drommer S & Heyer R. Severe head injury in children: impact of risk factors on outcome. *J Trauma* 1999; 47(1):33-8.

Feindel W, Penfield W & McNaughton E. The tentorial nerves and localisation of intracranial pain in man. *Neurology* 1960; 10:555-63.

Fishman RA. Brain edema. *N Engl Med J* 1975; 293: 706-11.

Fleminger S & Ponsford J. Long term outcome after traumatic brain injury. *BMJ* 2005; 331(7530):1419-20.

Forbes HS, Nason GI, Cobb S et al. Cerebral circulation XLV: vasodilation in the pia following stimulation of the geniculate ganglion. *Arch Neurol Psychiatry* 1937; 37:777-86.

Frosch MP, Anthony DC & De Girolami U. The Central Nervous System. In: Kumar V, Abbas AK, Fausto N, eds. Robbins and Cotran: *Pathologic Basis of Disease*, 7th ed. Philadelphia: Elsevier, 2005: 1347-420.

Furlan M, Marchal G, Viader F et al. Spontaneous neurological recovery after stroke and the fate of the ischemic penumbra. *Ann Neurol* 1996: 40(2): 216-26.

Furness JB, Papka RE, Della NG, et al. Substance P-like immunoreactivity in nerves associated with the vascular system in guinea pigs. *Neuroscience* 1982; 7: 447-59.

Gennarelli TA, Thibault LE & Graham DI. Diffuse axonal injury: an important form of traumatic brain injury. *Neuroscientist* 1998; 4: 202-15.

Geppetti P, Bertrand C, Ricciardolo FL et al. New aspects on the role of kinins in neurogenic inflammation. *Can J Physiol Pharmacol* 1995; 73(7):843-7.

Gibbins IL, Furness JB & Costa M. Pathway-specific patterns of the co-existence of substance P, calcitonin gene-related peptide, cholecystokinin and dynorphin in neurons of the dorsal root ganglia of the guinea-pig. *Cell Tissue Res* 1987; 248(2):417-37.

Go KG. The normal and pathological physiology of brain water. *Adv Techn Stand Neurosurg* 1997; 23:142-7.

Goadsby PJ & Duckworth JW. Effect of stimulation of trigeminal ganglion on regional cerebral blood flow in cats. *Am J Physiol* 1987; 253:R270-R4.

Goadsby PJ, Edvinsson L & Ekman R. Release of vasoactive peptides in the extracerebral circulation of man and the cat during activation of the trigeminovascular system. *Ann Neurol* 1988; 23:193-6.

Goadsby PJ. Effect of stimulation of the facial nerve on regional cerebral blood flow and glucose utilization in cats. *Ant J Phy.siol* 1989; 257:R517-R21.
Goldstein, M. Traumatic brain injury: a silent epidemic. *Ann Neurol* 1990: 27(3): 327.

Goadsby PJ, Zagami AS & Lambert GA. Neural processing of craniovascular pain: a synthesis of the central structures involved in migraine. *Headache* 1991; 31:365-71.

Goadsby PJ & Edvinsson L. Examination of the involvement of neuropeptide Y (NPY) in cerebral autoregulation using the novel NPY antagonist PP56. *Neuropeptides* 1993; 24:27-33.

Goadsby PJ & Hoskin KL. The distribution of trigeminovascular afferents in the non-human primate brain Macaca nemestrina: an immunocytochemical study. *J Anat* 1997;190: 367-75.

Goadsby PJ & Edvinsson L. Neurovascular control of the cerebral circulation. In: Edvinsson L, Krause DN, ed. *Cerebral Blood Flow and Metabolism*, 2nd ed. Philadelphia: Lippincott Williams and Wilkins, 2002:172-90.

Goldstein GW. Endothelial cell-astrocyte interactions. A cellular model of the blood-brain barrier. *Ann NY Acad Sci* 1988; 529: 31-9.

Goldstein M. Traumatic brain injury: a silent epidemic. *Ann Neurol* 1990; 27(3): 327.

Gorelova E, Loesch A, Bodin P et al. Localisation of immunoreactive factor VIII, nitric oxide synthase, substance P, endothelin-1 and 5hydroxytryptamine in human postmortem middle cerebral artery. *J Anat* 1996;188: 97-107.

Graeber MB, Blakemore WF & Kreutzberg GW. Cellular pathology of the central nervous system. In: Graham DI, Lantos PL, eds. *Greenfield's Neuropathology*, 7th ed. New York: Arnold, 2002: 123-91.

Graham DI, Gennarelli TA & McIntosh TK. Trauma. In: Graham DI, Lantos PL, eds. *Greenfield's Neuropathology*, 7th ed. New York: Arnold, 2002: 823-98.

Harrison S & Geppetti P. Substance p. *Int J Biochem Cell Biol* 2001; 33(6):555-76.

Hasenohrl RU, Souza-Silva MA, Nikolaus S et al. Substance P and its role in neural mechanisms governing learning, anxiety and functional recovery. *Neuropeptides* 2000; 34(5):272-80.

Hassin GB. The nerve supply of the cerebral blood vessels. *Arch Neurol Psychiatry* 1929; 22:375-91.

Hausmann R, Kaiser A, Lang C et al. A quantitative immunohistochemical study on the time-dependent course of acute inflammation cellular response to human brain injury. *Int J Legal Med* 1999; 112: 227-32.

Helke CJ. Neuroanatomical localization of substance p: implications for central cardiovascular control. *Peptides* 1982; 3(3):479-83.

Helke CJ & Hill KM. Immunohistochemical study of neuropeptides in vagal and glossopharyngeal afferent neurons in the rat. *Neuroscience* 1988; 26(2):539-51.

Henry JL. Effects of substance P on functionally identified units in cat spinal cord. *Brain Res* 1976; 114(3):439-51.

Heymann E & Mentlein R. Liver dipeptidyl aminopeptidase IV hydrolyzes substance P. *FEBS Lett* 1978; 91(2):360-4.

Hoff JT, MacKenzie ET & Harper AM. Responses of the cerebral circulation to hypercapnia and hypoxia after 7th cranial nerve transection in baboons. *Circ Res* 1977; 40:258-62.

Hokfelt T, Kellerth JO, Nilsson G et al. Substance p: localization in the central nervous system and in some primary sensory neurons. *Science* 1975; 190(4217):889-90.

Holmin S & Mathiesen T. Intracerebral administration of interleukin-1beta and induction of inflammation, apoptosis, and vasogenic edema. *J Neurosurg* 2000; 92(1):108-20.

Hooper NM & Turner AJ. Isolation of two differentially glycosylated forms of peptidyl-dipeptidase A (angiotensin converting enzyme) from pig brain: a re-evaluation of their role in neuropeptide metabolism. *Biochem J* 1987; 241(3):625-33.

Hossmann, K A. Viability thresholds and the penumbra of focal ischemia. *Ann Neurol* 1994: 36(4): 557-65.

Hüber GC. Observations on the innervation of intracranial vessels. *J Comp Neurol* 1899; 9:1-34.

Hulmin S, Soderlund I, Biberfeld P et al. Intracerebral inflammation after brain contusion. *Neurosurgery* 1998; 42: 291-8.

Humphreys SP. Anatomic relations of cerebral vessels and perivascular nerves. *Arch Neurol Psychiatry* 1939; 41:1207-21.

Iannotti F & Hoff J. Ischemic brain edema with and without reperfusion: an experimental study in gerbils. *Stroke* 1983: 14(4): 562-7.

Ironside JW & Pickard JD. Raised intracranial pressure, oedema and hydrocephalus. In: Graham DI, Lantos PL, eds. *Greenfield's Neuropathology*, 7th ed. New York: Arnold, 2002: 193-232.

Itakura T, Oken T, Nakakita K et al. A light and electron microscopic immunohistochemical study of vasoactive intestinal polypeptide- and substance P-containing nerve fibers along the cerebral blood vessels: comparison with aminergic and cholinergic nerve fibers. *J Cereb Blood Flow Metab* 1984; 4: 407-14.

Jansen I, Alafaci C, Uddman R et al. Evidence that calcitonin gene-related peptide contributes to the capsaicin-induced relaxation of guinea pig cerebral arteries. *Regul Pept* 1990; 31:167-78.

Jansen I, Uddman R, Ekman R et al. Distribution and effects of neuropeptide Y, vasoactive intestinal peptide, substance P, and calcitonin gene-related peptide in human middle meningeal arteries: comparison with cerebral and temporal arteries. *Peptides* 1992; 13: 527-36.

Jansen-Olesen I, Mortensson A & Edvinsson L. Calcitonin gene-related peptide is released from capsaicin sensitive nerve fibres and induce vasodilatation of human cerebral arteries concomitant with activation of adenylyl cyclase. *Cephalalgia* 1996;16:310-16.

Janzer RC & Raff MC. Astrocytes induce blood-brain barrier properties in endothelial cells. *Nature* 1987; 325: 2513-17.

Juul R, Edvinsson L, Gisvold SE et al. Calcitonin gene-related peptide-IR in subarachnoid haemorrhage in man. Signs of activation of the trigemino-cerebrovascular system? *Br J Neurosurg* 1990; 4:171-80.

Kalimo H, Kaste M & Haltia M. Vascular Diseases. In: Graham DI, Lantos PL, eds. *Greenfield's Neuropathology*, 7th ed. New York: Arnold, 2002: 281-356.

Kennedy PG, Rodgers J, Jennings FW et al. A substance P antagonist, RP-67,580, ameliorates a mouse meningoencephalitic response to Trypanosoma brucei brucei. *Proc Natl Acad Sci* (USA) 1997; 94(8): 4167-70.

Kennedy PG, Rodgers J, Bradley B et al. Clinical and neuroinflammatory responses to meningoencephalitis in substance P receptor knockout mice. *Brain*, 2003; 126: 1683-90.

Kido MA, Yamaza T, Goto T et al. Immunocytochemical localization of substance P neurokinin-1 receptors in rat gingival tissue. *Cell Tissue Res* 1999; 297(2):213-22.

Kincy-Cain T & Bost KL. *Substance* P-induced IL-12 production by murine macrophages. *J Immunol* 1997; 158(5): 2334-9.

Klatzo I. Presidental address. Neuropathological aspects of brain edema. *J Neuropathol Exp Neurol* 1967; 26(1): 1-14.

Kogure K, Busto R, Scheinberg P et al. The role of hydrostatic pressure in ischemic brain edema. *Ann Neurol* 1981; 9(3): 273-82.

Kontos HA. Oxygen radicals in cerebral vascular injury. *Circ Res* 1985; 57:508-16.

Kostyk, SK, Kowall NW & Hauser SL. Substance P immunoreactive astrocytes are present in multiple sclerosis plaques. *Brain Res* 1989; 504(2): 284-8.

Kotani H, Hoshimaru M, Nawa H et al. Structure and gene organization of bovine neuromedin K precursor. Proc Natl Acad Sci U S A. 1986 Sep;83(18):7074-8.

Lai JP, Zhan GX, Campbell DE et al. Detection of substance P and its receptor in human fetal microglia. *Neuroscience* 2000; 101(4): 1137-44.
Lee Y, Kawai Y, Shiosaka S et al. Coexistence of calcitonin gene-related peptide and substance P-like peptide in single cells of the trigeminal ganglion of the rat: immunohistochemical analysis. *Brain Res* 1985; 330(1):194-6.

Lenzlinger PM, Morganti-Kossmann MC, Laurer HL et al. The duality of the inflammatory response to traumatic brain injury. *Mol Neurobiol* 2001; 24(1-3):169-81.

Leon-Carrion J & Dominguez-Morales Mdel R. Epidemiology of traumatic brain injury and subarachnoid hemorrhage. *Pituitary* 2005; 8(3-4):197-202.

Lin RC. Reactive astrocytes express substance-P immunoreactivity in the adult forebrain after injury. *Neuroreport* 1995; 7(1): 310-2.

Linder J. Effects of facial nerve section and stimulation on cerebral and ocular blood flow in hemorrhagic hypotension. *Acta Physiol Scand* 1981; 112:185-93.

Linnik MD & Moskowitz MA. Identification of immunoreactive substance P in human and other mammalian endothelial cells. *Peptides* 1989;10: 957-62.

Liu-Chen LY, Mayberg MR & Moskowitz MA. Immunohistochemical evidence for a substance P-containing trigeminovascular pathway to pial arteries in cats. *Brain Res* 1983a; 268:162-6.

Liu-Chen LY, Han DH & Moskowitz MA. Pia arachnoid contains substance P originating from trigeminal neurons. *Neuroscience* 1983b; 9:803-8.

Ljungdahl A, Hokfelt T & Nilsson G. Distribution of substance P-like immunoreactivity in the central nervous system of the rat- I. Cell bodies and nerve terminals. *Neuroscience*. 1978; 3(10):861-943.

Luebke AE, Dahl GP, Roos BA et al. Identification of a protein that confers calcitonin gene-related peptide responsiveness to oocytes by using a cyclic fibrosis transmembrane conductance regulator assay. *Proc Natl Acad Sci (*USA) 1996; 93:3455-60.

Lundberg JM, Saria A, Brodin E et al. A substance P antagonist inhibits vagally induced increase in vascular permeability and bronchial smooth muscle contraction in the guinea pig. *Proc Natl Acad Sci* (U S A) 1983; 80(4):1120-4.

Maggi, CA. Tachykinins and calcitonin gene-related peptide (CGRP) as cotransmitters released from peripheral endings of sensory nerves. *Prog Neurobiol* 1995; 45(1): 1-98.

Maggi CA & Schwartz TW. The dual nature of the tachykinin NK1 receptor. *Trends Pharmacol Sci* 1997; 18(10):351-5.

Mantyh PW, Johnson DJ, Boehmer CG et al. Substance P receptor binding sites are expressed by glia in vivo after neuronal injury. *Proc Natl Acad Sci* (USA) 1989; 86(13): 5193-7.

Markowitz S, Saito K & Moskowitz MA. Neurogenically mediated plasma extravasation in dura mater: effect of ergot alkaloids. A possible mechanism of action in vascular headache. *Cephalalgia* 1988; 8(2):83-91.

Marmarou A. Traumatic brain edema: an overview. *Acta Neurochir* 1994; 60 (Suppl): 421-4.

Marmarou A, Portella G, Barzo P et al. Distinguishing between cellular and vasogenic edema in head injured patients with focal lesions using magnetic resonance imaging. *Acta Neurochir Suppl* 2000; 76: 349-51.

Martin FC, Charles AC, Sanderson MJ et al. Substance P stimulates IL-1 production by astrocytes via intracellular calcium. *Brain Res* 1992; 599(1): 13-8.

Matsas R, Kenny AJ & Turner AJ. The metabolism of neuropeptides. The hydrolysis of peptides, including enkephalins, tachykinins and their analogues, by endopeptidase-24.11. *Biochem J* 1984; 223(2):433-40.

Mayberg M, Langer RS, Zervas NT et al. Perivascular meningeal projections from cat trigeminal ganglia: possible pathway for vascular headaches in man. *Science* 1981; 213:228-30.

Mayberg M, Zervas NT & Moskowitz MA. Trigeminal projections to supratentorial pial and dural blood vessels in cats demonstrated by horseradish peroxidase histochemistry. *J Comp Neurol* 1984; 223: 46-56.

Mayhan WG. Nitric oxide donor-induced increase in permeability of the brain barrier. *Brain Res* 2000; 866: 101-8.

McCulloch J, Uddman R, Kingman T et al. Calcitonin gene-related peptide: functional role in cerebrovascular regulation. *Proc Nail Acad Sci* (USA) 1986; 83:5731-5.

McDonald DM, Thurston G & Baluk P. Endothelial gaps as sites for plasma leakage in inflammation. *Microcirculation* 1999; 6:7-13.

Mejia JA, Pernow J, von Holst H et al. Effects of neuropeptide Y, calcitonin gene-related peptide, substance P, and capsaicin on cerebral arteries in man and animals. *J Neurosurg* 1988; 69:913-8.

Michel JP, Sakamoto N, Bouvier R et al. Substance P-immunoreactive astrocytes related to deep white matter and striatal blood vessels in human brain. *Brain Res* 1986; 377(2): 383-7.

Millikan CH & McDowell F. *Stroke* 1987, Philadelphia, Lea & Febiger.

Mirra SS, Heyman A, McKeel D et al. The Consortium to Establish a Registry for Alzheimer's Disease (CERAD). Part II. Standardization of the neuropathologic assessment of Alzheimer's disease. *Neurology* 1991; 41(4):479-86.

Moreno MJ, Abounader R, Hebert E et al. Efficacy of the non-peptide CGRP receptor antagonist BIBN4096BS in blocking CGRP induced dilations in human and bovine cerebral arteries: potential implications in acute migraine treatment. *Neuropharmacology* 2002; 42: 568-76.

Mori E, del Zoppo GJ, Chambers JD et al. Inhibition of polymorphonuclear leukocyte adherence suppresses no-reflow after focal cerebral ischemia in baboons. *Stroke* 1992; 23: 712-18.

Mraovitch S, Iadecola C, Ruggiero DA et al. Widespread reductions in cerebral blood flow and metabolism elicited by electrical stimulation of the parabrachial nucleus in rat. *Brain Res* 1985; 341:283-96.

Mraovitch S, Lasbennes F, Calando Y et al. Cerebrovascular changes elicited by electrical stimulation of the centromedian-parafascicular complex in the rat. *Brain Res* 1986; 380:42-53.

Murray GD, Teasdale GM, Braakman R et al. The European Brain Injury Consortium survey of head injuries. *Acta Neurochir* (Wien) 1999; 141(3): 223-36.

Nadel JA. Neutral endopeptidase modulates neurogenic inflammation. *Eur Respir J* 1991; 4(6):745-54.

Nag S, Robertson DM & Dinsdale HB. Blood-brain barrier opening to horseradish peroxidase in acute experimental hypertension. *Acta Neuropathol* 1979; 46:107-16.

Nakai M, Iadecola C, Ruggiero DA et al. Electrical stimulation of cerebellar fastigial nucleus increases cerebral cortical blood flow without change in local metabolism: evidence for an intrinsic system in brain for primary vasodilation. *Brain Res* 1983; 260:35-49.

Nakanishi S. Mammalian tachykinin receptors. *Annu Rev Neurosci* 1991;14:123-36.

Nakata H, Yoshimine T, Murasawa A et al. Early blood-brain barrier disruption after high-dose single-fraction irradiation in rats. *Acta Neurochir* (Wien) 1995; 136(1-2):82-6.

Nilsson G, Larsson LI, Hakanson R et al. Localization of substance P-like immunoreactivity in mouse gut. *Histochemistry* 1975; 43(1):97-9.

Nimmo AJ, Cernak I, Heath DL et al. Neurogenic inflammation is associated with development and functional defecits following traumatic brain injury in rats. *Neuropeptides* 2004; 38(1): 40-7.

Obrenovitch, TP. The ischaemic penumbra: twenty years on. *Cerebrovasc Brain Metab Rev* 1995; 7(4): 297-323.

Oka M. Experimental study on the vasodilator innervation of the face. *Med J Osaka Unit* 1950; 2:109-16.

Okada Y, Copeland BR, Mori E et al. P-selectin and intercellular adhesion molecule-1 expression after focal brain ischemia and reperfusion. *Stroke* 1994; 25: 202-11.

Oldendorf WH, Cornford ME & Brown WJ. The large apparent work capability of the blood-brain barrier: A study of the mitochondrial content of capillary endothelial cells in brain and other tissues of the rat. *Ann Neurol* 1977; 1:409 - 17.

Oldendorf WH, Cornford ME & Brown WJ. Some unique ultrastmctural characteristics of rat brain capillaries. In: *Cerebral microcirculation and metabolism.* Cervos-Navarro J, Fritschka E, eds. New York: Raven Press, 1981:9-15.

Onofrio BM. Radiofrequency percutaneous Gasserian ganglion lesions. Results in 140 patients with trigeminal pain. *J Neurasurg* 1975; 42:132-43.

Penfield W. Intracerebral vascular nerves. *Arch Neurol Psychiatry* 1932; 27:30-114.

Penfield W. A contribution to the mechanism of intracranial pain. *Proc Assoc Res Nerv Mental Dis* 1934; 15:399-415.

Penfield W & McNaughton FL. Dural headache and the innervation of the dura mater, *Arch Neural Psychiatry* 1940;44:43-75.

Petersen KA, Nilsson E, Olesen J et al. Presence and function of the calcitonin gene-related peptide receptor on rat pial arteries investigated in vitro and in vivo, *Cephalalgia* 2005; 25(6):424-32.

Povlishock JT, Becker DP, Sullivan HG et al. Vascular permeability alterations to horseradish peroxidase in experimental brain injury. *Brain Res* 1978;153:223-39.

Povlishock JT. The pathophysiology of blood-brain barrier dysfunction due to traumatic brain injury. In: Partridge WM ed. *Introduction* to the blood-brain barrier. Cambridge: Cambridge University Press, 1998: 441-53.

Probert L & Hanley MR. The immunocytochemical localisation of 'substance-P-degrading enzyme' within the rat spinal cord. *Neurosci Lett* 1987; 78(2):132-7.

Purves MJ. *The physiology of the cerebral circulation.* Cambridge: Cambridge University Press, 1972.

Raichle ME, Eichling JO, Grubb RL et al. Central noradrenergic regulation of brain micro-circulation. In: Pappius HM, Feindel W, eds. *Dynamics of brain edema.* New York: Springer-Verlag, 1976: 11-17.

Rapoport SI. *Blood brain* barrier in physiology and medicine. New York: Raven Press, 1976.

Read SJ, Hirano T, Abbott DF et al. Identifying hypoxic tissue after acute ischemic stroke using PET and 18F-fluoromisonidazole. *Neurology* 1998;51(6): 1617-21.

Reilly PL, Graham DI, Adams JH et al. Patients with head injury who talk and die. *Lancet* 1975; (7931): 375-7.

Reilly PL. Brain injury: the pathophysiology of the first hours. Talk and Die revisited'. J Clin Neurosci2001: 8(5): 398-403.

Reese TS & Kamovsky M. Fine structural localization of a blood-brain barrier to exogenous peroxidase. *J Cell Biol* 1967; 4:207-17.

Rupniak NM & Kramer MS. Discovery of the antidepressant and anti-emetic efficacy of substance P receptor (NK1) antagonists. *Trends Pharmacol* Sci 1999; 20(12):485-90.

Sakurada C, Yokosawa H & Ishii S. The degradation of somatostatin by synaptic membrane of rat hippocampus is initiated by endopeptidase-24.11. *Peptides* 1990; 11(2):287-92.

Sams A, Knyihar-Csillik E, Engberg J et al. CGRP and adrenomedullin receptor populations in human cerebral arteries: in vitro pharmacological and molecular investigations in different artery sizes. *Eur J Pharmacol* 2000; 08:183-93.

Schilling L & Wahl M. Mediators of cerebral edema. Adv *Exp Med Biol* 1999; 474: 123-41.

Schoettle RJ, Kochanek PM, Magargee MJ et al. Early polymorphonuclear leukocyte accumulation correlates with the development of posttraumatic cerebral edema in rats. *J Neurotrauma* 1990; 7(4):207-17.

Schultzberg M, Hokfelt T, Nilsson G et al. Distribution of peptide- and catecholamine-containing neurons in the gastro-intestinal tract of rat and guinea-pig: immunohistochemical studies with antisera to substance P, vasoactive intestinal polypeptide, enkephalins, somatostatin, gastrin/cholecystokinin, neurotensin and dopamine beta-hydroxylase. *Neuroscience* 1980; 5(4):689-744.

Standring S, Crossman AR & Collins P. Vascular supply of the brain. In: Standring S, ed. *Gray's Anatomy*, 39th ed. Amsterdam: Elsevier, 2005a:295-306.

Standring S, Wigley C, Collins P et al. Smooth muscle and the cardiovascular and lymphatic systems. In: Standring S, ed. *Gray's Anatomy*, 39th ed. Amsterdam: Elsevier, 2005b:137-56.

Shimizu T, Koto A, Suzuki N et al. Occurrence and codistribution of substance P receptors in the cerebral blood vessels of the rat. *Brain Res* 1999; 30:372-78.

Shivers RR, Arthur FE & Bowman PD. Induction of gap junctions and brain enthothelium-like tight junctions in cultured bovine endothelial cells: local control of cell specialization. *J Submicrosc Cytol* 1988; 20: 1-14.

Shults CW, Quirion R, Chronwall B et al. A comparison of the anatomical distribution of substance P and substance P receptors in the rat central nervous system. *Peptides* 1984; 5(6):1097-128.

Siesjo BK & Kristian T. *Cerebrovascular Disease*. Ginsberg D and Bogousslavasky J. Blackwell Science1998: 1-13.

Skidgel RA & Erdos EG. Cleavage of peptide bonds by angiotensin I converting enzyme. *Agents Actions Suppl* 1987; 22:289-96.

Souza DG, Mendonca VA, de A Castro MS et al. Role of tachykinin NK receptors on the local and remote injuries following ischaemia and reperfusion of the superior mesenteric artery in the rat. *Br J Pharmacol* 2002; 135(2):303-12.

Stahel PF, Kossmann T, Joller H et al. Increased interleukin-12 levels in human cerebrospinal fluid following severe head trauma. *Neurosci Lett* 1998; 249(2-3):123-6.

Stanimirovic D & Satoh K. Inflammatory mediators of cerebral endothelium: a role in brain inflammation. *Brain Pathol* 2000; 10:113-26.

Sternini C, Su D, Gamp PD et al. Cellular sites of expression of the neurokinin-1 receptor in the rat gastrointestinal tract. *J Comp Neurol* 1995; 358(4):531-40.

Stubbs CM, Waldron GJ, Connor HE et al. Characterization of the receptor mediating relaxation to substance P in canine middle cerebral artery: no evidence for involvement of substance P in neurogenically mediated relaxation. *Br J Pharmacol* 1992; 105:875-80.

Stumm RK, Culmsee C, Schafer MK-H et al. Adaptive plasticity in tachykinin and tachykinin receptor expression after focal cerebral ischemia is differentially linked to GABAergic and glutamatergic cerebrocortical circuits and cerebrovenular endothelium. *J Neurosci* 2001; 21:798-811.

Sweet WM & Wepsic JG. Controlled thermocoagulation of V ganglion and rootlets for differential destruction of pain fibres. *J Neurosurg* 1974; 40:143-56.

Takahashi T, Konishi S, Powell D et al. Identification of the motoneuron-depolarizing peptide in bovine dorsal root as hypothalamic substance P. Brain Res. 1974 Jun 14;73(1):59-69.

Takahashi T & Otsuka M. Regional distribution of substance P in the spinal cord and nerve roots of the cat and the effect of dorsal root section. *Brain Res* 1975; 87(1):1-11.

Taylor TN, Davis PH, Torner JC et al. Lifetime cost of stroke in the United States. *Stroke* 1996; 27(9): 1459-66.

Tehranian R, Andell-Jonsson S, Beni SM et al. Improved recovery and delayed cytokine induction after closed head injury in mice with central overexpression of the secreted isoform of the interleukin-1 receptor antagonist. *J Neurotrauma* 2002; 19(8):939-51.

Todd NV, Picozzi P, Crockard A et al. Duration of ischemia influences the development and resolution of ischemic brain edema. *Stroke* 1986; 17(3): 466-71.

Too, HP, Marriott DR & Wilkin GP. Preprotachykinin A and substance P receptor (NKI) gene expression in rat astrocytes in vitro. *Neurosci Lett* 1994; 182(2):185-7.

Tooney PA, Au GG & Chahl LA. Tachykinin NK1 and NK3 receptors in the prefrontal cortex of the human brain. *Clin Exp Pharmacol Physiol* 2000; 27(11): 947-9.

Torrens Y, Beaujouan JC, Saffroy M et al. Substance P receptors in primary cultures of cortical astrocytes from the mouse. *Proc Natl Acad Sci* (USA) 1986; 83(23): 9216-20.

Toulmond S & Rothwell NJ. Interleukin-1 receptor antagonist inhibits neuronal damage caused by fluid percussion injury in the rat. *Brain Res* 1995; 671(2):261-6.

Tregear GW, Niall HD, Potts JT Jr et al. Synthesis of substance P. *Nat New Biol* 1971; 232(29):87-9.

Uddman R, Edvinsson L, Owman C et al. Perivascular substance P: occurrence and distribution in mammalian pial vessels. *J Cereb Blood Flow Metab* 1981; 1: 227-32.

Uddman R, Edvinsson L, Ekman R et al. Innervation of the feline cerebral vasculature by nerve fibers containing calcitonin gene-related peptide: tdgeminal origin and co-existence with substance P. *Neurosci Lett* 1985; 62:131-36.

Uddman R, Edvinsson L, Ekblad E et al. Calcitonin gene related peptide (CGRP): perivascular distribution and vasodilatory effects. *Regulatory Peptides* 1986; 15: 1-26.

Underwood MD, Iadecola C, Sved A et al. Stimulation *of* C1 area neurons globally increases regional cerebral blood-flow but not metabolism. *J Cereb Blood Flow Metab* 1992; 12:844-55.

Vaz R, Sarmento A, Borges N et al. Ultrastructural study of brain microvessels in patients with traumatic cerebral contusions. *Acta Neurochir* (Wien) 1997; 139: 215-20.

Venero JL, Vizute ML, Machado A et al. Aquaporins in the central nervous system. *Prog Neurobiol* 2001; 63: 321-36.

Verbeek MM, Otte-Holler I, Fransen JA et al. Accumulation of the amyloid-beta precursor protein in multivesicular body-like organelles.
J Histochem Cytochem 2002; 50(5):681-90

Vink R. Personal communication. 2006

Wakai S, Aritake K, Asano T et al. Selective destruction of the outer leaflet of the capillary endothelial membrane after intracetebral injection of arachidonic acid in the rat. *Acta Neuropathol* 1982; 58:303-6.

Walters DW, Gillespie SA & Moskowitz M. Cerebrovascular projections from the sphenopalatine and otic ganglia to the middle cerebral artery of the cat. *Stroke* 1986;17:488-94.

Wang LH, Ahmad S, Benter IF et al. Differential processing of substance P and neurokinin A by plasma dipeptidyl (amino) peptidase IV, aminopeptidase M and angiotensin converting enzyme. *Peptides* 1991; 12(6):1357-64.

Wardlaw JM & Warlow CP. Thrombolysis in acute ischemic stroke: does it work? *Stroke* 1992; 23: 1826-39.

Wardlaw JM, del Zoppo G & Yamaguchi T. Thrombolysis for acute ischaemic stroke. *Cochrane Database Syst Rev* 2000; No. 2: CD000213.

Waugh DJ, Bockman J, Smith CS et al. Limitations in using peptide drugs to characterize calcitonin gene-related peptide receptors. *J Pharmacol Exp Ther* 1999; 289:1419-26.

Westergaard E. Enhanced vesicular transport of exogenous peroxidase across cerebral vessels, induced by serotonin. *Acta Neuropathol* 1975; 32:27-42.

Westergaard E, Van Deurs B & Brondsted HE. Increased vesicular transfer of horseradish peroxidase across cerebral endothelium, evoked by acute hypertension. *Acta Neuropathvl* 1977; 37:141-52.

Westergaard E, Hertz MM & Bolwig TG. Increased permeability to horseradish peroxidase across cerebral vessels, evoked by electrically induced seizures in the rat. *Acta Neuropathol* 1978; 41:73-80.

Willis T. *Cerebri Anatomi.* London: Martin & Allestry, 1664.

Wimalawansa SJ & El-Kholy AA. Comparative study of distribution and biochemical characterisation of brain calcitonin gene related peptide receptors in five different species. *Neuroscience* 1993; 54: 513-19.

Yamamoto K, Matsuyama T, Shiosaka S et al. Overall distribution of substance P-containing nerves in the wall of the cerebral arteries of the guinea pig and its origin. *J Comp Neurol* 1983; 215: 421-26.

Yu Z, Cheng G, Huang X et al. Neurokinin-1 receptor antagonist SR140333: a novel type of drug to treat cerebral ischemia. *Neuroreport* 1997; 8:2117-19.

Chapter 6

APPENDICES

Appendix 1: Hematoxylin and eosin (H&E) staining technique

1. Mount sections on glass slides and dry at 60°C (20min).
2. Dewax slides in xylene (2x2min) and dehydrate in graded alcohol (2x2min).
3. (If section is visibly hemorrhagic, to avoid formation of artefactual formalin pigment) immerse in saturated alcoholic solution of picric acid (20min) and then immerse in absolute alcohol (1hr).
4. (If section is visibly hemorrhagic, to avoid formation of artefactual formalin pigment) rinse in water (10 dips).
5. Immerse in hematoxylin (5min).
6. Rinse in water (10 dips).
7. Place in acid alcohol (10 dips).
8. Rinse in water (10 dips).
9. Place in lithium carbonate (15sec).
10. Rinse in water (10 dips).
11. Immerse in eosin for (2min).
12. Dehydrate in graded alcohol (2x10 dips) and 2 changes of histolene (2x10 dips).
13. Coverslip.

Appendix 2: Immunohistochemical staining (streptavidin-biotin) technique

1. Mount sections on poly-lysine-coated glass slides and dry at 60°C (20min).
2. Dewax slides in xylene (2x2min) and dehydrate in graded alcohol (2x2min).
3. (If section is visibly hemorrhagic, to avoid formation of artefactual formalin pigment) immerse in saturated alcoholic solution of picric acid (20min) and then immerse in absolute alcohol (1hr).
4. Immerse in 500ml methanol with 8.3ml H_2O_2 (30min) to block endogenous peroxidase activity.
5. Rinse in phosphate-buffered saline (PBS) buffer (pH 7.38-7.42) (2x3min).
6. Apply appropriate pretreatment (boiling for 10min in citrate, ethylenediamine tetra-acetic acid (EDTA) or target retrieval solution (TRS) depending on primary antibody (see Table 6.1) for optimum antigen retrieval. Then allow cooling to below 40°C.
7. Rinse in PBS buffer (2x3min).
8. Circle section with wax marker (Dako cytomation) and incubate with 3% normal horse serum (NHS) (30min).
9. Drain NHS and apply primary antibody overnight in humidified chamber.
10. Rinse in PBS buffer (2x3 min).
11. Incubate with biotinylated secondary antibody* (Vector) at 1/250 (30min).
12. Rinse in PBS buffer (2x3 min).
13. Incubate with streptavidin peroxidase tertiary antibody (Pierce) at 1/1,000 (60min).
14. Rinse in PBS buffer (2x3 min).
15. Apply diaminobenzidene (DAB) (pH 7.65-7.70) and excess H_2O_2 to obtain optimum staining at approximately 7min.
16. Rinse in PBS buffer (2x3 min).
17. Lightly counterstain (1 min) in Mayer's hematoxylin.
18. Rinse in water (10 dips).
19. Place in acid alcohol (10 dips).
20. Rinse in water (10 dips).
21. Place in lithium carbonate (15sec).
22. Rinse in water (10 dips).
23. Dehydrate in graded alcohol (2x10 dips) and 2 changes of histolene (2x10 dips).
24. Coverslip.

* For confocal microscopy, at step 11, instead of biotinylated secondary antibody, incubate for 30 min with specified fluorophores (see Table 6.1). Then, rinse in PBS (2x3min) and coverslip using an aqueous mounting medium with antifade.

Table 6.1: Details of primary antibodies and fluorophores used in immunohistochemical staining.

Antibody/fluorophore	Manufacturer (catalog number)	Dilution*	Retrieval solution
anti-SP (goat polyclonal)	Santa Cruz (sc-9758)	1/2,000	EDTA
anti-albumin (goat polyclonal)	Cappel (0113-0341)	1/20,000	none
anti-APP (mouse monoclonal)	Boehringer (22C 11)	1/2,000	citrate
anti-NK1 (rabbit polyclonal)	Advanced Targeting Systems (AB-N04)	1/1,500	TRS
anti-CGRP (rabbit polyclonal)	Serotec (PEPA27)	1/20,000	citrate
anti-GFAP (rabbit polyclonal)	Dako (Z0334)	1/20,000	EDTA
Alexa 546 (donkey anti-goat)	Molecular Probes	1/200	N/A
FITC 488 (donkey anti-rabbit)	Jackson	1/200	N/A

* Dilutions decrease 10 fold for double immunolabeling
APP: amyloid precursor protein; CGRP: calcitonin gene-related peptide; EDTA: ethylenediamine tetra-acetic acid; FITC: fluorescein isothiocyanate; GFAP: glial fibrillary acidic protein; N/A: not applicable; NK1: neurokinin-1; SP: substance P; TRS: target retrieval solution

Addendum

(Cont'd from inside of front cover)

(Added references):

Berry M, Butt AM, Wilkin G et al. Structure and function of glia in the central nervous system. In: Graham DI & Lantos PL, eds. *Greenfield's Neuropathology*, 7th ed. New York: Arnold, 2002: 75-122.

Neumann H, Misgeld T, Matsumuro K et al. Neurotrophins inhibit major histocompatibility class II inducibility of microglia: involvement of the p75 neurotrophin receptor. *Proc Natl Acad Sci USA* 1998; 95: 5779-84.

Schmidtmayer J, Jacobsen C, Miksch G et al. Blood monocytes and spleen macrophages differentiate into microglia-like cells on monolayers of astrocytes: membrane currents. *Glia* 1994; 12: 259-67.

Sievers J, Parwaresch R & Wottge HU. Blood monocytes and spleen macrophages differentiate into microglia-like cells on monolayers of astrocytes: morphology. *Glia* 1994; 12: 245-58.